BioMed Research International

Genetic Treatments for Aging Diseases

Lead Guest Editor: Yun-Feng Yang
Guest Editors: Xiangyu Chu, Gang Zhang, and Huachao Shen

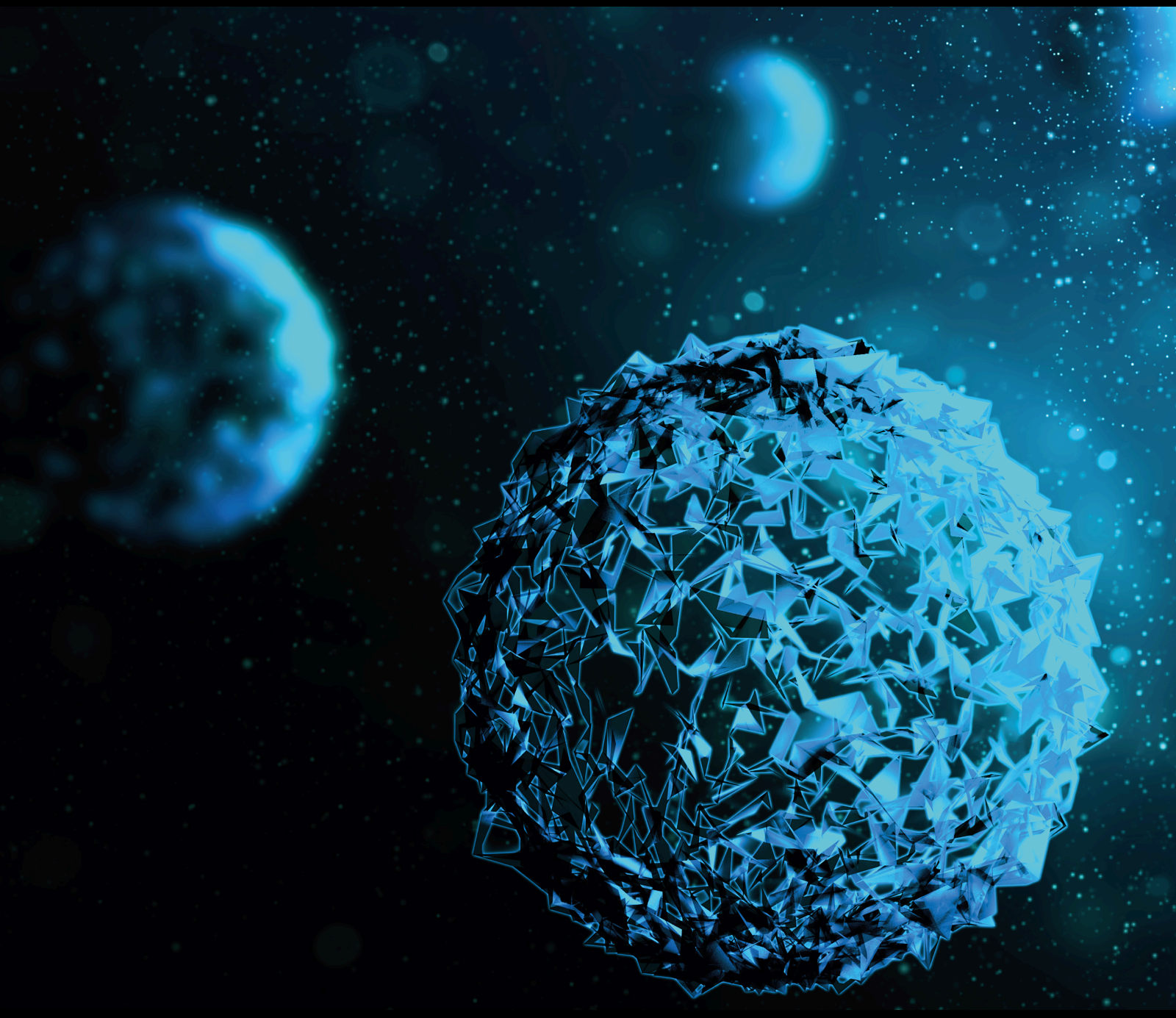

Genetic Treatments for Aging Diseases

BioMed Research International

Genetic Treatments for Aging Diseases

Lead Guest Editor: Yun-Feng Yang
Guest Editors: Xiangyu Chu, Gang Zhang, and Huachao Shen

Section Editors

Academic Editors

Biomedical Genetics & Genomics

Contents

[Retracted] The Effect on the Fracture Healing following Femoral Neck Shortening after Osteoporotic Femoral Neck Fracture Treated with Internal Fixation: Finite Element Analysis
Xiao Yu, Peng-ze Rong, Qing-jiang Pang, Xian-jun Chen, Lin Shi, and Cheng-hao Wang
Research Article (7 pages), Article ID 3490881, Volume 2021 (2021)

[Retracted] Analysis of Extended Resection of Limb Soft Tissue Leiomyosarcoma
Qiang Liu, Lijun Tang, Xinhua Hu, Jianxing Ye, Pengcheng Liang, Adriana C. Panayi, Shuhua Wang, and Jingde Deng
Research Article (4 pages), Article ID 2106972, Volume 2021 (2021)

[Retracted] Trophinin Is an Important Biomarker and Prognostic Factor in Osteosarcoma: Data Mining from Oncomine and the Cancer Genome Atlas Databases
Pan Cai, Yan Lu, Zhifeng Yin, Xiuhui Wang, Xiaoxiao Zhou, and Zhuokai Li
Research Article (9 pages), Article ID 6885897, Volume 2021 (2021)

[Retracted] Nomogram for Predicting Deep Venous Thrombosis in Lower Extremity Fractures
Ze Lin, Bobin Mi, Xuehan Liu, Adriana C. Panayi, Yuan Xiong, Hang Xue, Wu Zhou, Faqi Cao, Jing Liu, Liangcong Hu, Yiqiang Hu, Lang Chen, Chenchen Yan, Xudong Xie, Junfei Guo, Zhiyong Hou, Yun Sun, Yingze Zhang, Yu Hu, and Guohui Liu
Research Article (8 pages), Article ID 9930524, Volume 2021 (2021)

[Retracted] Increased EHHADH Expression Predicting Poor Survival of Osteosarcoma by Integrating Weighted Gene Coexpression Network Analysis and Experimental Validation
Juncheng Cui, Guoliang Yi, Jinxin Li, Yangtao Li, and Dongyang Qian
Research Article (13 pages), Article ID 9917060, Volume 2021 (2021)

Hindawi
BioMed Research International
Volume 2024, Article ID 9852153, 1 page
https://doi.org/10.1155/2024/9852153

Retraction

Retracted: Analysis of Extended Resection of Limb Soft Tissue Leiomyosarcoma

BioMed Research International

Received 12 March 2024; Accepted 12 March 2024; Published 20 March 2024

This article has been retracted by Hindawi following an investigation undertaken by the publisher [1]. This investigation has uncovered evidence of one or more of the following indicators of systematic manipulation of the publication process:

(1) Discrepancies in scope

(2) Discrepancies in the description of the research reported

(3) Discrepancies between the availability of data and the research described

(4) Inappropriate citations

(5) Incoherent, meaningless and/or irrelevant content included in the article

(6) Manipulated or compromised peer review

The presence of these indicators undermines our confidence in the integrity of the article's content and we cannot, therefore, vouch for its reliability. Please note that this notice is intended solely to alert readers that the content of this article is unreliable. We have not investigated whether authors were aware of or involved in the systematic manipulation of the publication process.

Wiley and Hindawi regrets that the usual quality checks did not identify these issues before publication and have since put additional measures in place to safeguard research integrity.

We wish to credit our own Research Integrity and Research Publishing teams and anonymous and named external researchers and research integrity experts for contributing to this investigation.

The corresponding author, as the representative of all authors, has been given the opportunity to register their agreement or disagreement to this retraction. We have kept a record of any response received.

References

[1] Q. Liu, L. Tang, X. Hu et al., "Analysis of Extended Resection of Limb Soft Tissue Leiomyosarcoma," *BioMed Research International*, vol. 2021, Article ID 2106972, 4 pages, 2021.

Hindawi
BioMed Research International
Volume 2024, Article ID 9838460, 1 page
https://doi.org/10.1155/2024/9838460

Retraction

Retracted: A New Survival Model Based on Cholesterol Biosynthesis-Related Genes for Prognostic Prediction in Clear Cell Renal Cell Carcinoma

BioMed Research International

Received 12 March 2024; Accepted 12 March 2024; Published 20 March 2024

This article has been retracted by Hindawi following an investigation undertaken by the publisher [1]. This investigation has uncovered evidence of one or more of the following indicators of systematic manipulation of the publication process:

(1) Discrepancies in scope

(2) Discrepancies in the description of the research reported

(3) Discrepancies between the availability of data and the research described

(4) Inappropriate citations

(5) Incoherent, meaningless and/or irrelevant content included in the article

(6) Manipulated or compromised peer review

The presence of these indicators undermines our confidence in the integrity of the article's content and we cannot, therefore, vouch for its reliability. Please note that this notice is intended solely to alert readers that the content of this article is unreliable. We have not investigated whether authors were aware of or involved in the systematic manipulation of the publication process.

Wiley and Hindawi regrets that the usual quality checks did not identify these issues before publication and have since put additional measures in place to safeguard research integrity.

We wish to credit our own Research Integrity and Research Publishing teams and anonymous and named external researchers and research integrity experts for contributing to this investigation.

The corresponding author, as the representative of all authors, has been given the opportunity to register their agreement or disagreement to this retraction. We have kept a record of any response received.

References

[1] X. Qi, X. Lv, X. Wang et al., "A New Survival Model Based on Cholesterol Biosynthesis-Related Genes for Prognostic Prediction in Clear Cell Renal Cell Carcinoma," *BioMed Research International*, vol. 2021, Article ID 9972968, 15 pages, 2021.

Hindawi
BioMed Research International
Volume 2024, Article ID 9834610, 1 page
https://doi.org/10.1155/2024/9834610

Retraction

Retracted: Trophinin Is an Important Biomarker and Prognostic Factor in Osteosarcoma: Data Mining from Oncomine and the Cancer Genome Atlas Databases

BioMed Research International

Received 12 March 2024; Accepted 12 March 2024; Published 20 March 2024

This article has been retracted by Hindawi following an investigation undertaken by the publisher [1]. This investigation has uncovered evidence of one or more of the following indicators of systematic manipulation of the publication process:

(1) Discrepancies in scope

(2) Discrepancies in the description of the research reported

(3) Discrepancies between the availability of data and the research described

(4) Inappropriate citations

(5) Incoherent, meaningless and/or irrelevant content included in the article

(6) Manipulated or compromised peer review

The presence of these indicators undermines our confidence in the integrity of the article's content and we cannot, therefore, vouch for its reliability. Please note that this notice is intended solely to alert readers that the content of this article is unreliable. We have not investigated whether authors were aware of or involved in the systematic manipulation of the publication process.

Wiley and Hindawi regrets that the usual quality checks did not identify these issues before publication and have since put additional measures in place to safeguard research integrity.

We wish to credit our own Research Integrity and Research Publishing teams and anonymous and named external researchers and research integrity experts for contributing to this investigation.

The corresponding author, as the representative of all authors, has been given the opportunity to register their agreement or disagreement to this retraction. We have kept a record of any response received.

References

[1] P. Cai, Y. Lu, Z. Yin, X. Wang, X. Zhou, and Z. Li, "Trophinin Is an Important Biomarker and Prognostic Factor in Osteosarcoma: Data Mining from Oncomine and the Cancer Genome Atlas Databases," *BioMed Research International*, vol. 2021, Article ID 6885897, 9 pages, 2021.

Hindawi
BioMed Research International
Volume 2024, Article ID 9826076, 1 page
https://doi.org/10.1155/2024/9826076

Retraction

Retracted: Nomogram for Predicting Deep Venous Thrombosis in Lower Extremity Fractures

BioMed Research International

Received 12 March 2024; Accepted 12 March 2024; Published 20 March 2024

This article has been retracted by Hindawi following an investigation undertaken by the publisher [1]. This investigation has uncovered evidence of one or more of the following indicators of systematic manipulation of the publication process:

(1) Discrepancies in scope

(2) Discrepancies in the description of the research reported

(3) Discrepancies between the availability of data and the research described

(4) Inappropriate citations

(5) Incoherent, meaningless and/or irrelevant content included in the article

(6) Manipulated or compromised peer review

The presence of these indicators undermines our confidence in the integrity of the article's content and we cannot, therefore, vouch for its reliability. Please note that this notice is intended solely to alert readers that the content of this article is unreliable. We have not investigated whether authors were aware of or involved in the systematic manipulation of the publication process.

Wiley and Hindawi regrets that the usual quality checks did not identify these issues before publication and have since put additional measures in place to safeguard research integrity.

We wish to credit our own Research Integrity and Research Publishing teams and anonymous and named external researchers and research integrity experts for contributing to this investigation.

The corresponding author, as the representative of all authors, has been given the opportunity to register their agreement or disagreement to this retraction. We have kept a record of any response received.

References

[1] Z. Lin, B. Mi, X. Liu et al., "Nomogram for Predicting Deep Venous Thrombosis in Lower Extremity Fractures," *BioMed Research International*, vol. 2021, Article ID 9930524, 8 pages, 2021.

Hindawi
BioMed Research International
Volume 2024, Article ID 9820387, 1 page
https://doi.org/10.1155/2024/9820387

Retraction

Retracted: The Effect on the Fracture Healing following Femoral Neck Shortening after Osteoporotic Femoral Neck Fracture Treated with Internal Fixation: Finite Element Analysis

BioMed Research International

Received 12 March 2024; Accepted 12 March 2024; Published 20 March 2024

This article has been retracted by Hindawi following an investigation undertaken by the publisher [1]. This investigation has uncovered evidence of one or more of the following indicators of systematic manipulation of the publication process:

(1) Discrepancies in scope

(2) Discrepancies in the description of the research reported

(3) Discrepancies between the availability of data and the research described

(4) Inappropriate citations

(5) Incoherent, meaningless and/or irrelevant content included in the article

(6) Manipulated or compromised peer review

The presence of these indicators undermines our confidence in the integrity of the article's content and we cannot, therefore, vouch for its reliability. Please note that this notice is intended solely to alert readers that the content of this article is unreliable. We have not investigated whether authors were aware of or involved in the systematic manipulation of the publication process.

Wiley and Hindawi regrets that the usual quality checks did not identify these issues before publication and have since put additional measures in place to safeguard research integrity.

We wish to credit our own Research Integrity and Research Publishing teams and anonymous and named external researchers and research integrity experts for contributing to this investigation.

The corresponding author, as the representative of all authors, has been given the opportunity to register their agreement or disagreement to this retraction. We have kept a record of any response received.

References

[1] X. Yu, P.-z. Rong, Q.-j. Pang, X.-j. Chen, L. Shi, and C.-h. Wang, "The Effect on the Fracture Healing following Femoral Neck Shortening after Osteoporotic Femoral Neck Fracture Treated with Internal Fixation: Finite Element Analysis," *BioMed Research International*, vol. 2021, Article ID 3490881, 7 pages, 2021.

Hindawi
BioMed Research International
Volume 2024, Article ID 9817540, 1 page
https://doi.org/10.1155/2024/9817540

Retraction

Retracted: Establishing and Validating an Aging-Related Prognostic Four-Gene Signature in Colon Adenocarcinoma

BioMed Research International

Received 12 March 2024; Accepted 12 March 2024; Published 20 March 2024

This article has been retracted by Hindawi following an investigation undertaken by the publisher [1]. This investigation has uncovered evidence of one or more of the following indicators of systematic manipulation of the publication process:

(1) Discrepancies in scope

(2) Discrepancies in the description of the research reported

(3) Discrepancies between the availability of data and the research described

(4) Inappropriate citations

(5) Incoherent, meaningless and/or irrelevant content included in the article

(6) Manipulated or compromised peer review

The presence of these indicators undermines our confidence in the integrity of the article's content and we cannot, therefore, vouch for its reliability. Please note that this notice is intended solely to alert readers that the content of this article is unreliable. We have not investigated whether authors were aware of or involved in the systematic manipulation of the publication process.

Wiley and Hindawi regrets that the usual quality checks did not identify these issues before publication and have since put additional measures in place to safeguard research integrity.

We wish to credit our own Research Integrity and Research Publishing teams and anonymous and named external researchers and research integrity experts for contributing to this investigation.

The corresponding author, as the representative of all authors, has been given the opportunity to register their agreement or disagreement to this retraction. We have kept a record of any response received.

References

[1] L. Zheng, Y. Yang, and X. Cui, "Establishing and Validating an Aging-Related Prognostic Four-Gene Signature in Colon Adenocarcinoma," *BioMed Research International*, vol. 2021, Article ID 4682589, 17 pages, 2021.

Hindawi
BioMed Research International
Volume 2024, Article ID 9782859, 1 page
https://doi.org/10.1155/2024/9782859

Retraction

Retracted: Increased EHHADH Expression Predicting Poor Survival of Osteosarcoma by Integrating Weighted Gene Coexpression Network Analysis and Experimental Validation

BioMed Research International

Received 12 March 2024; Accepted 12 March 2024; Published 20 March 2024

This article has been retracted by Hindawi following an investigation undertaken by the publisher [1]. This investigation has uncovered evidence of one or more of the following indicators of systematic manipulation of the publication process:

(1) Discrepancies in scope

(2) Discrepancies in the description of the research reported

(3) Discrepancies between the availability of data and the research described

(4) Inappropriate citations

(5) Incoherent, meaningless and/or irrelevant content included in the article

(6) Manipulated or compromised peer review

The presence of these indicators undermines our confidence in the integrity of the article's content and we cannot, therefore, vouch for its reliability. Please note that this notice is intended solely to alert readers that the content of this article is unreliable. We have not investigated whether authors were aware of or involved in the systematic manipulation of the publication process.

Wiley and Hindawi regrets that the usual quality checks did not identify these issues before publication and have since put additional measures in place to safeguard research integrity.

We wish to credit our own Research Integrity and Research Publishing teams and anonymous and named external researchers and research integrity experts for contributing to this investigation.

The corresponding author, as the representative of all authors, has been given the opportunity to register their agreement or disagreement to this retraction. We have kept a record of any response received.

References

[1] J. Cui, G. Yi, J. Li, Y. Li, and D. Qian, "Increased EHHADH Expression Predicting Poor Survival of Osteosarcoma by Integrating Weighted Gene Coexpression Network Analysis and Experimental Validation," *BioMed Research International*, vol. 2021, Article ID 9917060, 13 pages, 2021.

Hindawi
BioMed Research International
Volume 2024, Article ID 9817540, 1 page
https://doi.org/10.1155/2024/9817540

Retraction

Retracted: Establishing and Validating an Aging-Related Prognostic Four-Gene Signature in Colon Adenocarcinoma

BioMed Research International

Received 12 March 2024; Accepted 12 March 2024; Published 20 March 2024

This article has been retracted by Hindawi following an investigation undertaken by the publisher [1]. This investigation has uncovered evidence of one or more of the following indicators of systematic manipulation of the publication process:

(1) Discrepancies in scope

(2) Discrepancies in the description of the research reported

(3) Discrepancies between the availability of data and the research described

(4) Inappropriate citations

(5) Incoherent, meaningless and/or irrelevant content included in the article

(6) Manipulated or compromised peer review

The presence of these indicators undermines our confidence in the integrity of the article's content and we cannot, therefore, vouch for its reliability. Please note that this notice is intended solely to alert readers that the content of this article is unreliable. We have not investigated whether authors were aware of or involved in the systematic manipulation of the publication process.

Wiley and Hindawi regrets that the usual quality checks did not identify these issues before publication and have since put additional measures in place to safeguard research integrity.

We wish to credit our own Research Integrity and Research Publishing teams and anonymous and named external researchers and research integrity experts for contributing to this investigation.

The corresponding author, as the representative of all authors, has been given the opportunity to register their agreement or disagreement to this retraction. We have kept a record of any response received.

References

[1] L. Zheng, Y. Yang, and X. Cui, "Establishing and Validating an Aging-Related Prognostic Four-Gene Signature in Colon Adenocarcinoma," *BioMed Research International*, vol. 2021, Article ID 4682589, 17 pages, 2021.

Hindawi
BioMed Research International
Volume 2021, Article ID 4682589, 17 pages
https://doi.org/10.1155/2021/4682589

Research Article

Establishing and Validating an Aging-Related Prognostic Four-Gene Signature in Colon Adenocarcinoma

Lian Zheng,[1] **Yang Yang**,[2] **and Xiaorong Cui**[2]

[1]*Department of Gastroenterology, Third Affiliated Hospital (Jie'er Hospital), Chongqing Medical University, Chongqing, China*
[2]*Department of Geriatrics and Secret Service, First Affiliated Hospital, Army Medical University, Chongqing, China*

Correspondence should be addressed to Xiaorong Cui; snailtv@163.com

Received 6 June 2021; Revised 16 September 2021; Accepted 22 October 2021; Published 8 November 2021

Academic Editor: Irene Bottillo

Background. Aging is a process that biological changes accumulate with time and lead to increasing susceptibility to diseases like cancer. This study is aimed at establishing an aging-related prognostic signature in colon adenocarcinoma (COAD). *Methods*. The transcriptome data and clinical variables of COAD patients were downloaded from TCGA database. The genes in GOBP_AGING gene set was used for prognostic evaluation by the univariate and multivariate Cox regression analyses. The model was presented by a nomogram and assessed by the Kaplan-Meier curves and calibration curves. The drug response and gene mutation were also performed to implicate the clinical significance. The GO and KEGG analyses were employed to unravel the potential functional mechanism. *Results*. The Gene Set Enrichment Analysis result indicates that GOBP_AGING pathway is significantly enriched in COAD samples. Four aging-related genes are finally used to construct the aging-related prognostic signature: FOXM1, PTH1R, KL, and CGAS. The COAD patients with high risk score have much shorter overall survival in both train cohort and test cohort. The nomogram is then assembled to predict 1-year, 3-year, and 5-year survival. Patients with high risk score have elevated infiltrating B cell naïve and attenuated cisplatin sensitivity. The mutation landscape shows that the TTN, FAT4, ZFHX4, APC, and OBSCN gene mutation are different between high risk score patients and low risk score patients. The differentially expressed genes between patients with high score and low score are enriched in B cell receptor signaling pathway. *Conclusion*. We constructed an aging-related signature in COAD patients, which can predict oncological outcome and optimize therapeutic strategy.

1. Introduction

Colorectal adenocarcinoma is the third most commonly diagnosed malignancy and the second leading cause of cancer-specific death worldwide [1]. Colon adenocarcinoma (COAD) is the main subtype of colorectal adenocarcinoma and the dominative pathological subtype colon cancer, accounting for over 90% colon cancer [2]. Although increasing therapeutic advancements in the past decades, the survival of COAD patients is still far from satisfactory since the initial diagnosis is usually delayed [3]. Besides, COAD is characterized by rapid progression and metastasis, which may cause worse prognosis [4]. Recently, some studies have shown that the variation of gene expression occurs during colon carcinogenesis and progression. Nevertheless, precise genetic alteration accounting for the initiation and development of COAD is poorly understood [5]. Therefore, establishment of gene signatures can help to develop clinical therapeutic strategies to improve patient prognosis.

Aging is a process that biological changes accumulate with time and lead to increasing susceptibility to diseases like cancer. The incidence of colon cancer is elevated by age, which may result from cumulative impact of long-term carcinogen exposure and gene mutation [6]. The *in vivo* research reports that aged colonic mucosa is more sensitive to carcinogen by stimulating higher ornithine decarboxylase and tyrosine kinase activities [7]. However, on the other hand, the activation of some molecule like transcription factor Nrf2 can prevent increasing oxidative stress in aging but also promote colon cancer chemoresistance and radioresistance [8]. In this study, we first explore the association between aging gene set and COAD. Then, the aging-

related prognostic signature is constructed by multivariate Cox regression. A prediction model is established to predict oncological outcome, chemosensitivity, and immune cell infiltration of COAD patients. A further functional evaluation under differential aging risk scores is performed to unravel underlying mechanism.

2. Materials and Methods

2.1. Data Procession. Transcriptome profiles and clinical metadata of COAD patients were retrieved from TCGA database (https://portal.gdc.cancer.gov/). Gene set "GOBP_AGING" was searched and downloaded from the Gene Set Enrichment Analysis- (GSEA-) MSigDB database (https://www.gsea-msigdb.org/gsea/msigdb). All the data was processed by R program version 4.0.0.

2.2. Exploration of the Aging Pathway. We sorted the transcriptional matrix and performed GSEA between normal tissues and tumor tissues by setting "GOBP_AGING" gene set as the enrichment pathway. Then, we extracted the expression of the aging-related genes in the pathway and separately performed differential expression analysis to find differentially expressed genes (DEGs) and univariate Cox regression to discover prognostic genes. Following this, we took an intersect of these two gene lists and got differentially expressed prognostic aging genes. The left aging genes were input to the String database to further explore their protein-protein interaction (PPI), and Pearson correlation test was performed to check the correlation of their expression and establish the correlation network.

2.3. Signature Construction. We firstly randomly split the COAD patients into training set and validation set at a ratio as 1 : 1. Then, we performed univariate Cox regression in training set to find the potential prognostic factors with $p < 0.05$ and carried out multivariate Cox regression to establish the prognostic signature in training group. Thus, each patient in both training set and validation set acquired a risk score according to the formula as follows: $\text{Riskscore} = \sum_{i=1}^{N}(\text{Exp}(i) \bullet \text{coef}(i))$; here, i represented the i th gene in the prognostic signature, $\text{Exp}(i)$ represented the expression value of i, and $\text{coef}(i)$ represented the coefficient of i in the signature.

2.4. Signature Verification and Immune Infiltration. Because the prognostic signature was constructed according to the data in training set, we set the medium value of risk score in training set as the cut-off to stratify patients in both training set and validation set. Then, log-rank survival analysis was performed, and the Kaplan-Meier-based survival curve was plotted to check the prognostic value of risk score. CIBERSORT algorithm was performed to emphasize the immune infiltration of each sample; then, we compared the infiltration between high-risk and low-risk patients to further investigate the differences in immunity.

2.5. Nomogram and Calibration Curves. Considering the effects of clinicopathological characteristics, we established a nomogram in the training group using age, gender, stage, and risk score. Then, this nomogram was examined in training set (internal cross-validation), validation set (external validation), and all patients (external validation). Notably, concordance index (C-index) was used to check the efficacy of this nomogram. The nomogram was assembled using R package "rms."

Table 1: Basic characteristics of COAD patients.

Covariates	Total ($n = 453$)	Train ($n = 228$)	Test ($n = 225$)
Age			
≤65	188 (41.5%)	86 (37.7%)	102 (45.3%)
>65	265 (58.5%)	142 (62.3%)	123 (54.7%)
Sex			
Female	214 (47.2%)	115 (50.4%)	99 (44.0%)
Male	239 (52.8%)	113 (49.6%)	126 (56.0%)
Stage			
Stages I and II	250 (55.2%)	133 (58.3%)	117 (52.0%)
Stages III and IV	192 (42.4%)	91 (39.9%)	101 (44.9%)
Unknown	11 (2.4%)	4 (1.8%)	7 (3.1%)
T			
T1-2	88 (19.4%)	53 (23.3%)	35 (15.6%)
T3-4	364 (80.3%)	174 (76.3%)	190 (84.4%)
Unknown	1 (0.2%)	1 (0.4%)	0 (0.0%)
M			
M0	332 (73.3%)	170 (74.6%)	162 (72.0%)
M1	64 (14.1%)	26 (11.4%)	38 (16.9%)
Unknown	57 (12.6%)	32 (14.0%)	25 (11.1%)
N			
N0	266 (58.7%)	139 (61.0%)	127 (56.4%)
N1-3	187 (41.3%)	89 (39.0%)	98 (43.6%)

2.6. DEGs, Mutation Atlas, and Drug Response between High- and Low-Risk Patients. DEGs between high- and low-risk patients were defined with the $|\text{logFC}| > 1$ and false discovery rate $(\text{FDR}) < 0.05$. Then, GO and KEGG enrichment analyses were performed to investigate the significant functions of these DEGs, and the PPI network was used to investigate the interaction and screen hub genes. Besides, the mutation atlas between high- and low-risk patients was explored, and the drug response to cisplatin and cyclopamine with the formation in half maximal inhibitory concentration (IC50) was predicted by the R package "pRRophetic," and finally, we compared the drug response between high- and low-risk patients to distinguish the potential beneficiaries to the chemotherapy [9].

2.7. Statistical Analysis. All the statistical analysis was processed by R program 4.0.0 and Statistical Product and Service Solutions version 24. In detail, the differential expression analysis was examined by R package "limma" [10]. The immune infiltration was emphasized by the R package "CIBERSORT" [11]. The difference between two survival curves was evaluated by log-rank test. The differences of

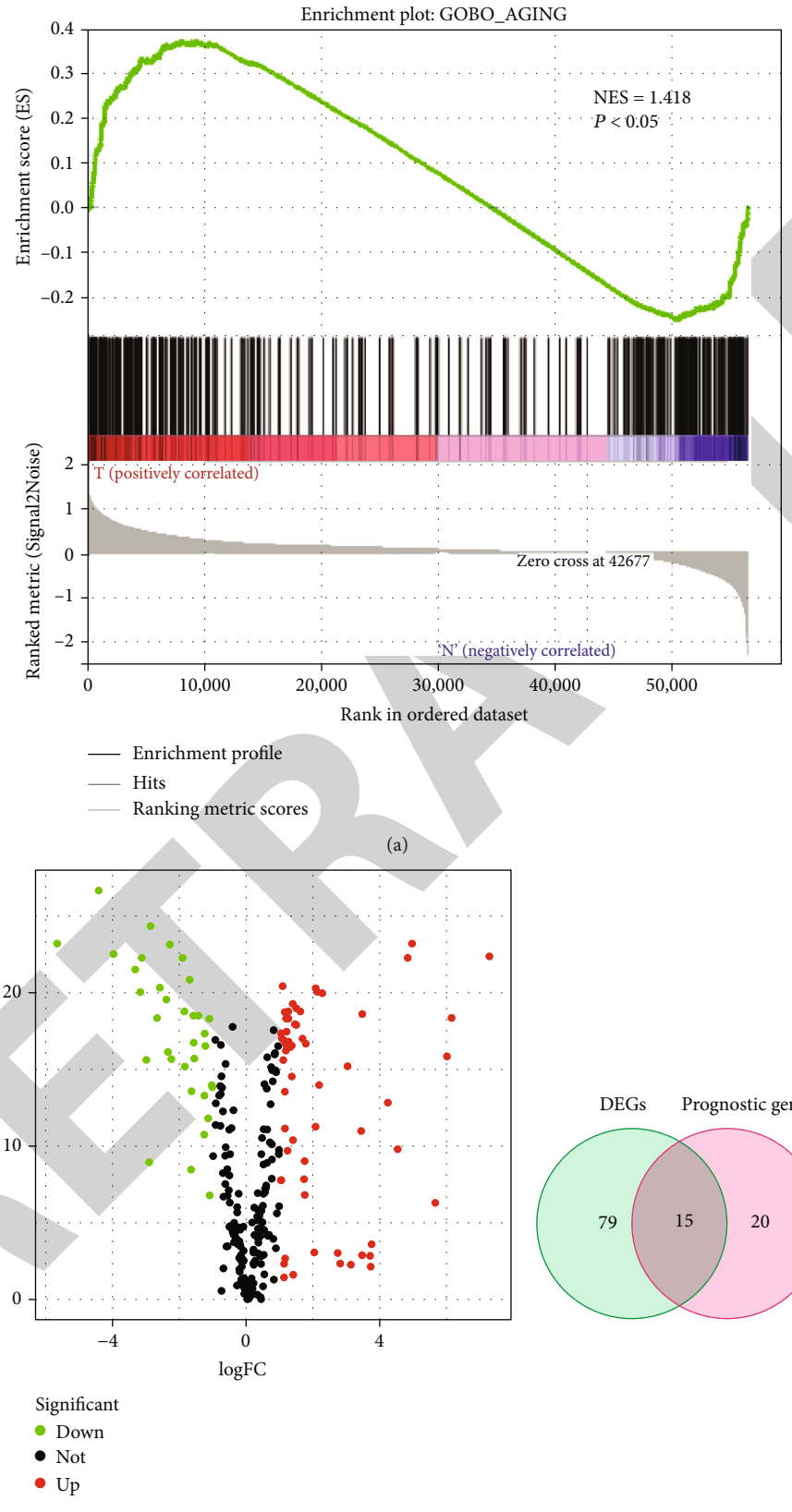

Figure 1: Continued.

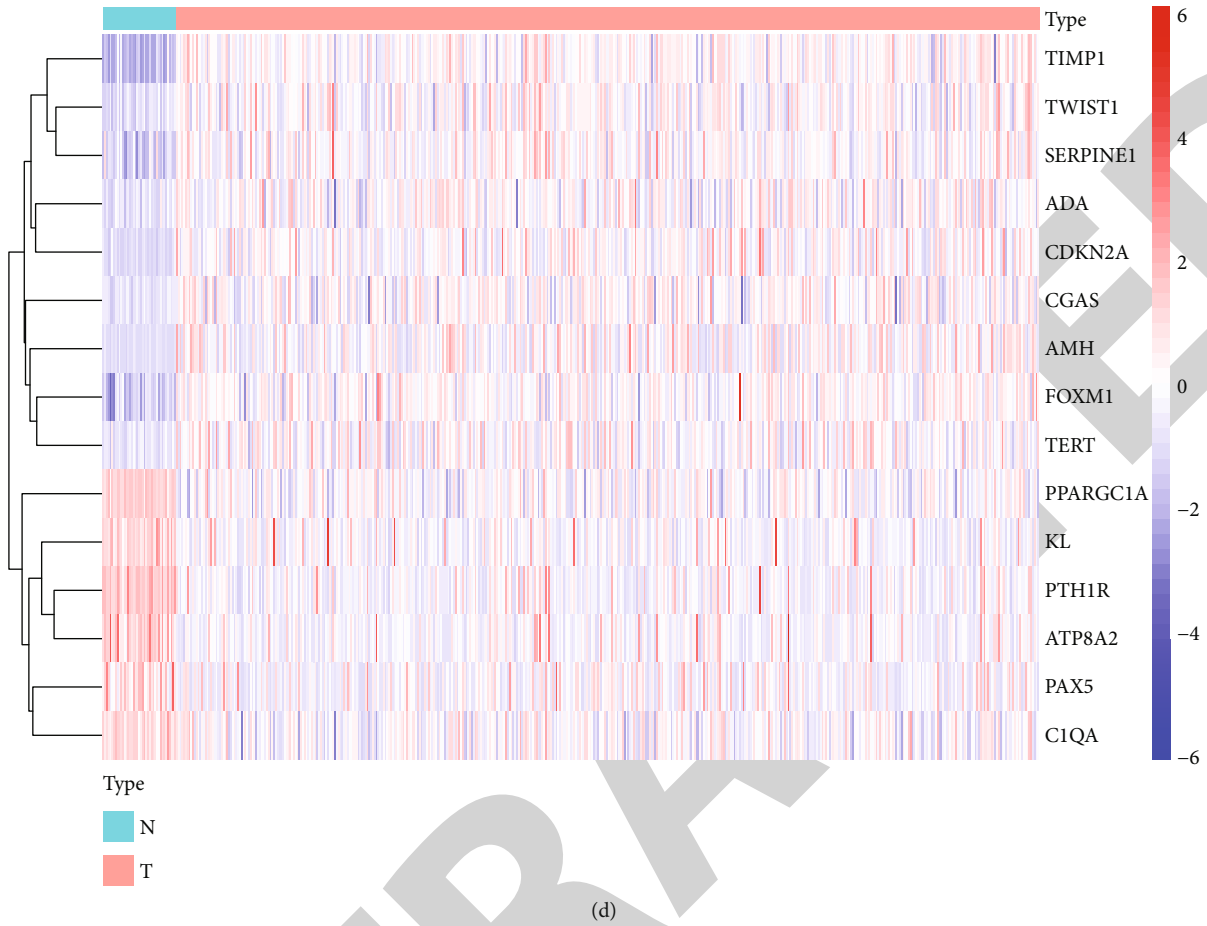

Figure 1: Evaluation of aging genes in colon cancer. (a) Gene Set Enrichment Analysis for colon cancer using GOBP_AGING gene set. (b) Volcano plot for aging genes in colon cancer. (c) Venn plot for differentially expressed aging genes and prognostic genes. (d) Heatmap for aging genes with prognostic value.

infiltrating immune cells and drug sensitivity between high-risk and low-risk patients were assessed by Wilcoxon rank-sum test when a nonnormal distribution was shown; otherwise, the t test or separate variance estimation t test was applied according to the equality of variances. The p value less than 0.05 was considered significant difference.

3. Results

3.1. Identification of Aging-Related Prognostic Signature. A total of 453 COAD patients from TCGA database are included in the study. The year of initial pathological diagnosis ranged from 1998 to 2013. (Table 1 shows the basic characteristics of the patients: age, sex, stage, tumor stage, regional lymph node status, and distant metastasis. The patients are randomly divided into train cohort ($n = 228$) and test cohort ($n = 225$). We use the train cohort to identify the signature. First, the GSEA result indicates that GOBP_AGING pathway is significantly enriched in COAD samples compared with normal colon tissue (Figure 1(a)). The results indicate that the aging genes in the GOBP_AGING pathway participant in the initiation of colon adenocarcinoma. We explore the expression pattern of individual genes in GOBP_AGING pathway (Figure 1(b)). There are 33 significantly downregulated genes and 61 upregulated genes in tumor samples. Among the differentially expressed genes, 15 genes have prognostic value for overall survival of COAD patients with log-rank test p value less than 0.05 (Figure 1(c)). Nine genes are downregulated (TMP1, TWIST1, SERPINE1, ADA, CDKN2A, CGAS, AMH, FOXM1, and TERT), and six genes are upregulated (PPARGC1A, KL, PTH1R, ATP8A2, PAX5, and C1QA) (Figure 1(d)).

Univariate Cox analysis shows that 6 genes can predict overall survival in COAD patients: FOXM1, PTH1R, PAX5, KL, CGAS, and ATP8A2 (Figure 2(a)). We performed multivariate Cox regression analysis to identify the independent predictor. Then, the aging-related prognostic signature is constructed by four genes: FOXM1, PTH1R, KL, and CGAS (Table 2). Figures 2(b) and 2(d) show the distribution of risk score in train cohort and test cohort, respectively. COAD patients with high risk score have much lower overall survival rate than the patients with low risk score in both train cohort ($p = 0.006$) and test cohort ($p = 0.013$) (Figures 2(c) and 2(e)). Highly enriched aging genes may impair the survival of COAD patients.

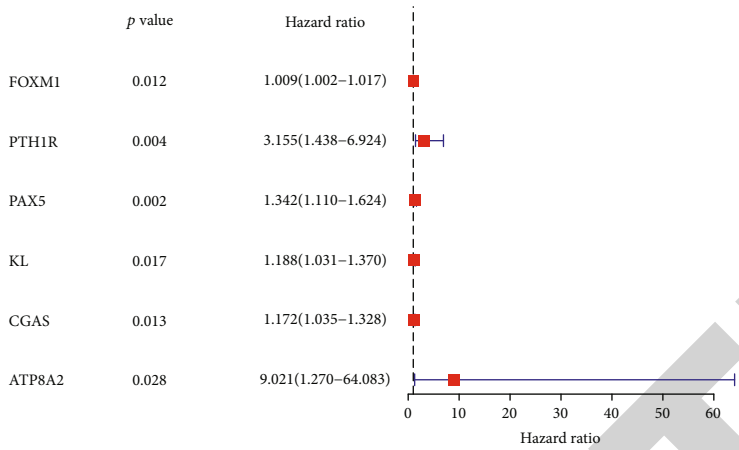

(a)

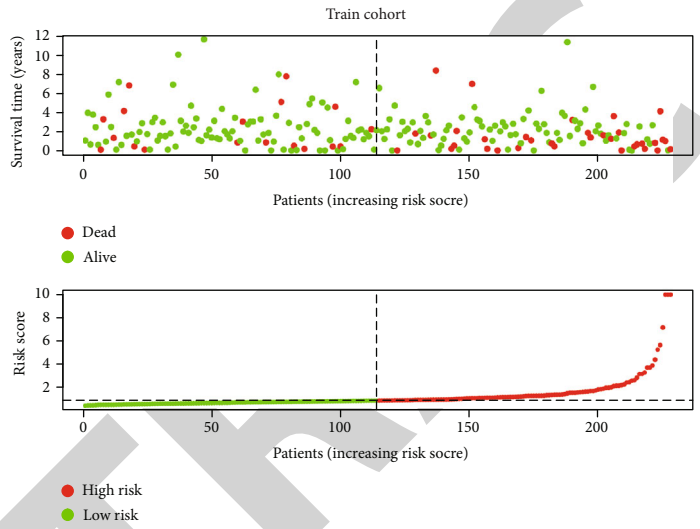

(b)

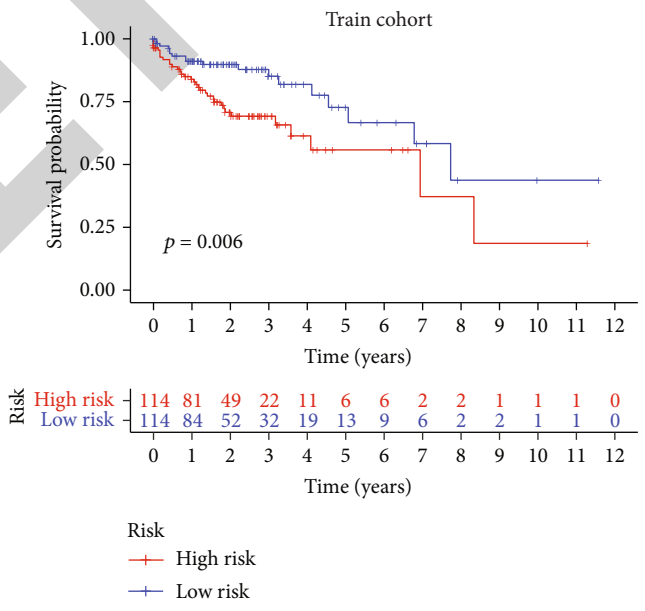

(c)

Figure 2: Continued.

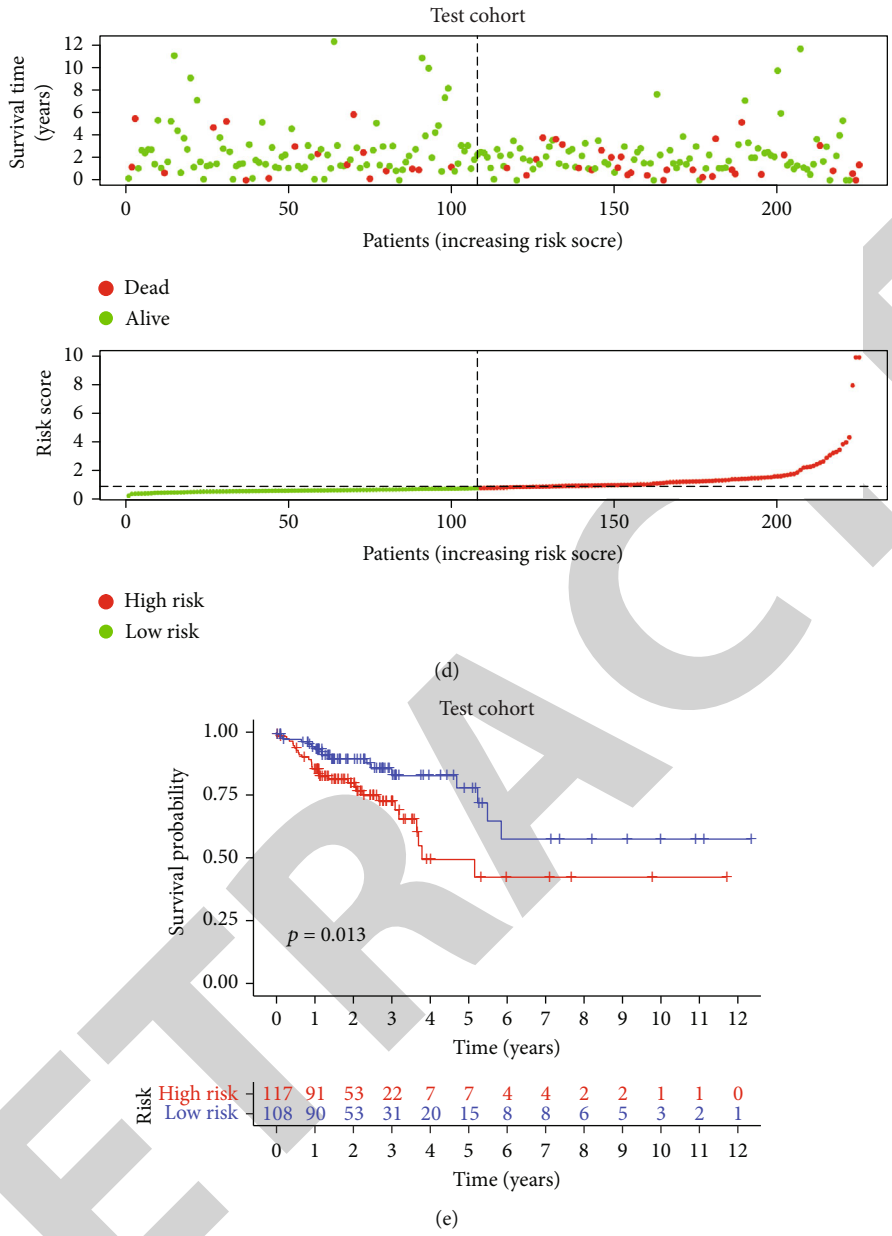

Figure 2: Identification of aging-related prognostic signature. (a) Univariate Cox analysis for significant aging genes. The distribution of risk scores and survival status of colon cancer patients with different risk scores in (b) train cohort and (d) test cohort. The survival curves for patients with high risk score and low risk score in (c) train cohort and (e) test cohort.

A nomogram is then established using the signature, age, and stage to predict 1-year survival, 3-year survival, and 5-year survival of COAD patients (Figure 3(a)). The calibration curves for train cohort, test cohort, and all patients show that the nomogram can effectively forecast the actual survival probability (Figures 3(b)–3(d)). These results identify an aging-related prognostic signature consisted of 4 genes that can be used to perform prognostic prediction.

3.2. Clinical Implication for the Aging-Related Prognostic Signature. We apply the CIBERSORT algorithm to estimate 22 types of infiltrating immune cells. The significant

Table 2: Components of aging-related prognostic signature.

Gene symbol	Coefficient	HR	95% CI	*p* value
FOXM1	0.010	1.010	1.003-1.018	0.007
PTH1R	1.445	4.243	1.321-13.630	0.015
PAX5	0.333	1.396	0.980-1.987	0.064
KL	0.174	1.190	1.029-1.377	0.019
CGAS	0.181	1.198	1.051-1.366	0.007
ATP8A2	-2.94	0.053	0.001-2.745	0.145

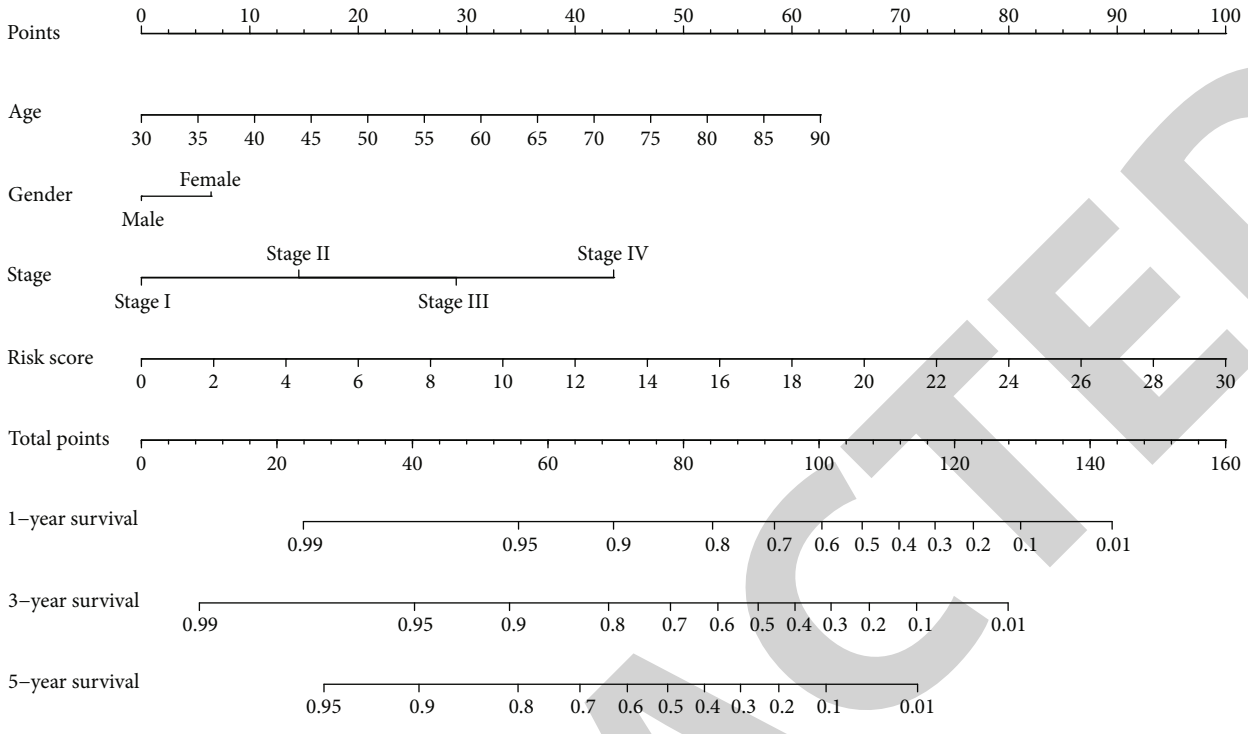

(a)

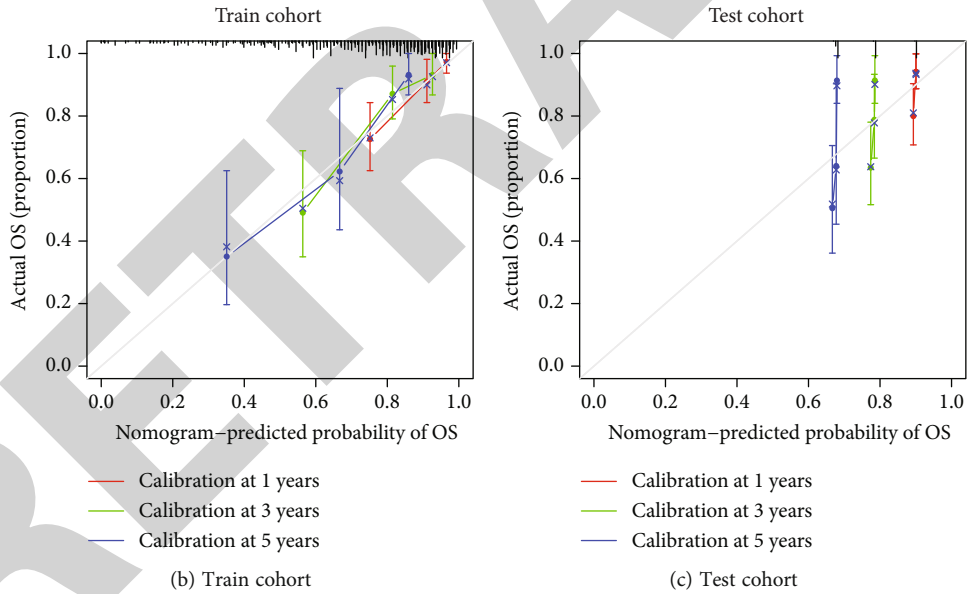

(b) Train cohort

(c) Test cohort

Figure 3: Continued.

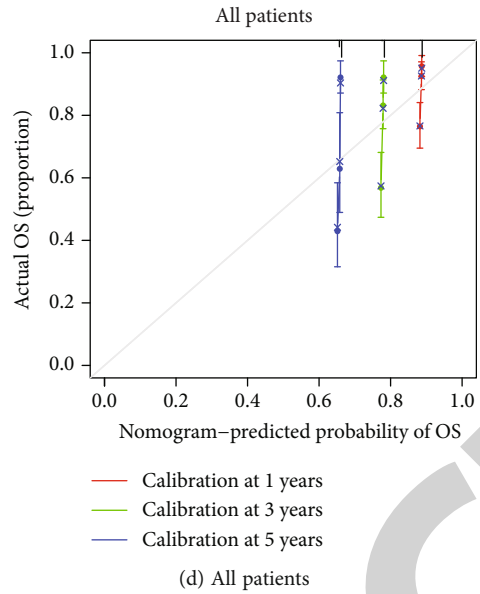

Figure 3: Establishment of an aging-related prognostic model to predict overall survival in colon cancer patients. (a) The nomogram presenting the aging-related prognostic model. The calibration curves in train cohort, test cohort, and all patients.

estimation with p value less than 0.05 is used for further analysis. The infiltrating immune cell profile is illustrated in Figure 4(a). COAD patients with high aging-related risk have higher infiltration level of B cell naïve ($p = 0.010$), T cell CD8 ($p = 0.010$), and T cell regulatory ($p = 0.045$), but lower infiltration level of B cell memory ($p = 0.017$), macrophage M0 ($p = 0.043$), and mast cells activated ($p = 0.027$) (Figures 4(b)–4(g)).

Chemotherapy is the main treatment for COAD patients. We evaluate the relationship between the aging-related prognostic signature and drug sensitivity (Figures 5(a)–5(c)). Patients with lower risk score are more sensitive to cisplatin ($p < 0.001$) and cyclopamine ($p = 0.011$), rather than paclitaxel ($p = 0.31$). The result indicates that patients with low risk score may have longer survival receiving cisplatin or cyclopamine treatments.

We also evaluate the gene mutation status in high-risk patients and low-risk patients (Figures 5(d) and 5(e)). Patients with high risk score have much higher mutation rate of TTN (53% vs. 45%), FAT4 (26% vs. 21%), and ZFHX4 (24% vs. 19%), but lower mutation rate of APC (72% vs. 77%) and OBSCN (18% vs. 23%) than patients with low risk score.

3.3. Functional Variance between High-Risk Patients and Low-Risk Patients. We investigate the differential expressed genes between high-risk patients and low-risk patients to unravel their functional variance. A total of 191 genes are significantly different between two groups (Figure 6(a)). Only one gene is downregulated. The GO analysis shows the gene participant in B cell-related biological process, such as B cell activation, B cell receptor signaling pathway, and B cell-mediated immunity (Figure 6(b)). The KEGG result indicates that the genes are enriched in pathways like PI3K −Akt signaling pathway and B cell receptor signaling pathway. These findings reveal that B cell-related molecule and pathways are highly activated in high score patients.

The PPI network is employed to depict the interaction profile and identify the hub genes (Figure 7). The top 5 hub genes are CD19, SNAP25, CD22, MS4A1, and CD79B, which play a central role in colon cancer initiation and development.

4. Discussion

In this research, we establish an aging-related prognostic signature consisting of four aging genes: FOXM1, PTH1R, KL, and CGAS. Among the four genes, FOXM1 and CGAS are highly expressed in COAD samples, while KL and PTH1R are downregulated during COAD initiation. In COAD patients, the elevated four genes all predict shorter survival. The aging-related prognostic signature can distinguish COAD patients with different overall survival in both train cohort and test cohort. The signature can also recognize the patients who are more sensitive to cisplatin and cyclopamine. The patients with high risk score have higher infiltrating B cell naïve and activating B cell-related pathways such as B cell activation and B cell receptor signaling pathway.

FOXM1 is a proliferation-related molecular belonging to the FOX transcription factor family. It widely participates in pathological process of tumor development, proliferation, invasion, metastasis, and chemoresistance [12, 13]. FOXM1 is repressed during human aging to cause mitotic decrease and aneuploidy, which further leads to aging-related disease [14]. In colon cancer, studies show that overexpression of FOXM1 is observed in tumor samples and dysregulated activation of FOXM1 promotes cancer growth and progression [15]. The aberrantly elevated expression of FOXM1 is

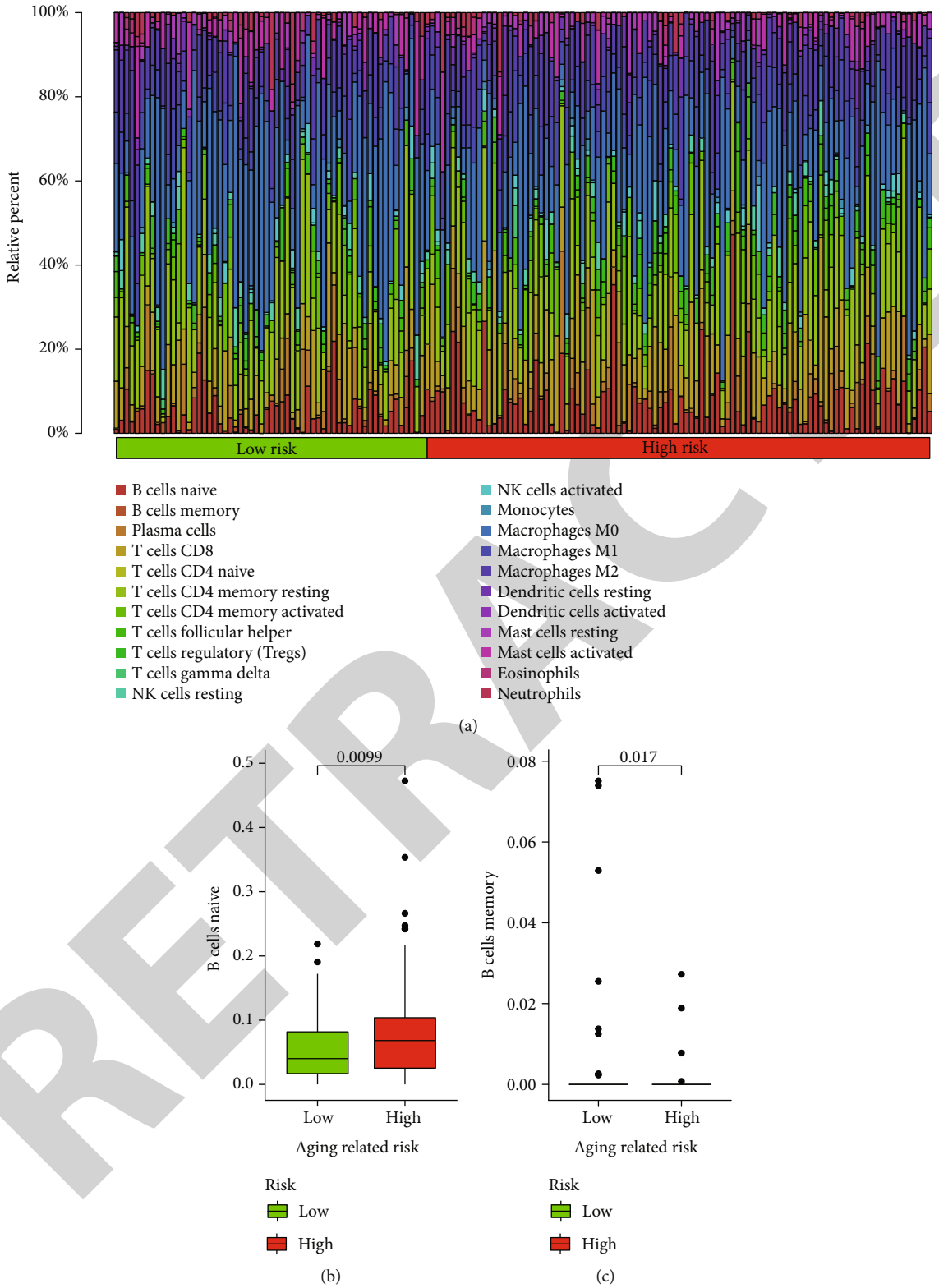

Figure 4: Continued.

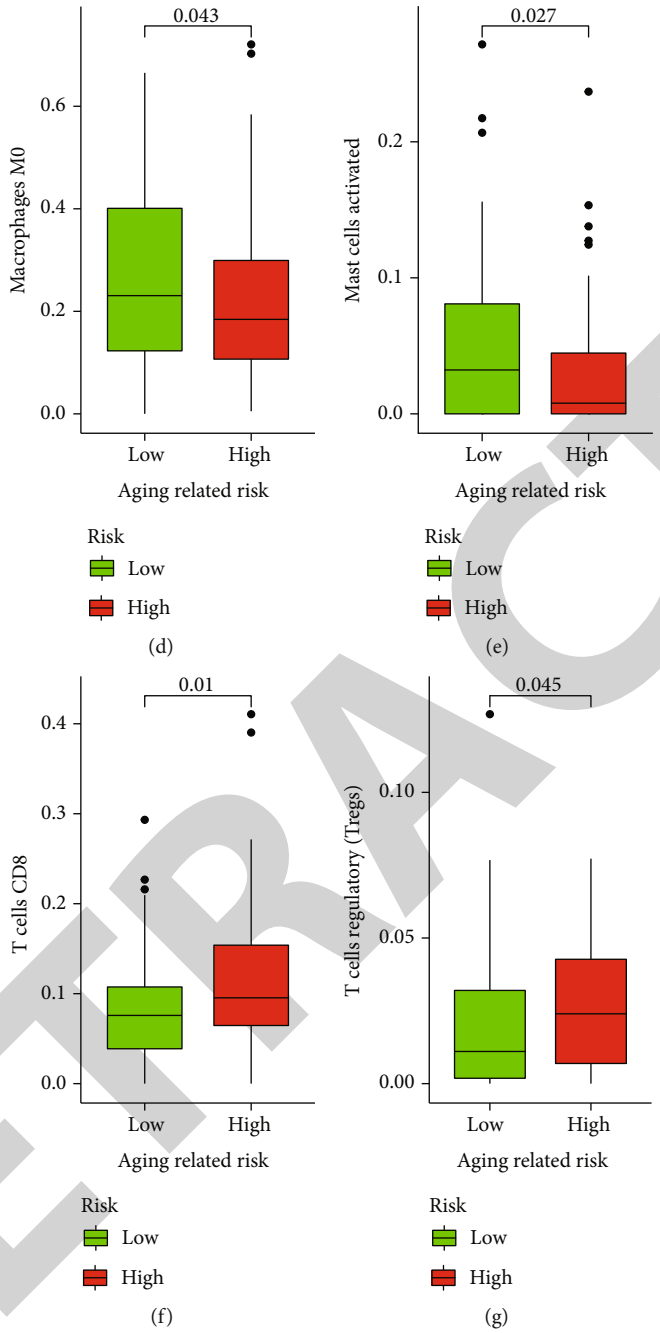

Figure 4: The differentially infiltrating immune cells in colon cancer patients with high risk score and low risk score. (a) Profile of infiltrating immune cells in colon cancer patients. Differentially infiltrating (a) B cell naïve, (c) B cell memory, (d) macrophage M0, (e) mast cells activated, (f) T cell CD8, and (g) T cell regulatory (Tregs) between high-risk patients and low-risk patients.

associated with poor survival of COAD patients [15, 16]. The cyclic GMP-AMP synthase (CGAS) is involved in aging by CGAS-STING signaling. During cell senescence, cytoplasmic DNA is accumulated through the CGAS-STING signaling to stimulate senescence-associated secretory phenotypes, which will cause downstream senescence responses [17, 18]. The CGAS can also sense cytoplasmic DNA escape from the nucleus due to DNA damage in cancer cells and prevent aberrant development of cells [19]. The deficiency of CGAS may lead to tumorigenesis. However, we found that the CGAS gene expression is much higher in COAD tumor samples compared to normal samples. The elevated CGAS expression is related to poor survival. The results may indicate that chronic inflammatory and aging accompanied by activating CGAS-STING signaling lead to the initiation of colon cancer. There may be a mechanism for cancer cell to escape the surveillance of CGAS-STING signaling.

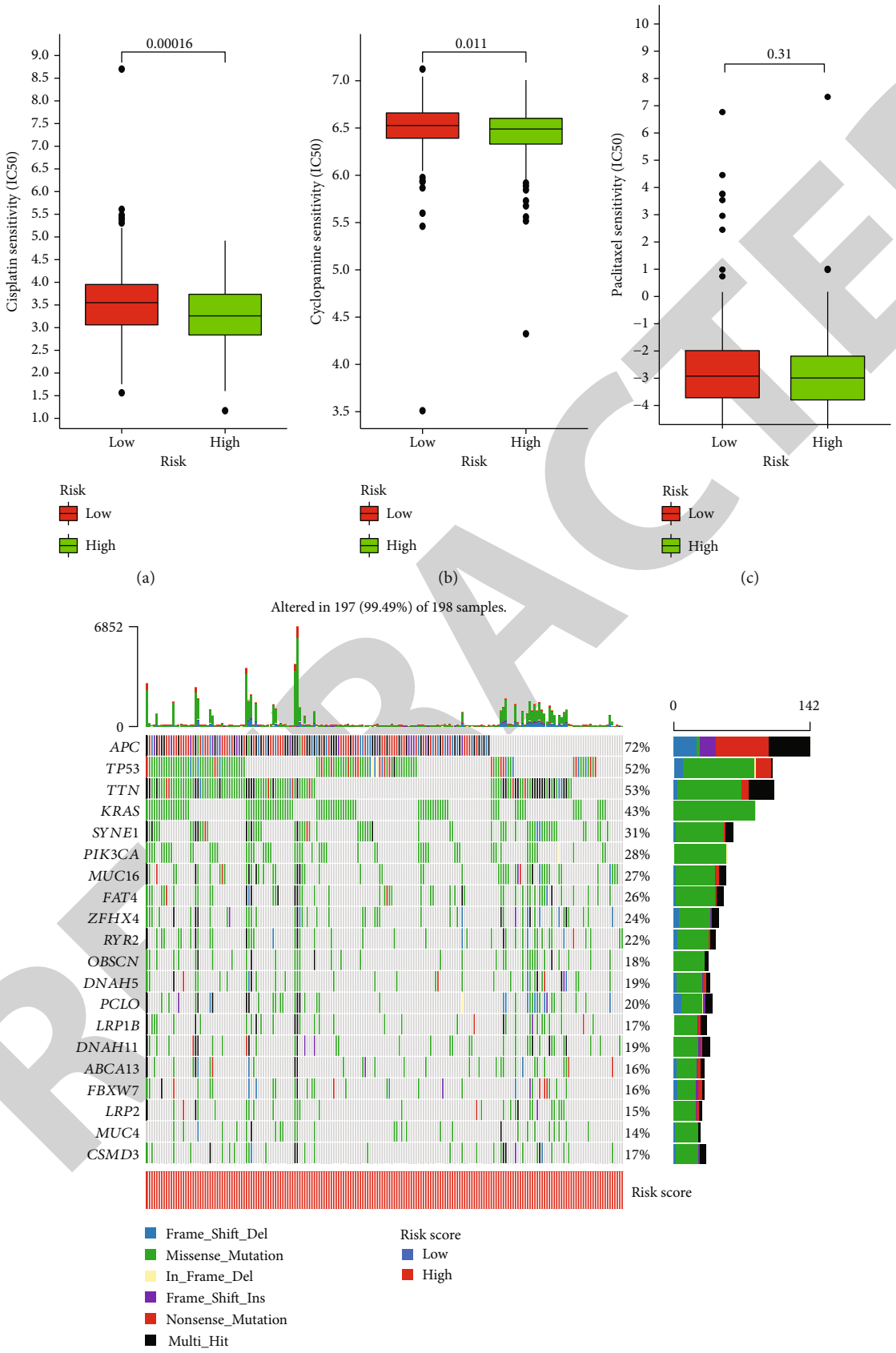

Figure 5: Continued.

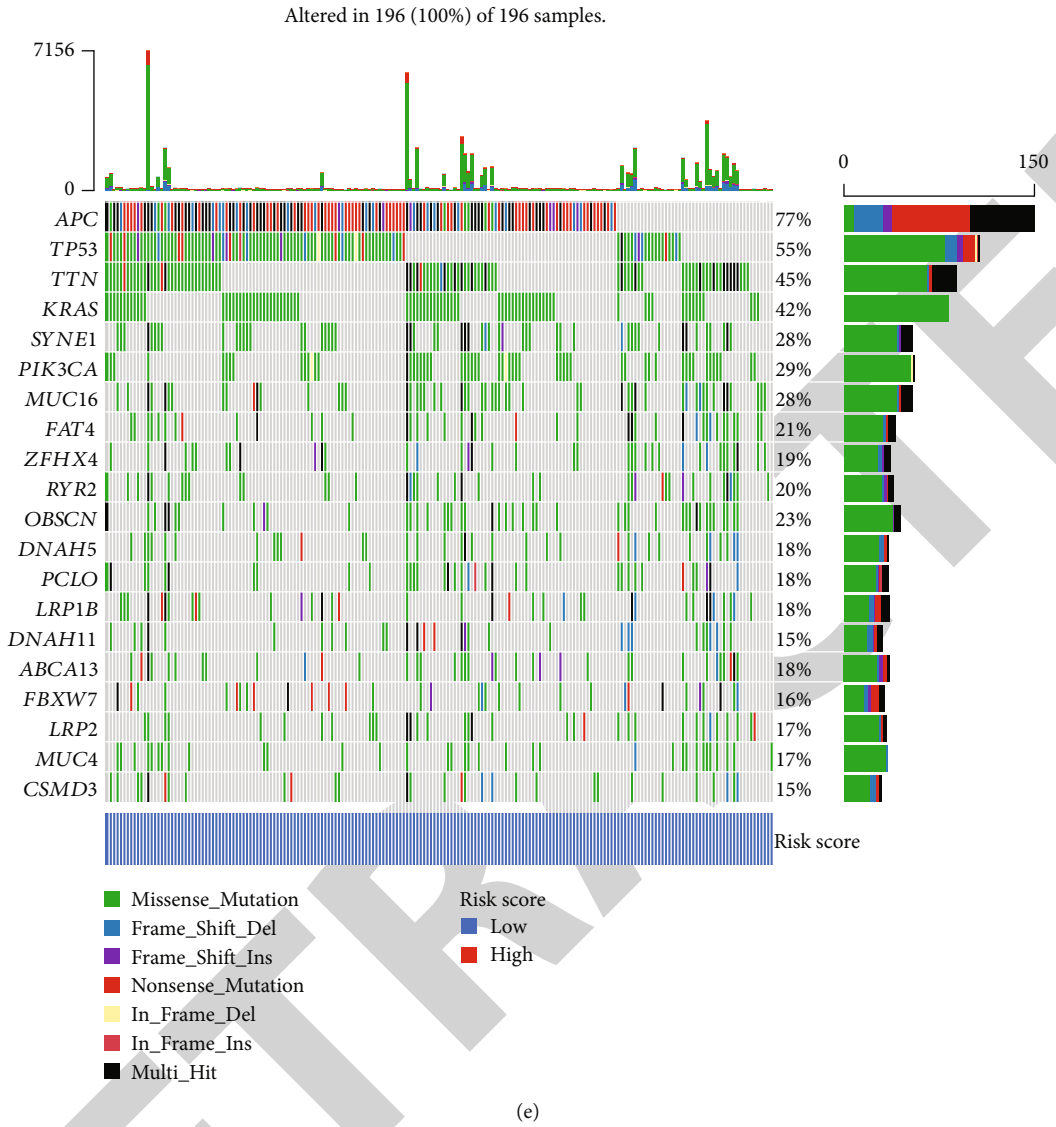

Figure 5: The sensitivity of high-risk patients and low-risk patients to (a) cisplatin, (b) cyclopamine, and (c) paclitaxel. Mutation frequency in (d) high-risk patients and (e) low-risk patients.

Hypercalcemia is reported as a critical factor associated with the progress and metastasis of malignancies [20, 21]. In colon cancer, slightly activated intracellular Ca^{2+} signaling can promote the initiation and development of colon cancer. But persistent Ca^{2+} influx and Ca^{2+} overload can lead to tumor cell death [22]. PTH1R is type 1 receptor of parathyroid hormone, regulating the serum concentrations of calcium and phosphate. Our study reveals that PTH1R is slightly reduced in COAD samples compared to normal samples. However, in COAD patients, higher PTH1R level is associated with poor prognosis. Liu and colleagues also suggested that PTH1R was correlated to miRNA and DNA methylation during liver metastasis of colorectal cancer [23]. The Klotho (KL) gene is also a key regulator during the aging process. The mice with overexpression KL gene have longer survival [24]. It is also identified as tumor suppressor gene in colon cancer. Rubinstein and colleagues found that KL can stimulate the unfolded protein response to inhibit colon cancer proliferation and viability [25]. Therefore, the aging signature that is constructed in our research can effectively predict the prognosis of COAD patients and participant in the pathological process of COAD.

Aging genes also regulate chemosensitivity of COAD patients. Our study reveals that the aging-related prognostic signature is associated with cisplatin sensitivity. Recent research shows that FOXM1, the direct target of miR-320, can diminish chemotherapy sensitivity with higher expression [26]. In addition, we identified the relationship between aging and B cell-related pathways in colon cancer. The patients with high risk score have upregulated B cell-related pathways. We speculate that the aging genes regulate tumor proliferation, invasion, metastasis, and chemosensitivity through remodeling B cell immunity. Further research needs to identify the role of B cell in aging-related colon cancer.

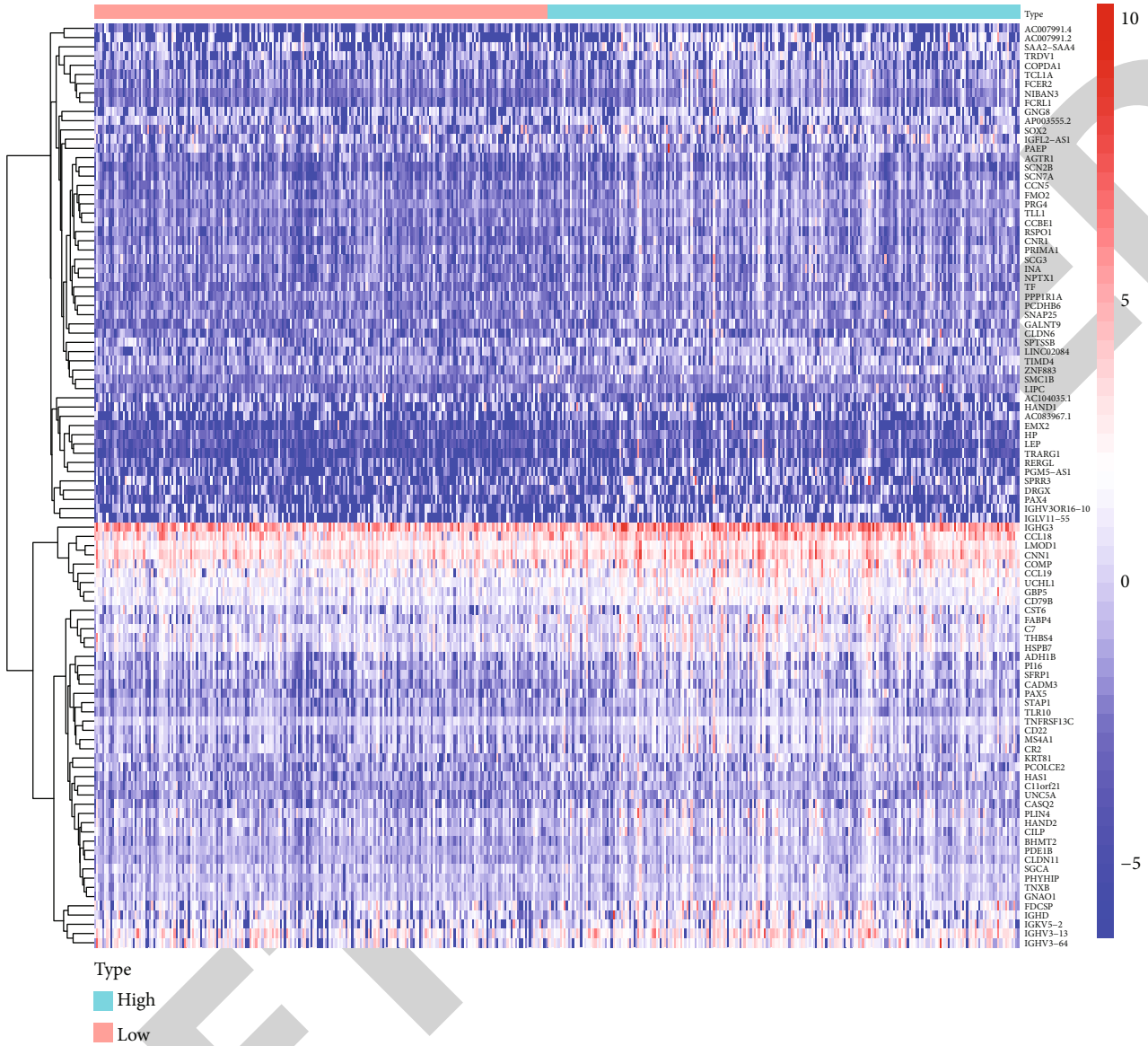

(a)

Figure 6: Continued.

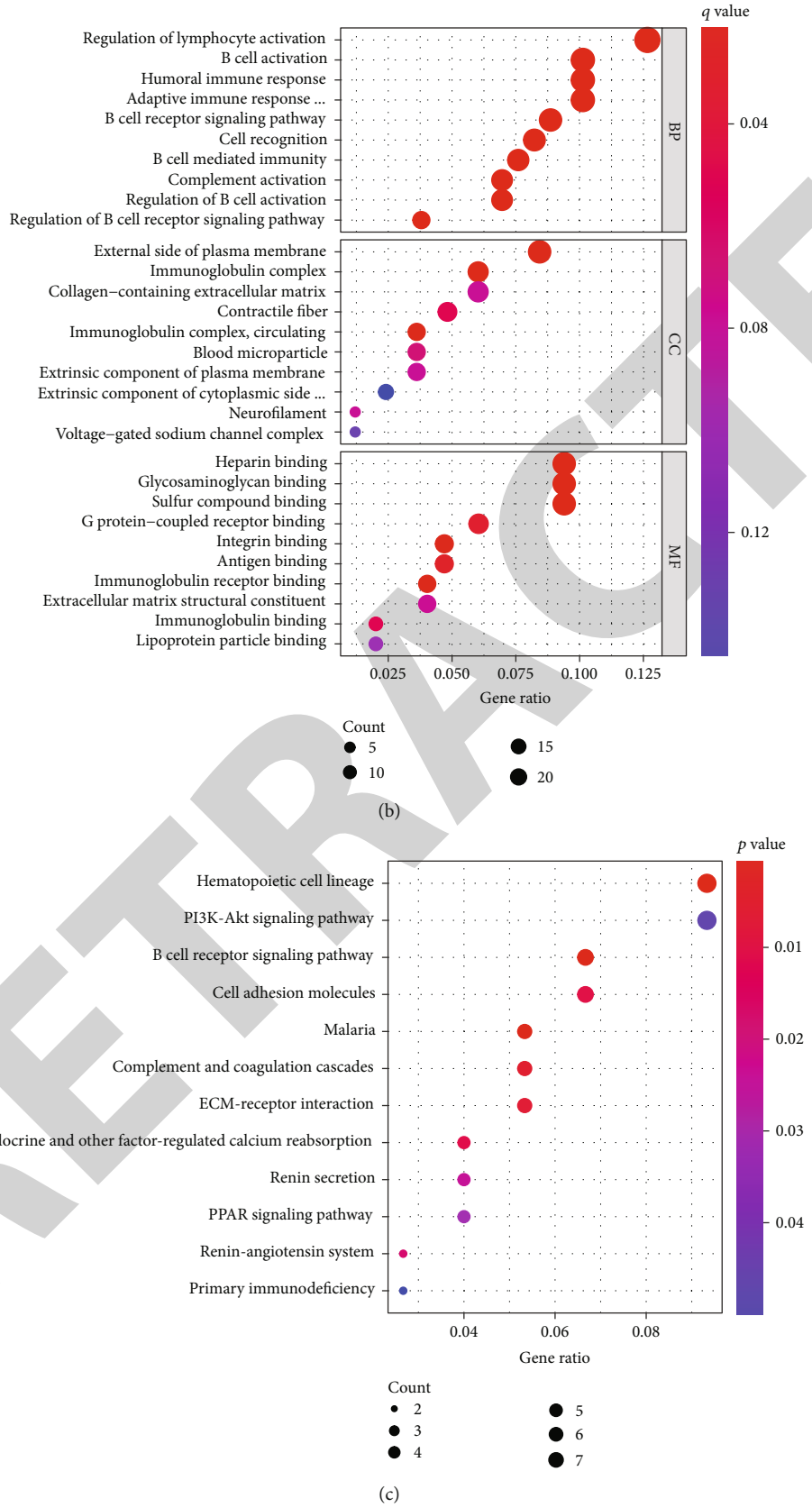

Figure 6: (a) Differentially expressed genes between high-risk patients and low-risk patients. (b) GO analysis and (c) KEGG analysis for differentially expressed genes.

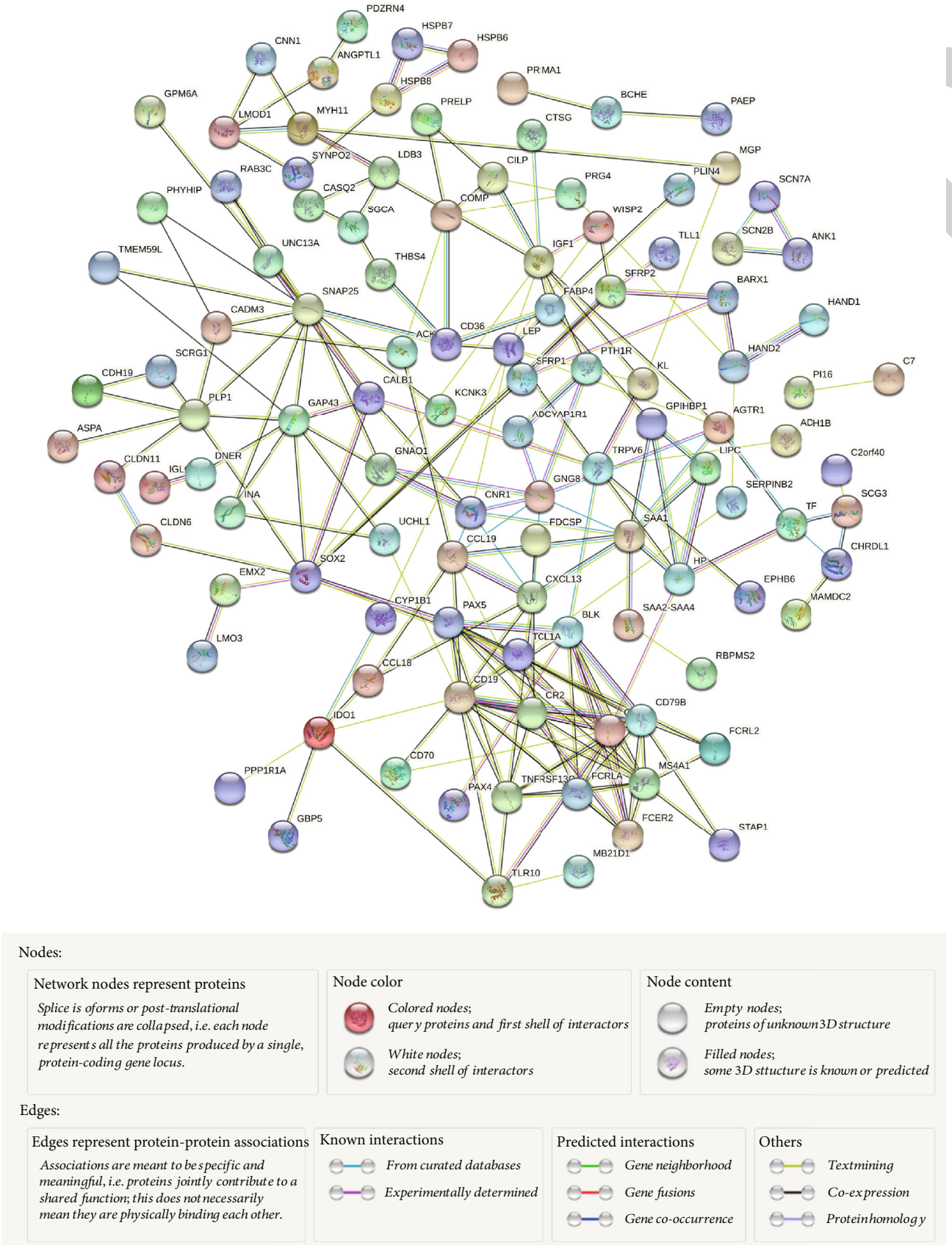

Figure 7: The protein-protein interaction network for differentially expressed genes.

5. Conclusions

In summary, we constructed an aging-related signature in COAD patients, which can predict oncological outcome and optimize therapeutic strategy.

Data Availability

All original data that supports the findings of the research can be available from the corresponding author upon reasonable request.

Conflicts of Interest

The authors declare that there is no conflict of interest.

Authors' Contributions

Lian Zheng and Yang Yang contributed equally to this work.

Acknowledgments

We thank Dr. Xiaoni Zhong for the instruction of statistical methods.

References

[1] F. Bray, J. Ferlay, I. Soerjomataram, R. L. Siegel, L. A. Torre, and A. Jemal, "Global cancer statistics 2018: GLOBOCAN estimates of incidence and mortality worldwide for 36 cancers in 185 countries," *CA: a Cancer Journal for Clinicians*, vol. 68, no. 6, pp. 394–424, 2018.

[2] M. K. Washington, "Colorectal carcinoma: selected issues in pathologic examination and staging and determination of prognostic factors," *Archives of Pathology & Laboratory Medicine*, vol. 132, no. 10, pp. 1600–1607, 2008.

[3] M. De Rosa, U. Pace, D. Rega et al., "Genetics, diagnosis and management of colorectal cancer (review)," *Oncology Reports*, vol. 34, no. 3, pp. 1087–1096, 2015.

[4] C. C. Compton, "Colorectal carcinoma: diagnostic, prognostic, and molecular features," *Modern Pathology*, vol. 16, no. 4, pp. 376–388, 2003.

[5] X. Wang, J. Fan, F. Yu et al., "Decreased MALL expression negatively impacts colorectal cancer patient survival," *Oncotarget*, vol. 7, no. 16, pp. 22911–22927, 2016.

[6] R. Jaszewski, M. N. Ehrinpreis, and A. P. Majumdar, "Aging and cancer of the stomach and colon," *Frontiers in Bioscience: a Journal and Virtual Library*, vol. 4, no. 1-3, pp. D322–D328, 1999.

[7] J. P. Issa, Y. L. Ottaviano, P. Celano, S. R. Hamilton, N. E. Davidson, and S. B. Baylin, "Methylation of the oestrogen receptor CpG island links ageing and neoplasia in human colon," *Nature Genetics*, vol. 7, no. 4, pp. 536–540, 1994.

[8] K. C. Cheng, R. J. Lin, J. Y. Cheng et al., "FAM129B, an antioxidative protein, reduces chemosensitivity by competing with Nrf2 for Keap1 binding," *eBioMedicine*, vol. 45, pp. 25–38, 2019.

[9] P. Geeleher, N. Cox, and R. S. Huang, "pRRophetic: an R package for prediction of clinical chemotherapeutic response from tumor gene expression levels," *PLoS One*, vol. 9, no. 9, article e107468, 2014.

[10] M. E. Ritchie, B. Phipson, D. Wu et al., "limma powers differential expression analyses for RNA-sequencing and microarray studies," *Nucleic Acids Research*, vol. 43, no. 7, article e47, 2015.

[11] A. M. Newman, C. B. Steen, C. L. Liu et al., "Determining cell type abundance and expression from bulk tissues with digital cytometry," *Nature Biotechnology*, vol. 37, no. 7, pp. 773–782, 2019.

[12] L. Bella, S. Zona, G. Nestal de Moraes, and E. W. Lam, "FOXM1: a key oncofoetal transcription factor in health and disease," *Seminars in Cancer Biology*, vol. 29, pp. 32–39, 2014.

[13] C. T. Karadedou, A. R. Gomes, J. Chen et al., "FOXO3a represses VEGF expression through FOXM1-dependent and -independent mechanisms in breast cancer," *Oncogene*, vol. 31, no. 14, pp. 1845–1858, 2012.

[14] J. C. Macedo, S. Vaz, B. Bakker et al., "FoxM1 repression during human aging leads to mitotic decline and aneuploidy-driven full senescence," *Nature Communications*, vol. 9, no. 1, 2018.

[15] D. Li, P. Wei, Z. Peng et al., "The critical role of dysregulated FOXM1-PLAUR signaling in human colon cancer progression and metastasis," *Clinical Cancer Research*, vol. 19, no. 1, pp. 62–72, 2013.

[16] V. Varghese, L. Magnani, N. Harada-Shoji et al., "FOXM1 modulates 5-FU resistance in colorectal cancer through regulating TYMS expression," *Scientific Reports*, vol. 9, no. 1, 2019.

[17] Y. Y. Lan, J. M. Heather, T. Eisenhaure et al., "Extranuclear DNA accumulates in aged cells and contributes to senescence and inflammation," *Aging Cell*, vol. 18, no. 2, article e12901, 2019.

[18] S. Glück, B. Guey, M. F. Gulen et al., "Innate immune sensing of cytosolic chromatin fragments through cGAS promotes senescence," *Nature Cell Biology*, vol. 19, no. 9, pp. 1061–1070, 2017.

[19] S. Hu, Y. Fang, X. Chen et al., "cGAS restricts colon cancer development by protecting intestinal barrier integrity," *Proceedings of the National Academy of Sciences of the United States of America*, vol. 118, no. 23, 2021.

[20] H. J. Wang, L. Wang, S. S. Song et al., "Decreased expression of PTH1R is a poor prognosis in hepatocellular carcinoma," *Cancer biomarkers: section A of Disease markers*, vol. 21, no. 3, pp. 723–730, 2018.

[21] H. Liang, Y. Zhong, Y. Huang, and G. Chen, "Type 1 receptor parathyroid hormone (PTH1R) influences breast cancer cell proliferation and apoptosis induced by high levels of glucose," *Medical Oncology*, vol. 29, no. 2, pp. 439–445, 2012.

[22] W. Wang, S. Yu, S. Huang et al., "A complex role for calcium signaling in colorectal cancer development and progression," *Molecular Cancer Research*, vol. 17, no. 11, pp. 2145–2153, 2019.

[23] J. Liu, H. Li, L. Sun et al., "Epigenetic alternations of microRNAs and DNA methylation contribute to liver metastasis of colorectal cancer," *Digestive Diseases and Sciences*, vol. 64, no. 6, pp. 1523–1534, 2019.

[24] Y. Xu and Z. Sun, "Molecular basis of Klotho: from gene to function in aging," *Endocrine Reviews*, vol. 36, no. 2, pp. 174–193, 2015.

Hindawi
BioMed Research International
Volume 2024, Article ID 9838460, 1 page
https://doi.org/10.1155/2024/9838460

Retraction

Retracted: A New Survival Model Based on Cholesterol Biosynthesis-Related Genes for Prognostic Prediction in Clear Cell Renal Cell Carcinoma

BioMed Research International

Received 12 March 2024; Accepted 12 March 2024; Published 20 March 2024

This article has been retracted by Hindawi following an investigation undertaken by the publisher [1]. This investigation has uncovered evidence of one or more of the following indicators of systematic manipulation of the publication process:

(1) Discrepancies in scope

(2) Discrepancies in the description of the research reported

(3) Discrepancies between the availability of data and the research described

(4) Inappropriate citations

(5) Incoherent, meaningless and/or irrelevant content included in the article

(6) Manipulated or compromised peer review

The presence of these indicators undermines our confidence in the integrity of the article's content and we cannot, therefore, vouch for its reliability. Please note that this notice is intended solely to alert readers that the content of this article is unreliable. We have not investigated whether authors were aware of or involved in the systematic manipulation of the publication process.

Wiley and Hindawi regrets that the usual quality checks did not identify these issues before publication and have since put additional measures in place to safeguard research integrity.

We wish to credit our own Research Integrity and Research Publishing teams and anonymous and named external researchers and research integrity experts for contributing to this investigation.

The corresponding author, as the representative of all authors, has been given the opportunity to register their agreement or disagreement to this retraction. We have kept a record of any response received.

References

[1] X. Qi, X. Lv, X. Wang et al., "A New Survival Model Based on Cholesterol Biosynthesis-Related Genes for Prognostic Prediction in Clear Cell Renal Cell Carcinoma," *BioMed Research International*, vol. 2021, Article ID 9972968, 15 pages, 2021.

Hindawi
BioMed Research International
Volume 2021, Article ID 9972968, 15 pages
https://doi.org/10.1155/2021/9972968

Research Article

A New Survival Model Based on Cholesterol Biosynthesis-Related Genes for Prognostic Prediction in Clear Cell Renal Cell Carcinoma

Xiaochen Qi,[1] Xin Lv,[1] Xiaoxi Wang,[2] Zihao Ruan,[3] Peizhi Zhang,[4] Qifei Wang,[1] Yingkun Xu,[5] and Guangzhen Wu[1]

[1]*Department of Urology, The First Affiliated Hospital of Dalian Medical University, Dalian 116011, China*
[2]*Department of Clinical Laboratory, The First Affiliated Hospital of Dalian Medical University, Dalian 116011, China*
[3]*The Nursing College of Zhengzhou University, Zhengzhou 450052, China*
[4]*Department of Urology, Shandong Provincial Hospital, Cheeloo College of Medicine, Shandong University, Jinan 250021, China*
[5]*Department of Endocrine and Breast Surgery, The First Affiliated Hospital of Chongqing Medical University, Chongqing 400042, China*

Correspondence should be addressed to Qifei Wang; wangqifei6008@hotmail.com, Yingkun Xu; yingkunxu@hotmail.com, and Guangzhen Wu; wuguang0613@hotmail.com

Xiaochen Qi, Xin Lv, and Xiaoxi Wang contributed equally to this work.

Received 20 March 2021; Revised 6 July 2021; Accepted 16 August 2021; Published 3 September 2021

Academic Editor: Yun-Feng Yang

In our study, the value of cholesterol biosynthesis is related to clinical analysis in 32 cancer forms in the GSEA database facility. We have a mutation between 25 CBRGs. In The Cancer Genome Atlas database, clear cell renal cell carcinoma (ccRCC, $n = 539$) was upregulated or downregulated in 22 out of 25 cases ($n = 72$) compared with normal kidney tissue. Then, using LASSO regression analysis, the survival model that is based on nine risk-related CBRGs (*CYP51A1*, *HMGCR*, *HMGCS1*, *IDI1*, *FDFT1*, *SQLE*, *ACAT2*, *FDPS*, and *NSDHL*) is established. ROC curves confirmed the good omen of the new survival mode, and the area under the curve is 0.72 (5 years) and 0.709 (10 years). High *SQLE* and *ACAT2* expression and low *NSDHL*, *FDPS*, *CYP51A1*, *FDFT1*, *HMGCS1*, *HMGCR*, and *IDI1* expression were closely related to patients with high-risk renal clear cell carcinoma. Two types of Cox regression, uni- and multivariate, were used to determine risk scores, age, staging, and grade as independent risk factors for prognosis in patients with clear cell renal cell carcinoma. The results showed the prediction model established by 9 selected CBRGs could predict the prognosis more accurately.

1. Introduction

The incidence of kidney cancer has been on the rise worldwide in recent decades, kidney cancer accounted for 2.2% of all cancers diagnosed and 1.8% of all cancer deaths, according to the report from GLOBOCAN 2018 released by the International Agency for Research on Cancer (IARC) [1]. Clear cell renal cell carcinoma (ccRCC) is the most common type of renal malignancy, and the histologic feature of tumor cells is a distinctive pale, glassy cytoplasm. Cholesterol, cholesterol esters, and other neutral lipids accumulate in large quantities in the cytoplasm [2, 3]. Cholesterol is mainly synthesized by the liver, and kidney cancer cells (including other tumor cells) need high levels of cholesterol to maintain their cell membrane biogenesis and other functional requirements compared to normal cells. Normal cells synthesize cholesterol through 21 enzymatic reactions, producing a large number of metabolites and participating in the control of physiological and developmental processes [4].

The contents of total cholesterol and esterified cholesterol in clear cell carcinoma tissues were 8 times and 35

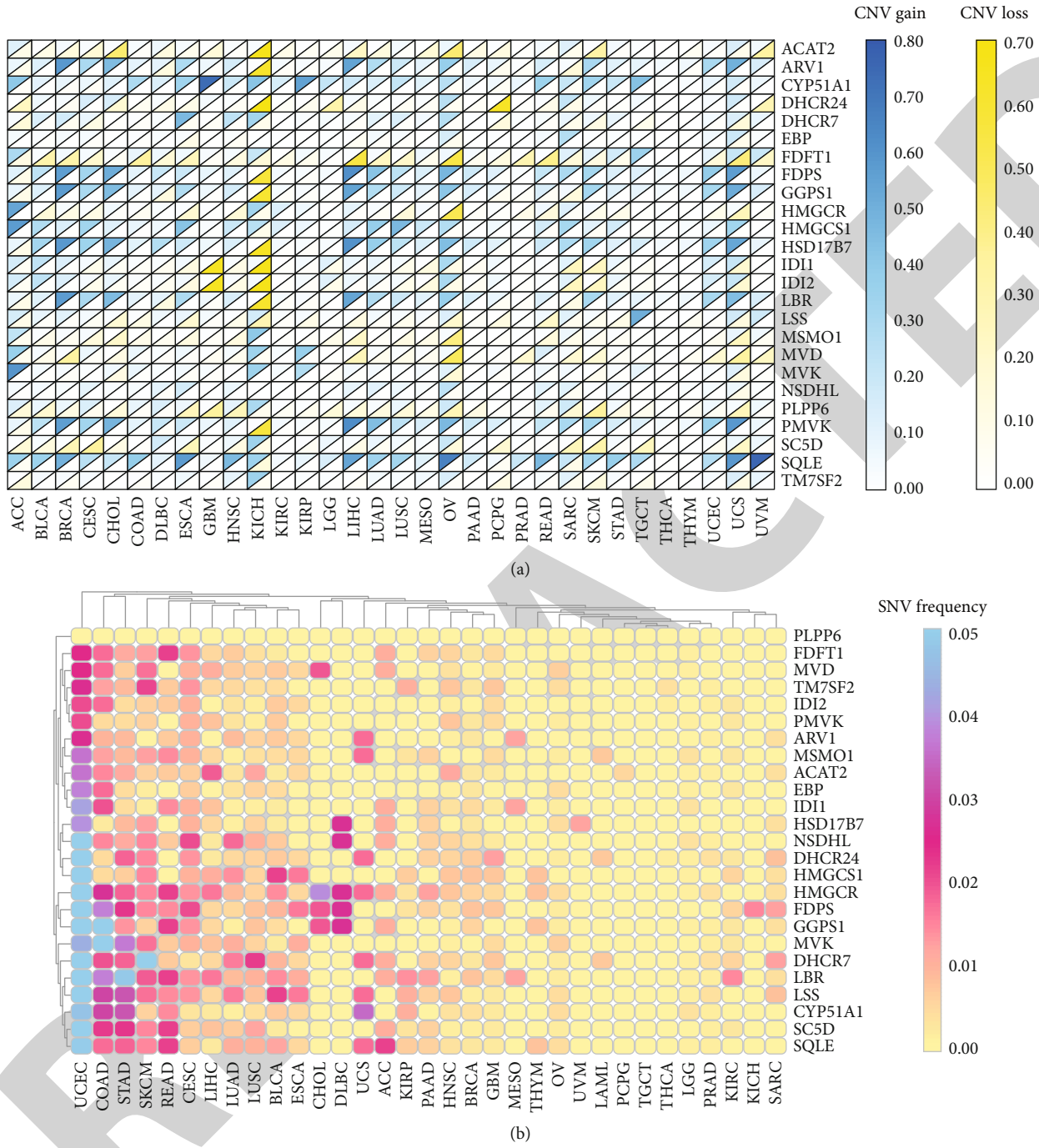

Figure 1: (a) CNV of 25 CBRGs is shown for 32 tumor types. The color code bar on the right side refers to the gain or loss of copy numbers. (b) SNV of the 25 CBRGs is shown for the 32 tumor types. The color code bar on the right side refers to frequencies of SNV.

times those in normal kidney tissue [5], respectively. In general, cholesterol metabolism plays a significant role in tumor progression, including cell proliferation, migration, and invasion.

In this study, we analyzed different expressions and mutations of cholesterol-related genes in 32 types of cancer systematically. We especially focused our attention on the ccRCC and analyzed the expression of cholesterol biosynthesis-related genes (CBRGs) in KIRC patients. Gene expression in cancer tissues is complex, so we summarized the coexpression relationships of these 32 genes in ccRCC patient tissues for researching the interactions between these multiple oncogenes. The samples were divided into high-risk group and low-risk group by judging gene expression. The survival of the two groups was demonstrated by the K-M survival curve. After that, we used LASSO regression to determine the nine strongest prognostic markers and use the ROC curve to determine authenticity. Then we use the heat map to show

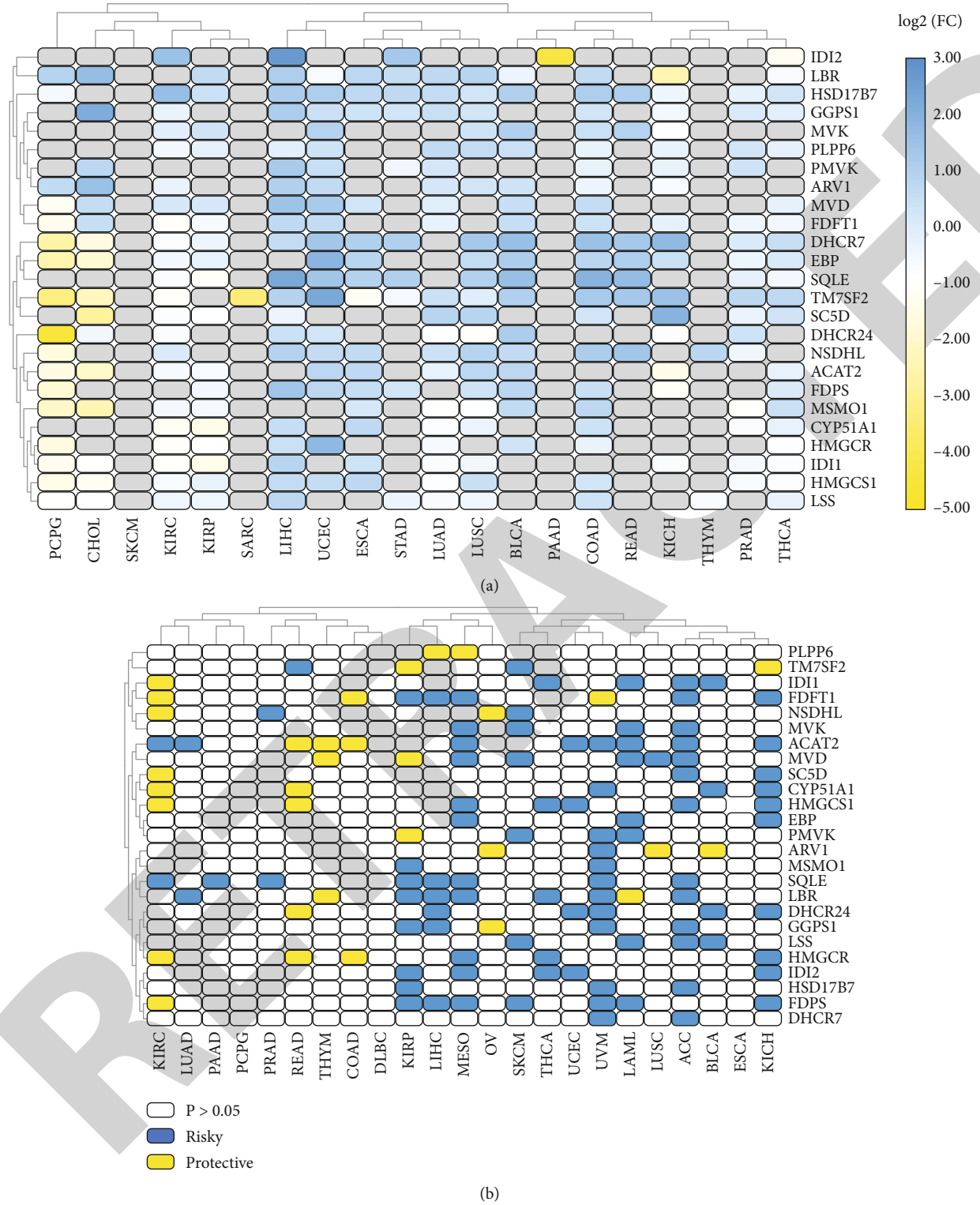

Figure 2: (a) There were changes in the expression of 25 CBRGs among 20 different types of cancer. The color code bar shows the corresponding value of log2(FC) on the right side. (b) Survival landscape of 25 Cholesterol Biosynthesis Pathway genes among 20 different types of cancers. The color bar shows $P > 0.05$ (white), risky gene (blue), and protective gene (yellow).

the profiles of the expression of survival model CBRGs and clinicopathological features in low-risk and high-risk ccRCC patients. Finally, we establish a survival prediction model for ccRCC patients with R language.

2. Materials and Methods

2.1. Analyzing the Collected Data. SNV and CNV data were obtained from TCGA (The Cancer Genome Atlas, https://

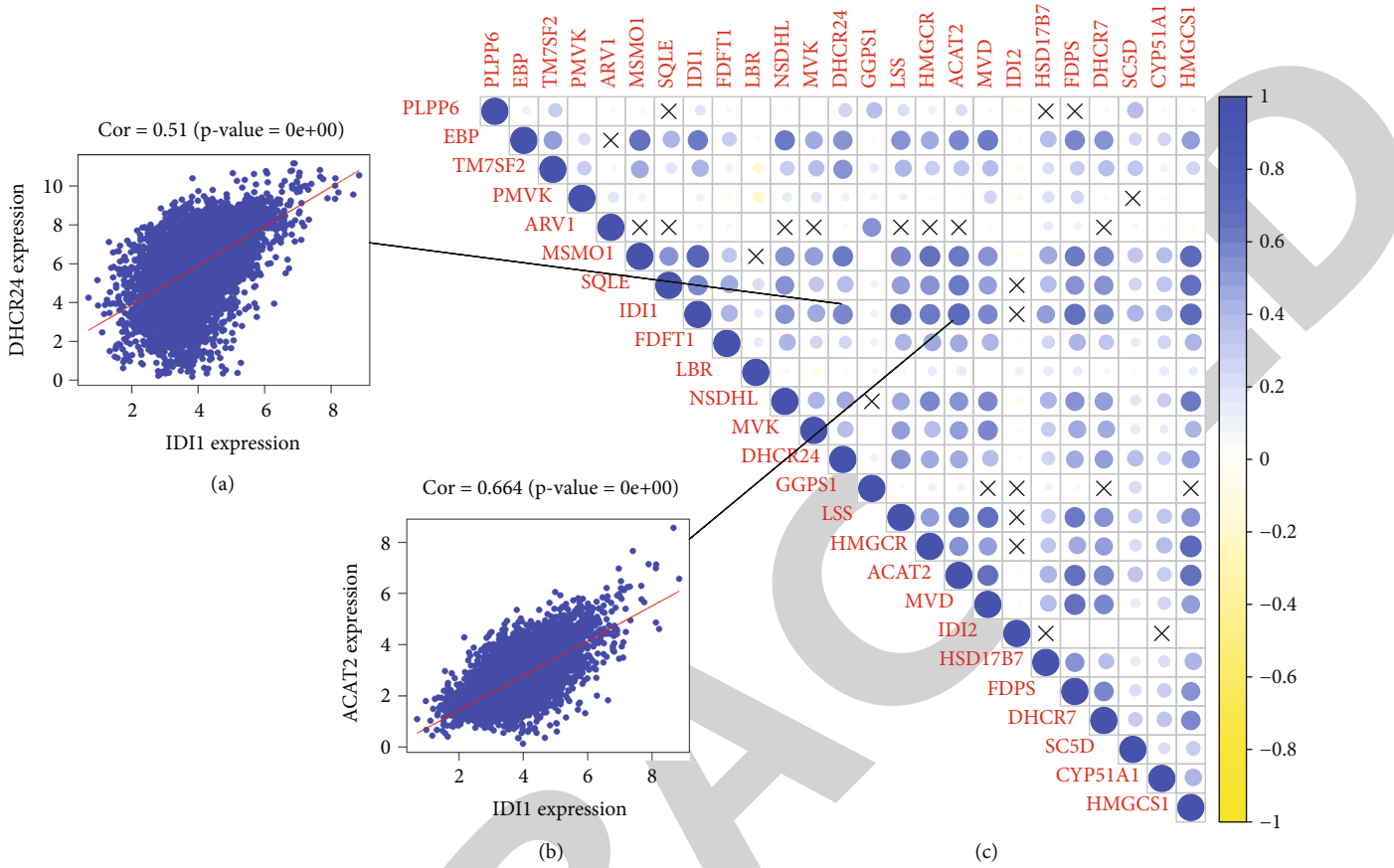

Figure 3: (a) The correlation coefficient between *IDI1* and *DHCR24* is 0.51. (b) The correlation coefficient between *IDI1* and *ACAT2* is 0.664. (c) Coexpression analysis showed that 25 CBRGs were correlated in tumor tissues.

cancergenome.nih.gov) database, and 32 cancers were downloaded [6]. The data is analyzed using the Perl language and then visualized using TB tools. Download the RNA-seq queue for KIRC from the R/Bioconductor package for TCGA Biolinks. Twenty-three different treatment regimens for TCGA were analyzed, each with its characteristics. We download clinical information about cancer from TCGA Biolinks, including age, life expectancy, tumor stage, tumor size, and metastasis [7]. Use the Corrplot package to analyze public data expressions in the Perl language and R studio. LASSO regression analysis was performed with Glmnet and survival packages. Survival time analysis was used to analyze the clinical manifestations of Cox risk factors by single factor and multifactor analysis.

2.2. Establishing Regression Models and Determining Risk Levels. Using the Cox model, we investigated the relationship between CBRG expression levels and OS (overall survival) in samples with KIRC. Patients with ccRCC remove samples without complete clinical data. Based on a P value (<0.05), CBRG was selected as a survival-related gene. Because we found collinearity among more than 30 selected genes in the previous coexpression analysis, they were highly correlated with each other, and we then used LASSO regression analysis which was performed to exclude the genes that did not fit the model. This analysis can reduce the number of variables affecting the prediction model, prevent overfitting, and simplify the prediction model while ensuring its authenticity. Then, we use multivariate analysis to determine the best CBRG, which was able to show prognostic situation. Risk score index = $\sum ni = 1$ (Expi ∗ Coei), where N represents the number of genes, Coei represents the regression coefficient, and Expi represents the level of gene expression. Samples were divided into two groups: low- and high-risk, median risk score as the critical value. Through time-dependent ROC analysis, the accuracy of the 5 and 10-year prediction model is evaluated.

2.3. Statistical Analyses. The expression of CBRG in tumor and normal tissues was observed with one-way ANOVA as control. The expression of CRG in ccRCC was examined by the Student's t-test according to gender, age, stage, T (tumor), and M (tumor metastasis). Because a large number of samples in TCGA database cannot be verified, N (tumor nodes) are not used in this study. "Er" software package and the patients were divided into a high-risk group. Each risk score of different groups was determined by the "survminer" software package. The samples are divided into high- and low-risk groups according to the optimal threshold. Statistical analysis was performed using the R Studio software package. A significant difference was found in $P < 0.05$.

(a)

Figure 4: Continued.

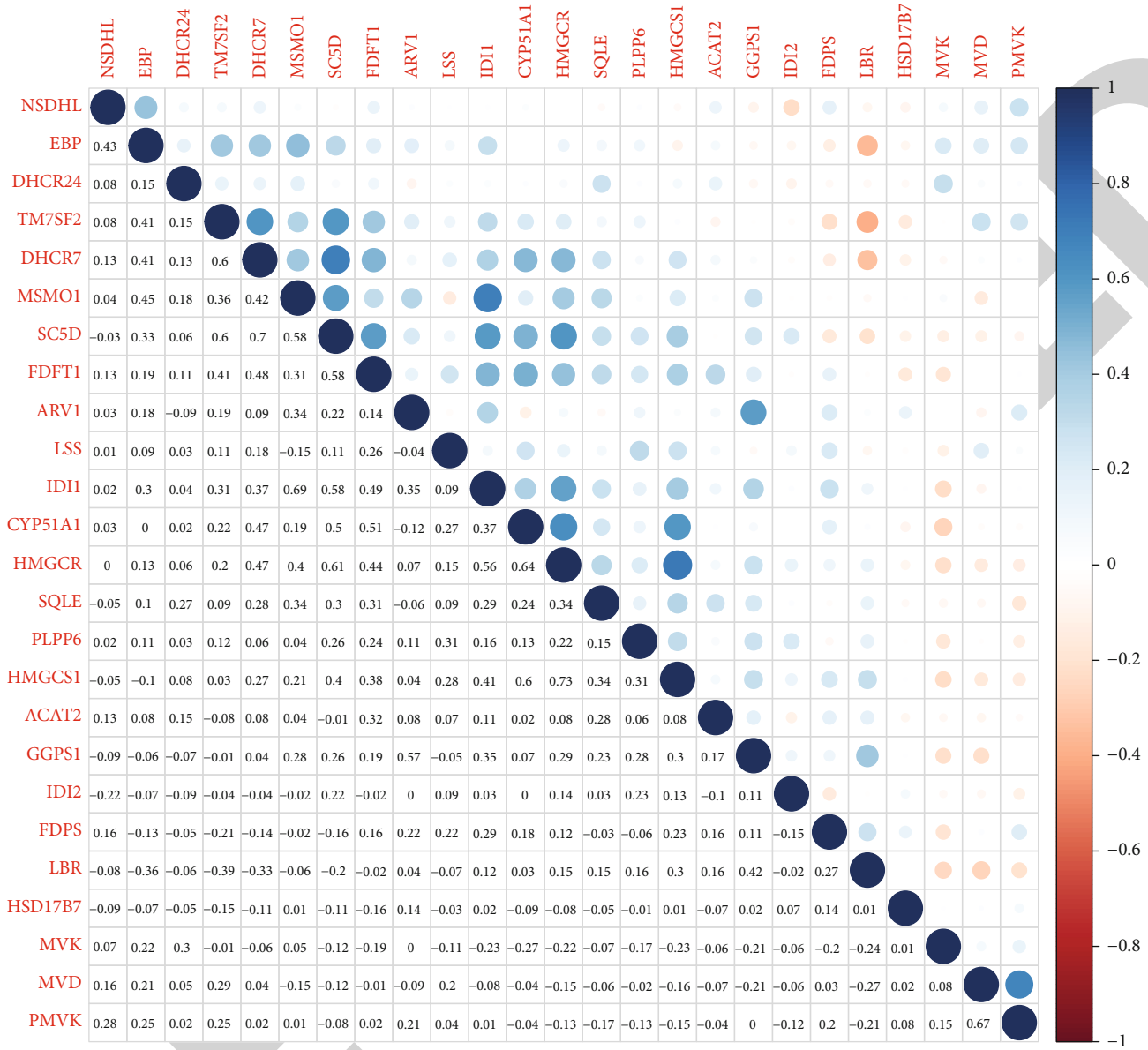

(b)

Figure 4: Continued.

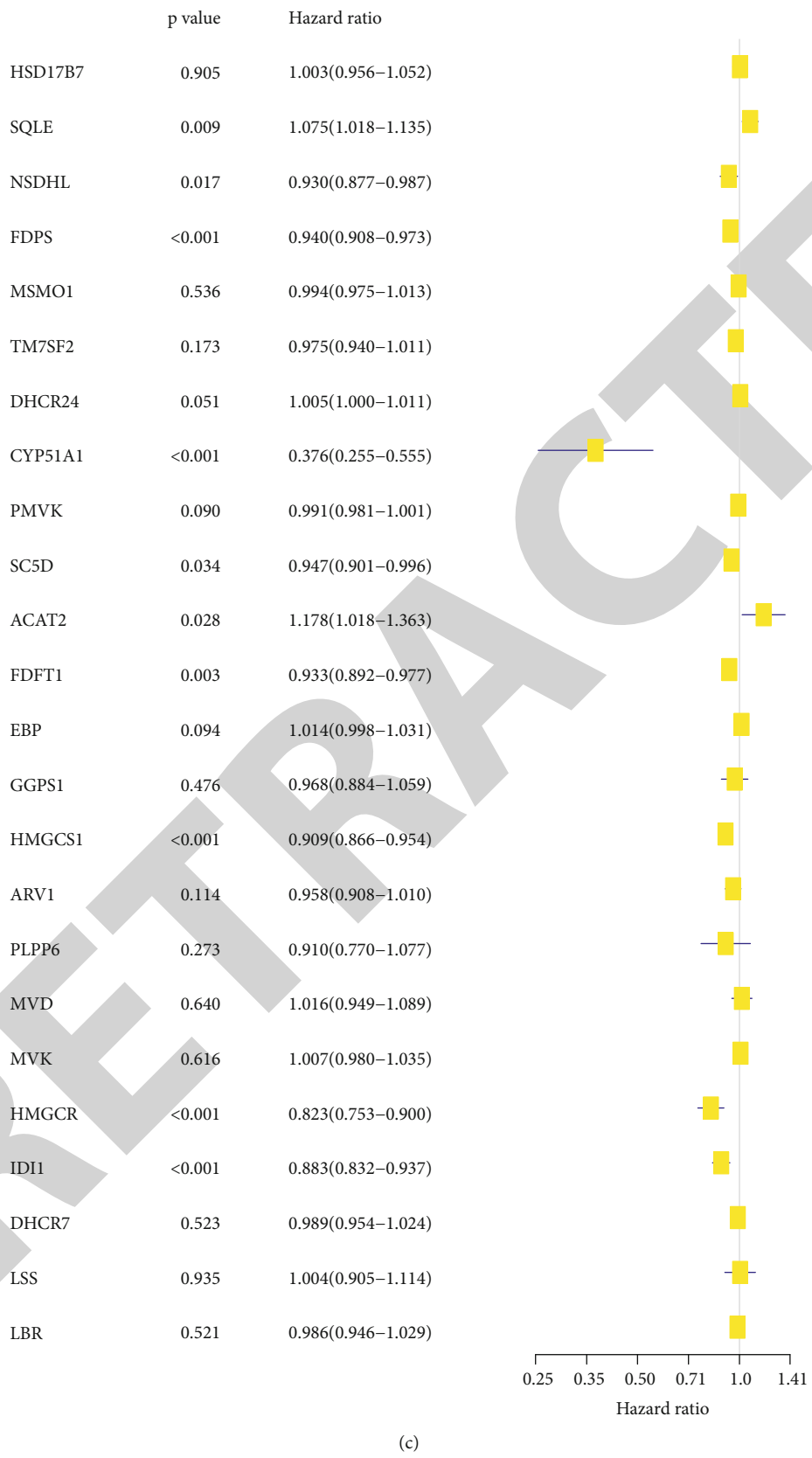

(c)

Figure 4: (a) The expression of 25 CBRGs in the sample of ccRCC patients. The blue color shows the upregulation of CBRGs, and the yellow color indicates the downregulation of CBRGs. N presents the normal sample, and T presents the tumor sample. (b) Coexpression analysis showed that 25 CBRGs were correlated in ccRCC tissues. (c) Forest plot of the hazard ratio (HR) analysis with 95% confidence intervals (CI) and *P* values for the 25 CBRGs.

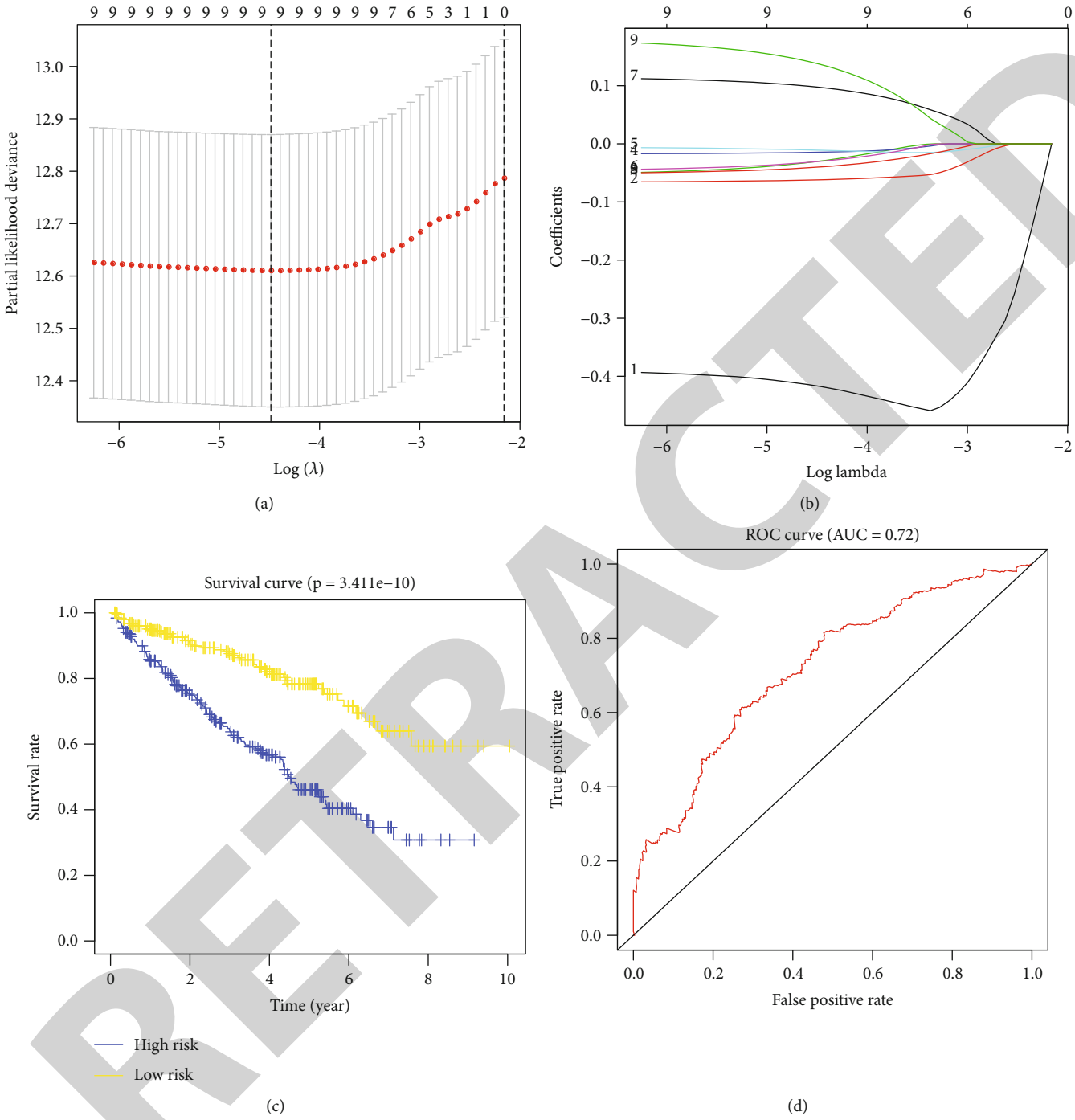

Figure 5: Continued.

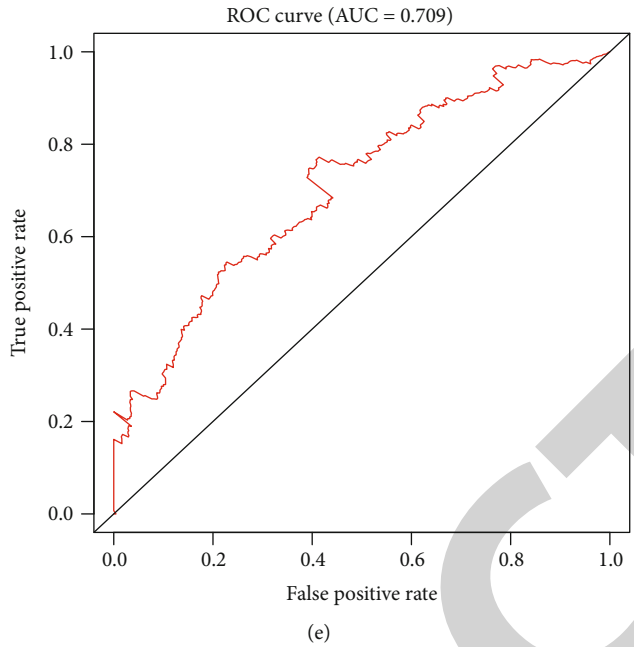

Figure 5: (a) Nine genes were selected by LASSO Cox regression analysis. (b) The LASSO coefficient profiles of CBRGs in KIRC. (c) The survival curve was obtained based on this model. Blue and yellow correspond, respectively, to the high-risk group and the low-risk group. (d, e) ROC curve of 5 and 10 years, and AUC of the curve is 0.72 and 0.709 in turn.

3. Results

3.1. Genetic Mutation of CBRGs in 32 Cancer Types. We determine the copy number variations (CNVs) and the single nucleotide variations (SNVs) in the 25 CBRGs among the 32 cancer types with the help of the GSEA database [8, 9]. Then, we analyzed the CNVs in the CBRGs among the 32 cancer types with R language. We use the 32 tumors' CNV and SNV data, which were downloaded from TCGA database, to verify the results with R language. We use TBtools to make the final result visual (Figures 1(a) and 1(b)).

3.2. Prognostic Significance of CBRGs in Various Tumors. Next, we analyzed the prognostic relevance of CBRGs in different tumors. We used R language and TBtools software to analyze the 32 tumors' mRNA expression data from TCGA database. The results show that *HSD17B7*, *GGPS1*, *MVK*, *PLPP6*, *PMVK*, and *ARV1*, 6 types of representative CBRGs, were upregulated in most of all tumors compared to the corresponding controls. *SQLE* and *NSDHL* were upregulated in KIRC, and *CYP51A1* and *FDFT1* were downregulated in KIRC compared to the corresponding controls (Figure 2(a)). Then, we analyzed the relevance between the survival landscape and CBRGs among 32 tumors. We analyzed the expression of CBRGs and the overall survival (OS) of the tumor patients with the help of the GEPIA online database and judged the gene that was risky or protective according to the result of the relationship between the expression and the OS (Figure 2(b)). We use R language and TBtools to analyze the data and show the consequence.

3.3. Functional Analysis of CBRG-Related Pathways in ccRCC. To find the relevance of any two genes, we performed the coexpression analysis on these 25 CBRGs among all tumor patients and found the Pearson correlation coefficient (PCC) of *IDI1* and *DHCR24* was 0.51 (Figure 3(a)), the PCC of *IDI1* and *ACAT2* was 0.664 (Figure 3(b)), and both of them were a positive correlation; the final results based on the figure show that most of the CBRGs were a positive correlation, and we observed strong correlation among the CBRGs (Figure 3(c)).

Since the metabolism of cholesterol has been established in ccRCC, we analyzed the expression of CBRGs in 72 normal kidneys and 539 ccRCC specimens through TCGA database, with the help of the Limma package in R language. The results showed that 22 out of 25 CBRGs were differentially expressed in ccRCC tissue and normal kidney tissue (Figure 4(a)). We also performed the coexpression analysis on these 25 CBRGs among ccRCC patients (Figure 4(b)). The results showed that the correlation between the CBRGs among the ccRCC patients is strong. Meanwhile, a negative correlation also existed in these CBRGs.

3.4. Creating and Testing a New Survival Mode CBRG. To further understand the role of CBRG in prognosis evaluation of clear cell renal cell carcinoma, analysis of TCGA data using Cox regression was used. High expression of *ACAT2* and *SQLE* in patients with renal clear cell carcinoma is associated with decreased survival. On the contrary, high expression of *NSDHL*, *FDPS*, *CYP51A1*, *FDFT1*, *HMGCS1*, *HMGCR*, and *IDI1* is correlated with better survival rates (Figure 4(c)). So according to the P value <0.05, we selected some of CBRGs as survival-related genes, and with the help of LASSO regression analysis, we determined the strongest prognostic index. We selected nine genes (*CYP51A1*, *HMGCR*, *HMGCS1*, *IDI1*, *FDFT1*, *SQLE*, *ACAT2*, *FDPS*, and *NSDHL*)

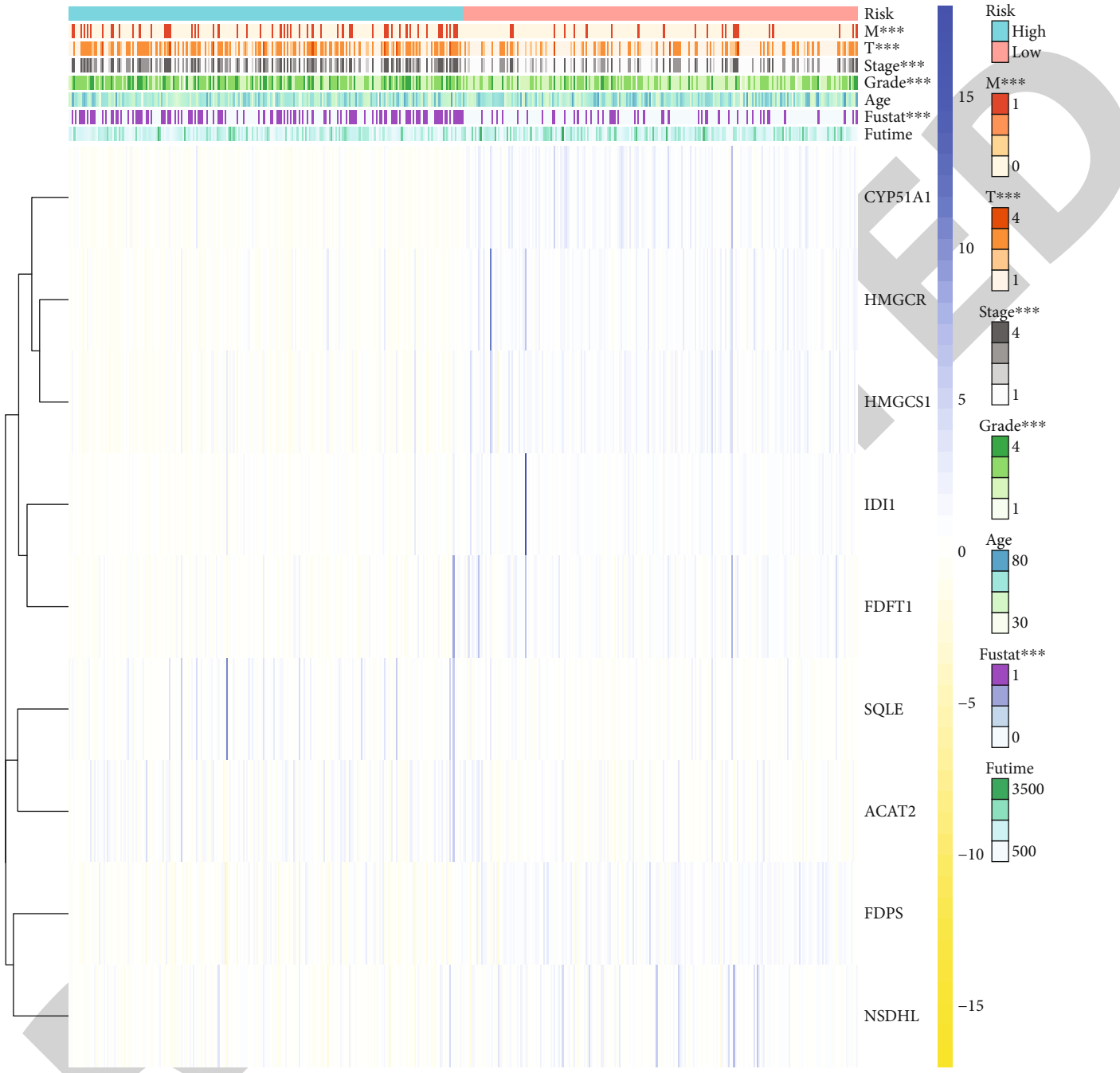

(a)

Figure 6: Continued.

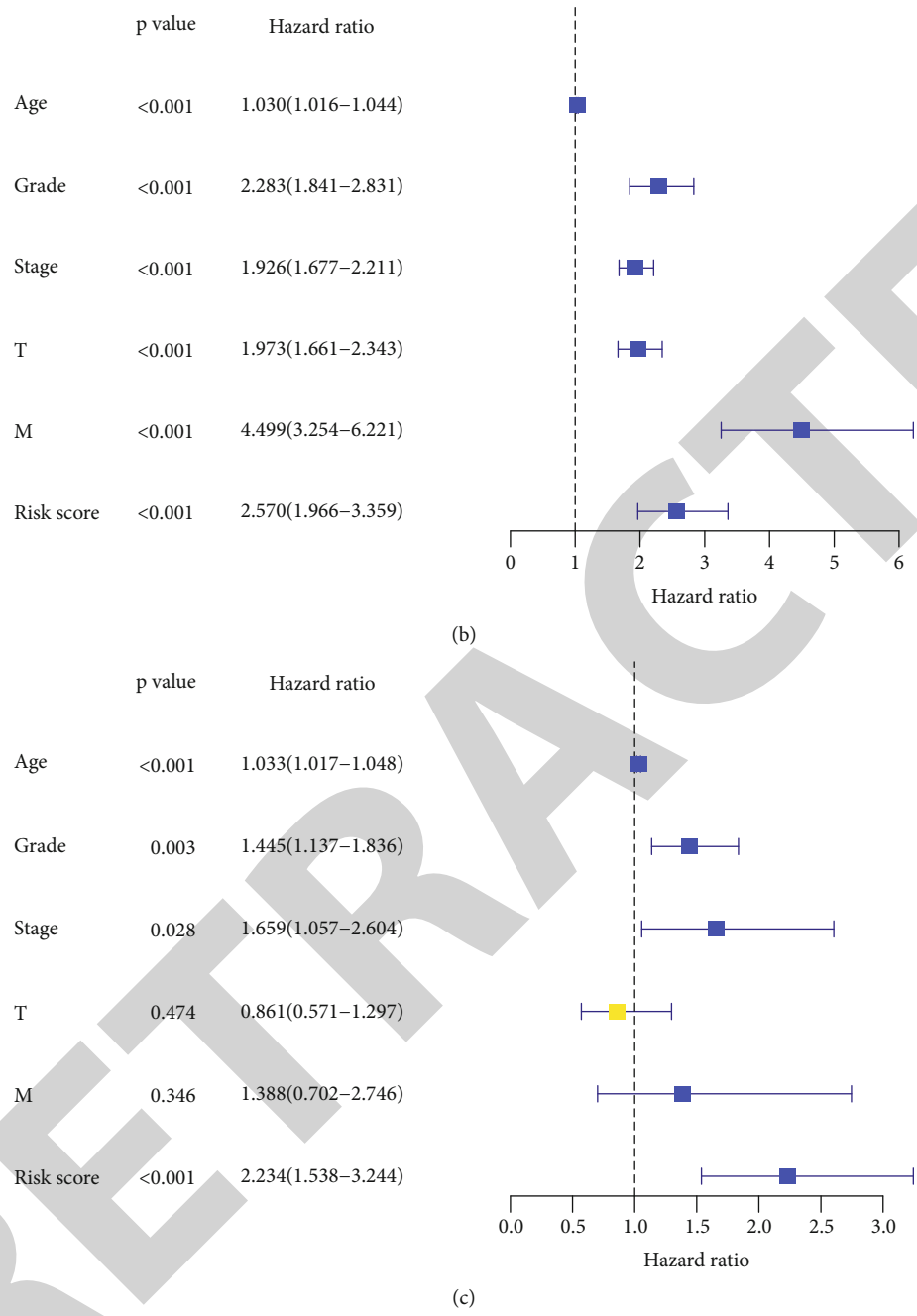

Figure 6: (a) The correlation of 9 selected genes and the clinicopathological characteristics in two groups. Blue represents upregulation, and yellow represents downregulation ($^{*}P < .05$, $^{**}P < .01$, and $^{***}P < .001$). (b) Forest plot of univariate Cox analysis. (c) Forest plot of multivariate Cox analysis.

based on results. Based on the minimum criterion, 9 genes were used to establish the risk characteristic model. Using the risk score as the median, patients with clear cell carcinoma of the kidney were divided into high and low control groups to observe the predictive power of new survival patterns composed of nine risk genetic characteristics (Figures 5(a) and 5(b)). The Kaplan-Meyer survival curve (K-M survival curve) analysis showed a significant reduction in survival in the high-risk group compared to the low-risk group (Figure 5(c)). In addition, the ROC curve was used to analyze the effect of new survival mode on the prognosis of renal clear cell carcinoma. The indices were 0.72 (5 years) and 0.709 (10 years) (Figures 5(d) and 5(e)). The results showed that the model's risk score calculated by the model could accurately predict the survival rates of renal clear cell carcinoma in 5 and 10 years.

3.5. The New CBRG-Based Survival Model Is Closely Related to the Clinicopathological Characteristics of ccRCC Patients. To further study the correlation between CBRGs and ccRCC, we used a heat map system to analyze the correlation between risk scores based on the expression of 9 CBRGs

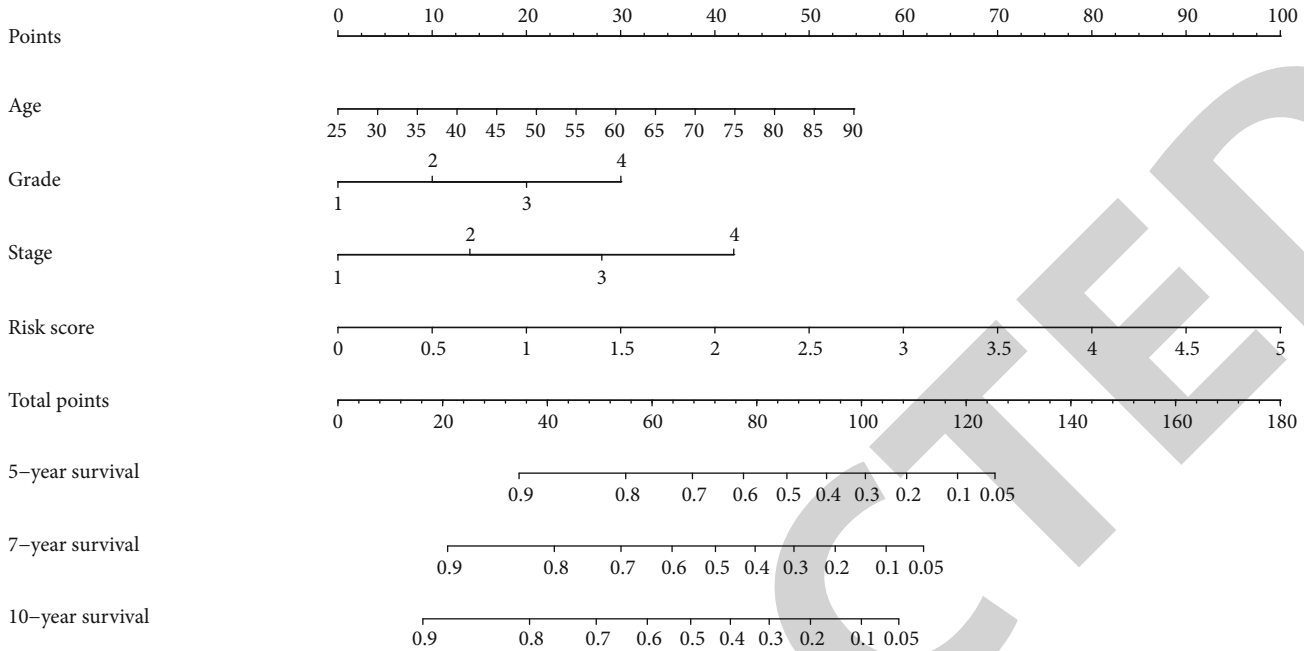

Figure 7: Nomogram of the predictive model.

and the clinicopathological characteristics of different samples obtained from TCGA data set. There is a strong correlation between the risk scores of high- and low-risk samples and clinical pathological characteristics such as T (tumor size), N (tumor lymph node), M (tumor metastasis), tumor grade, tumor stage, gender, and survival. The expressions of *SQLE* and *ACAT2* were significantly upregulated in the high-risk group, and the expressions of *CYP51A1*, *HMGCR*, *HMGCS1*, *IDI1*, *FDFT1*, *FDPS*, and *NSDHL* were significantly downregulated (Figure 6(a)). Cox regression analysis showed that age, tumor grade, tumor stage, tumor size (T), tumor metastasis (M), and risk score were related to ccRCC patients' OS (Figure 6(b)). The risk score, age, stage, and grade were independent risk factors affecting ccRCC patients' prognosis showed by multivariate Cox regression analysis (Figure 6(c)). Finally, we built a scoring table in R language and added the total scores of age, tumor stage, tumor grade, and risk score to get the corresponding survival rate of ccRCC patients in 5 and 10 years.

3.6. Based on the Risk Model, Draw the Nomogram and the Verification Process. We use a nomogram to predict the risk of KIRC patients. Nomogram generates a total of 9 lines. The first row represents fractional meters. Age is in the second row, grade is in the third, the stage is in the fourth, and risk score is fifth. The total score in row 6 is obtained by adding up the scores for each item of age, grade, stage, and risk score. We can easily estimate the survival rates in 5 and 10 years of ccRCC patients from the total score (Figure 7(a)). To improve the reliability of the research results, we conducted random internal sampling validation in the KIRC data set of TCGA database. Based on this risk model, we divided 45 randomly selected KIRC patients into high-risk and low-risk groups. In the generated survival curve, we found that the prognosis of patients in the high-risk group was significantly lower than that of the low-risk group ($P = 0.002$) (Supplementary Materials Figure S1A). In order to verify more results in this study, based on the expression of key genes HMGCR, IDI1, and HMGCS1 in this study, we divided ccRCC patients into high expression groups and low expression groups and plotted the corresponding survival curves. The results show that the expression of these three key genes is correlated with the poor prognosis of ccRCC (Supplementary Materials Figure S1B-D).

4. Discussion

The genesis and development of cancer cells are inseparable from cell division, which requires a large amount of cholesterol to form the cell membrane. There is a balance of cholesterol metabolism among them, Higher levels of etherified phospholipids, cholesterol esters, and triacylglycerols and lower levels of phospholipids (except phosphatidylcholine) and lower levels of polyunsaturated fatty acids were present in the canceled tissues [10], and it means that the metabolic balance of cholesterol is disrupted. Many studies have shown that preoperative cholesterol levels in cancer patients can influence postoperative prognosis, and cholesterol level has been used to construct a model to predict patient survival [11–14]. Cholesterol accumulation is a common feature of cancer tissue, and recent studies have shown that it plays an important role in breast, bladder, colorectal, and other cancers [15]. The mechanism of cholesterol metabolism in cells has been largely understood through current studies. There is a dynamic balance between synthesis, uptake, output, and esterification of intracellular cholesterol. That is, cholesterol is converted into neutral cholesterol ester, stored in lipid droplets, or secreted as a lipoprotein [16].

There are four different anomalous metabolic explanations for cholesterol accumulation [2]: (1) Absorb a large amount of free cholesterol in serum. (2) Synthesize excessive amount of endogenous cholesterol in cancer cells. (3) The activity of enzymes and other factors that regulate cholesterol synthesis in cancer cells increases. (4) Cholesterol cannot be normally excreted from cancer cells [17]. In vitro inoculation tests have confirmed that cholesterol accumulation in RCC cells is not dependent on extracellular uptake, but rather is likely due to intracellular endogenous cholesterol synthesis and efflux [18]. Most research, however, has focused on the role of cholesterol and its typical metabolites in cells [19], and little is known about changes in cholesterol synthesis and its pathways in cancer cells, particularly in the genes involved. Therefore, we chose to start with the synthesis pathway of endogenous cholesterol synthesis in cells.

When it comes to the synthesis of substances, genetic changes must be taken into account. Studies on the gene related to kidney cancer have been carried out for a long time, and the sequencing of the gene related to kidney cancer has also been reported [20]. At present, the main direction focuses on differentially expressed genes, miRNA, etc., among which mutations of immune-related genes, lipid-synthesis-related genes, and similar genes have been found to play their roles in cancer cells [21]. miRNA, on the other hand, affects gene expression by cutting off mRNA or inhibiting translation [22]. However, there are still few studies on the relationship between cholesterol biosynthesis-related genes (CBRGs) and clear cell renal cell carcinoma (ccRCC).

A complex set of related genes regulates cholesterol homeostasis. For example, in the process of cholesterol production by *HMG-COA* in cancer cells, the synthesis pathways of many associated proteins and enzymes are regulated by different associated genes such as *HMGCR* and *HMGCS1* [23]. Therefore, we believe that these CBRGs affect the cholesterol synthesis of cancer cells, and the study of the biosynthetic pathway of these genes can also provide references for the clinical treatment and prognosis of ccRCC.

In this study, we investigated for the first time the effect of CBRG expression in ccRCC tissues on the prognosis of patients. We worked backward, identifying the path-related raw materials and enzymes and then looking backward for the genes involved in their synthesis. Previous studies have shown that the upregulated differentially expressed genes (DEGs) in ccRCC are significantly enriched in the inflammatory and hypoxia responses in the immune response injury response. In contrast, the downregulated genes are mainly concentrated in the genes related to ion transport [24]. We systematically analyzed the clinical relevance of CBRGs selected from TCGA database and through the analysis of CNV and SNV to determine whether they are risky genes or protective genes [25, 26]. Then, LASSO regression was used to select 9 of these genes and construct a model to predict survival rate. Age, grade, and stage of cancer are also factors that take into account [27–30]. We included all of these factors in the nomogram. All these analyses were performed in R language. Referring to other experiments with R, we used several good software packages such as Limma and Glmnet [31, 32]. Because cholesterol synthesis involves many biosynthetic pathways, the number and types of pathways affected by CBRGs are also very large. Among the nine selected genes, 7 are protective genes and 2 are risky genes, among which *ACAT2* is a risky gene [16]. *ACAT2*, as a gene related to cholesterol ester synthesis and its influence on cholesterol intestinal absorption, has been deeply studied. *HMGCR* and other genes associated with the synthesis of *HMG-COA* have also been thoroughly studied in the treatment of lung cancer and breast cancer [23, 33]. In a 2012 review, Borgquist et al. [34] suggested that genes involved in sterol synthesis and cholesterol synthesis, especially enzymes downstream of squalene, could potentially have far-reaching implications for cancer treatment. This view was also confirmed by the establishment of a predictive survival model for ccRCC patients with nine CBRGs, including *SQLE* and *CYP51A1*. After this, Clayman et al. [19] also put forward the view that mutations of *SQLE*, *HMGCR*, and other genes could affect cholesterol metabolism, thus further affecting cancer, and the conclusion is put forward. A single pathway to inhibit cholesterol metabolism may cause a low impact on tumor growth. Further, exploration and prevention of biochemical cholesterol changes in cancer may provide new ideas for the next generation of metabolic therapies. Therefore, how to perfect the influence factors used to construct the model, including cholesterol metabolism and transport, is the next thing we need to solve.

Abbreviations

GSEA: Gene Set Enrichment Analysis
ccRCC: Clear cell renal cell carcinoma
CYP51A1: Cytochrome P450 family 51 subfamily a member 1
HMGCR: 3-Hydroxy-3-methylglutaryl-CoA reductase
HMGCS1: 3-Hydroxy-3-methylglutaryl-CoA synthase 1
IDI1: Isopentenyl-diphosphate delta isomerase 1
FDFT1: Farnesyl-diphosphate farnesyltransferase 1
SQLE: Squalene epoxidase
ACAT2: Acetyl-CoA acetyltransferase 2
FDPS: Farnesyl diphosphate synthase
NSDHL: NAD(P)-dependent steroid dehydrogenase-like
IARC: International Agency for Research on Cancer
TCGA: The Cancer Genome Atlas
KIRC: Kidney renal clear cell carcinoma
LASSO: Least absolute shrinkage and selection operator
OS: Overall survival
CNVs: Copy number variations
SNV: Single nucleotide variation.

Data Availability

The data used to support the findings of this study are available from the corresponding author upon request.

Conflicts of Interest

The authors declare that they have no conflicts of interest.

Authors' Contributions

Guangzhen Wu, Yingkun Xu, and Qifei Wang designed the research methods and analyzed the data. Xiaochen Qi, Xin Lv, and Xiaoxi Wang participated in data collection. Xin Lv, Zihao Ruan, Peizhi Zhang, and Yingkun Xu drafted and revised the manuscript. All authors approved the version to be released and agreed to be responsible for all aspects of the work. Xiaochen Qi, Xin Lv, and Xiaoxi Wang contributed equally to this study and are considered co-first authors.

Acknowledgments

We thank The Cancer Genome Atlas (TCGA) for providing publicly available data. This project is supported by the Scientific Research Fund of Liaoning Provincial Education Department (no. LZ2020071) and the Liaoning Province Doctoral Research Startup Fund Program (no. 2021-BS-209).

Supplementary Materials

Figure S1: random sampling validation. (A) Based on this risk model, 45 patients with ccRCC randomly sampled from TCGA database were divided into high- and low-risk groups, and the corresponding survival curves were drawn. (B-D) Based on the expression of key genes of HMGCR, IDI1, and HMGCS1, the corresponding survival curves were drawn in ccRCC. *(Supplementary Materials)*

References

[1] F. Bray, J. Ferlay, I. Soerjomataram, R. L. Siegel, L. A. Torre, and A. Jemal, "Global cancer statistics 2018: GLOBOCAN estimates of incidence and mortality worldwide for 36 cancers in 185 countries," *CA: a Cancer Journal for Clinicians*, vol. 68, no. 6, pp. 394–424, 2018.

[2] R. L. Gebhard, R. V. Clayman, W. F. Prigge et al., "Abnormal cholesterol metabolism in renal clear cell carcinoma," *Journal of Lipid Research*, vol. 28, no. 10, pp. 1177–1184, 1987.

[3] G. M. Zhang, Y. Zhu, L. Luo et al., "Prevalence of dyslipidaemia in patients with renal cell carcinoma: a case-control study in China," *BJU International*, vol. 113, no. 5b, pp. E75–E81, 2014.

[4] S. Silvente-Poirot and M. Poirot, "Cancer. Cholesterol and cancer, in the balance," *Science*, vol. 343, no. 6178, pp. 1445-1446, 2014.

[5] J. Wang, M. Tan, J. Ge et al., "Lysosomal acid lipase promotes cholesterol ester metabolism and drives clear cell renal cell carcinoma progression," *Cell Proliferation*, vol. 51, no. 4, article e12452, 2018.

[6] K. Tomczak, P. Czerwińska, and M. Wiznerowicz, "The Cancer Genome Atlas (TCGA): an immeasurable source of knowledge," *Contemporary Oncology/Współczesna Onkologia*, vol. 19, no. 1a, pp. A68–A77, 2015.

[7] A. Colaprico, T. C. Silva, C. Olsen et al., "TCGAbiolinks: an R/Bioconductor package for integrative analysis of TCGA data," *Nucleic Acids Res*, vol. 44, no. 8, p. e71, 2016.

[8] V. K. Mootha, C. M. Lindgren, K. F. Eriksson et al., "PGC-1alpha-responsive genes involved in oxidative phosphorylation are coordinately downregulated in human diabetes," *Nature Genetics*, vol. 34, no. 3, pp. 267–273, 2003.

[9] A. Subramanian, P. Tamayo, V. K. Mootha et al., "Gene set enrichment analysis: a knowledge-based approach for interpreting genome-wide expression profiles," *Proceedings of the National Academy of Sciences of the United States of America*, vol. 102, no. 43, pp. 15545–15550, 2005.

[10] W. M. Linehan and C. J. Ricketts, "The Cancer Genome Atlas of renal cell carcinoma: findings and clinical implications," *Nature Reviews. Urology*, vol. 16, no. 9, pp. 539–552, 2019.

[11] K. Saito, E. Arai, K. Maekawa et al., "Lipidomic signatures and associated transcriptomic profiles of clear cell renal cell carcinoma," *Scientific Reports*, vol. 6, no. 1, p. ???, 2016.

[12] KOrean Renal Cell Carcinoma (KORCC) Group, H. Lee, Y. J. Kim et al., "Preoperative cholesterol level as a new independent predictive factor of survival in patients with metastatic renal cell carcinoma treated with cyto-reductive nephrectomy," *BMC Cancer*, vol. 17, no. 1, p. 364, 2017.

[13] M. de Martino, C. V. Leitner, C. Seemann et al., "Preoperative serum cholesterol is an independent prognostic factor for patients with renal cell carcinoma (RCC)," *BJU International*, vol. 115, no. 3, pp. 397–404, 2015.

[14] B. Li, D. Huang, H. Zheng, Q. Cai, Z. Guo, and S. Wang, "Preoperative serum total cholesterol is a predictor of prognosis in patients with renal cell carcinoma: a meta- analysis of observational studies," *International Braz J Urol*, vol. 46, no. 2, pp. 158–168, 2020.

[15] B. Hao, X. Peng, B. Bi, M. Yu, C. Sang, and Z. Chen, "Preoperative serum high-density lipoprotein cholesterol as a predictor of poor survival in patients with clear cell renal cell cancer," *The International Journal of Biological Markers*, vol. 34, no. 2, pp. 168–175, 2019.

[16] T. Murai, "Cholesterol lowering: role in cancer prevention and treatment," *Biological Chemistry*, vol. 396, no. 1, pp. 1–11, 2015.

[17] J. Luo, H. Yang, and B. L. Song, "Mechanisms and regulation of cholesterol homeostasis," *Nature Reviews. Molecular Cell Biology*, vol. 21, no. 4, pp. 225–245, 2020.

[18] B. Sharma and N. Agnihotri, "Role of cholesterol homeostasis and its efflux pathways in cancer progression," *The Journal of Steroid Biochemistry and Molecular Biology*, vol. 191, p. 105377, 2019.

[19] R. V. Clayman, R. Gonzalez, A. Y. Elliott, D. E. Gleason, and M. E. Dempsey, "Cholesterol accumulation in heterotransplanted renal cell cancer," *The Journal of Urology*, vol. 129, no. 3, pp. 621–624, 1983.

[20] H. Xu, S. Zhou, Q. Tang, H. Xia, and F. Bi, "Cholesterol metabolism: new functions and therapeutic approaches in cancer," *Biochimica et Biophysica Acta (BBA) - Reviews on Cancer*, vol. 1874, no. 1, article 188394, 2020.

[21] I. Varela, P. Tarpey, K. Raine et al., "Exome sequencing identifies frequent mutation of the SWI/SNF complex gene _PBRM1_ in renal carcinoma," *Nature*, vol. 469, no. 7331, pp. 539–542, 2011.

[22] B. Wan, B. Liu, Y. Huang, and C. Lv, "Identification of genes of prognostic value in the ccRCC microenvironment from TCGA database," *Biochimica et Biophysica Acta (BBA) - Reviews on Cancer*, vol. 8, no. 4, p. e1159, 2020.

[23] S. Mishra, T. Yadav, and V. Rani, "Exploring miRNA based approaches in cancer diagnostics and therapeutics," *Critical Reviews in Oncology/Hematology*, vol. 98, pp. 12–23, 2016.

Hindawi
BioMed Research International
Volume 2024, Article ID 9820387, 1 page
https://doi.org/10.1155/2024/9820387

Retraction

Retracted: The Effect on the Fracture Healing following Femoral Neck Shortening after Osteoporotic Femoral Neck Fracture Treated with Internal Fixation: Finite Element Analysis

BioMed Research International

Received 12 March 2024; Accepted 12 March 2024; Published 20 March 2024

This article has been retracted by Hindawi following an investigation undertaken by the publisher [1]. This investigation has uncovered evidence of one or more of the following indicators of systematic manipulation of the publication process:

(1) Discrepancies in scope

(2) Discrepancies in the description of the research reported

(3) Discrepancies between the availability of data and the research described

(4) Inappropriate citations

(5) Incoherent, meaningless and/or irrelevant content included in the article

(6) Manipulated or compromised peer review

The presence of these indicators undermines our confidence in the integrity of the article's content and we cannot, therefore, vouch for its reliability. Please note that this notice is intended solely to alert readers that the content of this article is unreliable. We have not investigated whether authors were aware of or involved in the systematic manipulation of the publication process.

Wiley and Hindawi regrets that the usual quality checks did not identify these issues before publication and have since put additional measures in place to safeguard research integrity.

We wish to credit our own Research Integrity and Research Publishing teams and anonymous and named external researchers and research integrity experts for contributing to this investigation.

The corresponding author, as the representative of all authors, has been given the opportunity to register their agreement or disagreement to this retraction. We have kept a record of any response received.

References

[1] X. Yu, P.-z. Rong, Q.-j. Pang, X.-j. Chen, L. Shi, and C.-h. Wang, "The Effect on the Fracture Healing following Femoral Neck Shortening after Osteoporotic Femoral Neck Fracture Treated with Internal Fixation: Finite Element Analysis," *BioMed Research International*, vol. 2021, Article ID 3490881, 7 pages, 2021.

Hindawi
BioMed Research International
Volume 2021, Article ID 3490881, 7 pages
https://doi.org/10.1155/2021/3490881

Research Article

The Effect on the Fracture Healing following Femoral Neck Shortening after Osteoporotic Femoral Neck Fracture Treated with Internal Fixation: Finite Element Analysis

Xiao Yu,[1] **Peng-ze Rong**,[2] **Qing-jiang Pang**,[1] **Xian-jun Chen**,[1] **Lin Shi**,[1] **and Cheng-hao Wang**[1]

[1]*Department of Orthopedics, HwaMei Hospital, University of Chinese Academy of Sciences; Ningbo Institute of Life and Health Industry, University of Chinese Academy of Sciences, Ningbo 315000, China*
[2]*Ningbo University School of Medicine, Ningbo 315211, China*

Correspondence should be addressed to Qing-jiang Pang; pqjey@sina.com

Received 14 June 2021; Accepted 9 July 2021; Published 5 August 2021

Academic Editor: Yun-Feng Yang

Objective. To evaluate the stress status of fracture site caused by femoral neck shortening and to analyze the stress of fracture site and the implants from the finite element point of view. *Methods*. CT scan data of hip of a normal adult female were collected. Three-dimensional reconstruction MICs and related module function simulation was used to establish the postoperative shortening model of femoral neck fracture with Pauwels angle > 50°, which was treated with cannulated screws. The models were divided into four groups: normal femoral neck, shortening in 2.5 mm, shortening in 7.5 mm, and shortening in 12.5 mm. The finite element analysis software msc.nastran2012 was used, and the data of maximum stress and stress nephogram of fracture site and implants were carried out. *Results*. From normal femoral neck to shortening in 12.5 mm of the femoral neck, the maximum tensile stress increased gradually in the fracture site above the cannulated screws while compressive stress decreased gradually in the fracture site below the cannulated screws, and the maximum stress of the cannulated screws increased gradually with obvious stress concentration at the screw holes in the fracture site, and the peak value of stress concentration was about 179 MPa. *Conclusion*. The biomechanical environment of the fracture site changed by femoral neck shortening. With the increasing of femoral neck shortening, the stress of the fracture site and implants would be uneven; then, the stability of fracture site would become worse, and the possibility of implant sliding or even breakage would be increased.

1. Introduction

Femoral neck fracture is a senile disease. However, the fracture in 60-65 years old is usually treated by internal fixation with cannulated screws, which was considered as an important method to preserve the hip joint [1, 2]. However, due to the situation such as osteoporosis, it is not uncommon to see the femoral neck shortening after cannulated screw placement [3]. The shortening of the femoral neck will inevitably cause the shortening of the lower limb, which will change the patient's gait. For a long time, it will affect the abduction function of hip joint and pelvic stability, thus affecting the quality of life [4, 5]. Some scholars reported their researches about the stability of the femoral neck fracture fixation by finite element analysis and the comparison with the dynamic hip screw and cannulated screws by biomechanical evaluation [6–8]; however, there was few biomechanical experiment to verify the biomechanical effect of neck shortening on fracture healing after internal fixation with cannulated screws. In fact, it is necessary to understand the biomechanical effect, which helps the surgeons to judge what kind of degree of shortening needs early intervention. It has been confirmed that femoral neck shortening after internal fixation with cannulated screws will significantly reduce the Harris score of hip joint due to the abnormal gait of claudication of the injured limb and limitation of the abduction of the injured hip [9–12]. Therefore, this study aims to establish a three-dimensional model of femoral neck fracture with

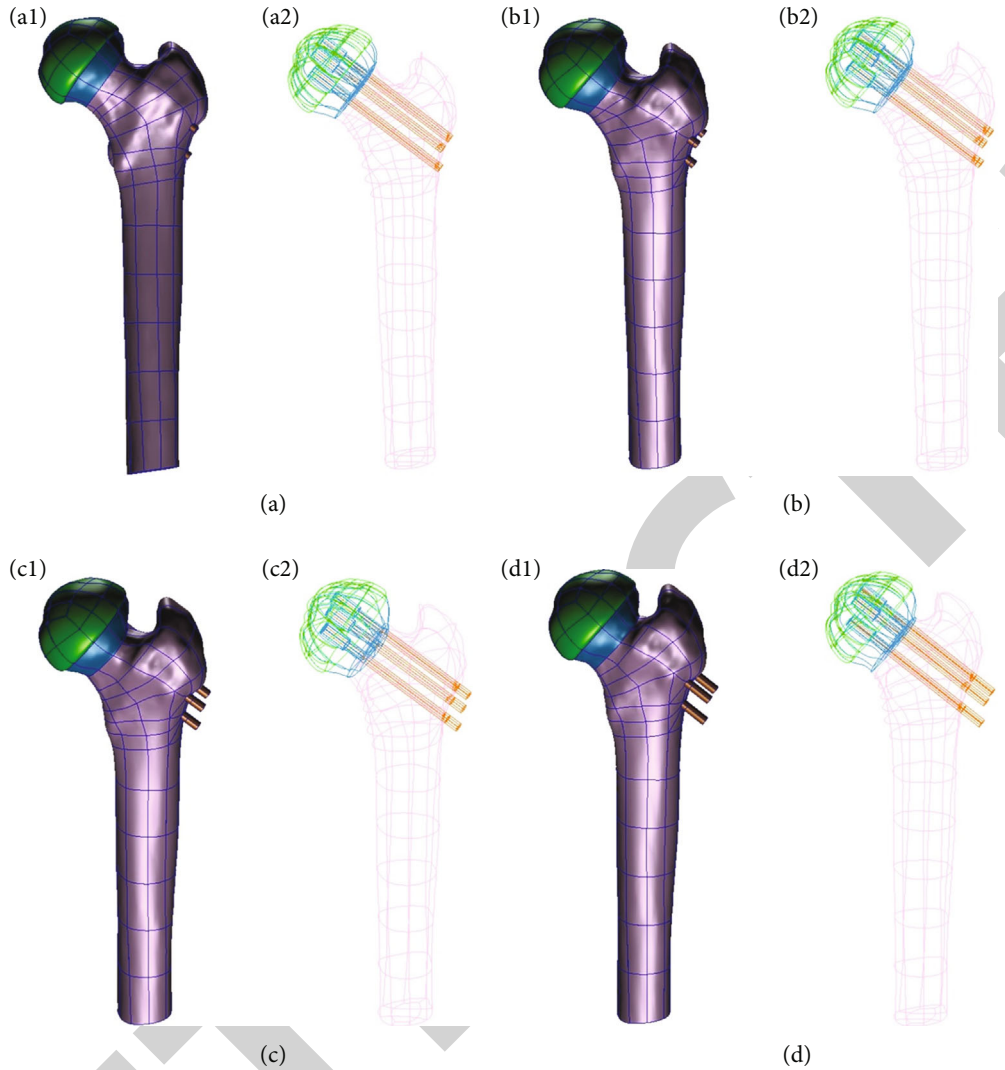

Figure 1: Geometric models and the cannulated screws retreat in different femoral neck shortening after cannulated screws fixation. (a) No shortening, (b) shortening in 2.5 mm, (c) shortening in 7.5 mm, and (d) shortening in 12.5 mm; 1: geometric models and 2: cannulated screws retreat.

cannulated screw fixation and analyze the stress distribution and changes on the fracture site and implants by finite element method, so as to explore the biomechanical effect of femoral neck shortening on fracture healing after internal fixation of femoral neck fracture.

2. Material and Method

2.1. The Establishment of Normal Hip Joint Model and Femoral Neck Fracture Model with Neck Shortening. A 60-year-old female volunteer, 160 cm in height and 55 kg in weight, was randomly selected in the hospital. The abnormal conditions such as necrosis of the femoral head, acetabular defect and dysplasia, and hip joint disease were excluded by X-ray examination. The patient was diagnosed as osteoporosis by dual energy X-ray absorptiometry (DXA). The study was approved by the ethics committee in the hospital, and the volunteers signed the informed consent before the examination.

The volunteer was supine on the CT bed, and the lower extremities were in the neutral position. The hip joint was scanned from the upper edge of the acetabulum to the middle part of the femoral shaft. After scanning, the CT image data of 512×512 matrix, 260 layers in total, was obtained, and the scanned data was stored directly in Dicom format. The Dicom files were loaded into software of Mimics 16.0. The original images were set in the directions of front, back, left, and right and accurately matched the orientation of the reconstructed 3D model with the human body coordinate axis. The osseous tissue was extracted by threshold method with the range of 122-1613 Hu. The extracted tissue was stored in a mask, and the pixels in the mask were modified by mask editing, region growing, and cavity filling. Then, the STL file was loaded into the software of Geomagic studio 2014, which could build a watertight nonuniform rational spline curve and could be optimized for surface fitting and fairing. It could be curved through the process of accurate surface and finally formed a three-dimensional solid model

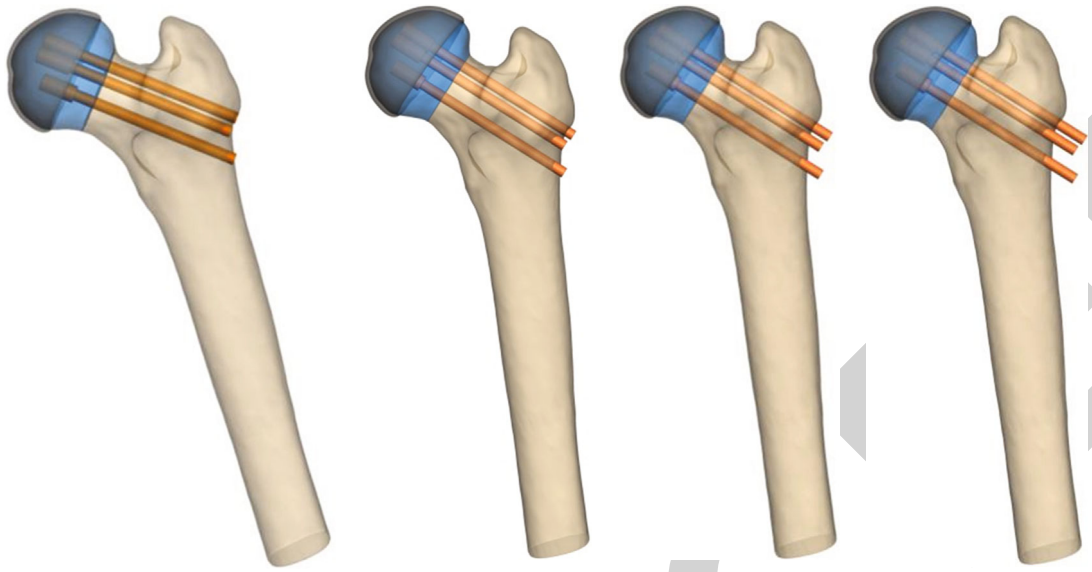

Figure 2: The models of shortening after internal fixation of femoral neck in four groups. (a) No shortening, (b) shortening in 2.5 mm, (c) shortening in 7.5 mm, and (d) shortening in 12.5 mm.

Table 1: The material parameters of femoral neck shortening model after cannulated screw fixation.

Structural region	Modulus of elasticity (MPa)	Poisson's ratio
Cortical bone of femur	16 800	0.30
Cancellous bone of femur	620	0.29
Acetabular cartilage	10	0.40
Cannulated screw (Ti6Al4VELI)	110 000	0.33

of the hip joint, which was conducive to the subsequent finite element model establishment and analysis (Figure 1).

3. The Model Assembly

In order to facilitate the establishment of hip joint finite element model and data processing, the implant size was referred to the operation of internal fixation of femoral neck fracture. Three cannulated screws (Synthes, Swiss) were commonly used with the screw diameter 4.8 mm, thread diameter 7.3 mm, and hollow diameter 2.6 mm. However, the screw length was depended on the actual length of the femoral neck. The cannulated screws were arranged in an inverted triangle, and the thread shape of the screw was ignored in the process of screw modeling. The contact setting was used in the calculation process to achieve a good contact between the thread of the cannulated screws and the femoral neck. It was assumed that the femoral neck was complete fracture and had been anatomical reduction. The Pauwels angle was more than 50°, and the friction coefficient between the two fracture surfaces was 0.15. The relationship between the femoral neck and the thread of the cannulated screws was set as binding without displacement; however, the relationship between the screw paths and the unthreaded part of the screws was set as contact, and the

Figure 3: Boundary constraints of femoral neck shortening model.

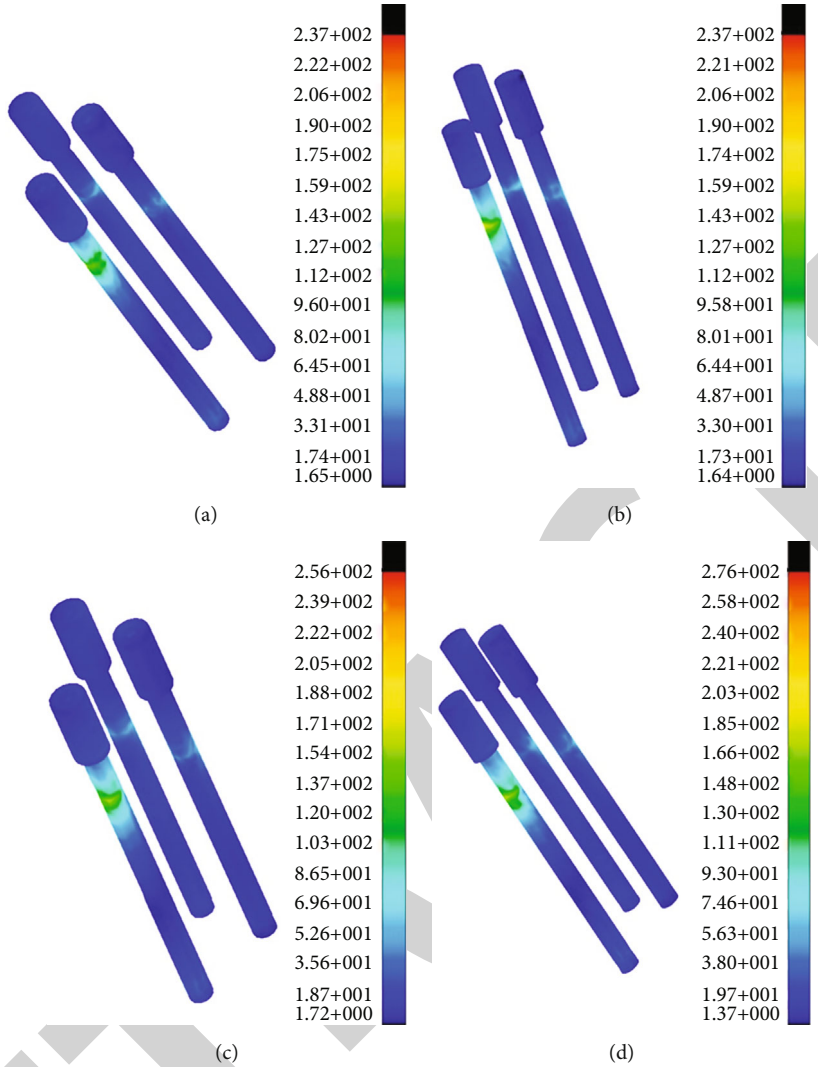

Figure 4: Von Mises stress diagram of cannulated screws with different degrees of femoral neck shortening. (a) No shortening, (b) shortening in 2.5 mm, (c) shortening in 7.5 mm, and (d) shortening in 12.5 mm.

friction coefficient was 0.2. The shortening model of femoral neck after internal fixation could be completely obtained. According to the shortening length, the models could be divided into four groups: no femoral neck shortening model (0 mm), mild shortening model (2.5 mm), moderate shortening model (7.5 mm), and severe shortening model (12.5 mm) (Figure 2).

4. Generating the Finite Element Model and Assigning Material to the Model

The IGES files of four groups of the models were imported into HyperMesh 13.0 software for mesh generation, the BDF format files were then exported, and the finite element postprocessing calculation and analysis were carried out in msc.nastran2012 software.

The modulus of elasticity and Poisson's ratio were selected as the parameters of material assignment. The femur is made up of cancellous bone, cortical bone, and hollow medullary cavity, and it has the characteristics of heterogeneity and belongs to anisotropic nonlinear body. Therefore, we referred to the published research data [13–15], titanium alloy (Ti6Al4VELI) material was used for the cannulated screws, and the material parameters of the model were listed in the table below (Table 1).

5. Constraint Condition and Mechanical Loading

The boundary constraint conditions for four groups of the models were hypothesized: (1) it was assumed that a distal femoral fixation constraint and the degrees of freedom in six directions for all nodes on the distal of femur are limited. (2) It was assumed that the structure of femur is a continuous, uniform, and isotropic linear elastic material [15]. In this study, the commonly used simplified model was adopted, the peak force of the single hip was tested when the 55 kg volunteer was walking normally, and the joint was loaded at the

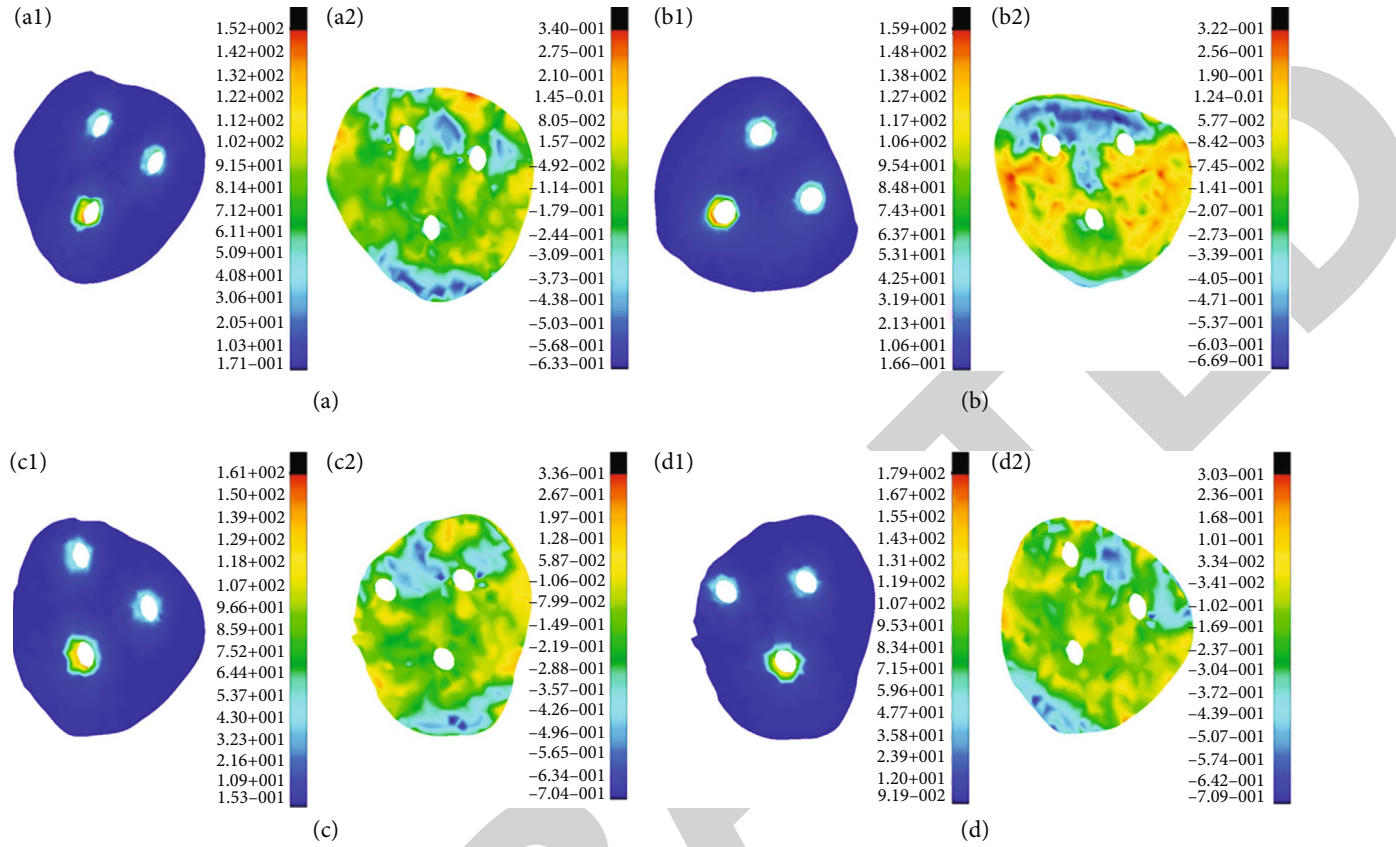

Figure 5: Von Mises stress maps and equivalent strain maps of femoral neck fractures with different shortening of femoral. (a) No shortening, (b) shortening in 2.5 mm, (c) shortening in 7.5 mm, and (d) shortening in 12.5 mm; 1: von Mises stress maps and 2: equivalent strain maps.

peak time [15]. The reaction resultant of the hip joint force was about 2072 N, and abductor muscle resultant force was about 8737 N. The resultant joint forces are distributed in a cosine fashion on the surface of the femoral head [15]. The model of assigned material was imported into the finite element analysis software Msc.Nastran2012 and loaded the constraints, and then, the calculation and analysis could be carried out (Figure 3).

6. Results

6.1. Finite Element Simulation of Cannulated Screws with Different Degree of Femoral Neck Shortening. From normal femoral neck without shortening to shortening in 2.5 mm, 7.5 mm, and 12.5 mm of the femoral neck, the maximum tensile stress of cannulated screws in the fracture site above femoral neck were 115.2 MPa, 117.3 MPa, 120.0 MPa, and 136.6 MPa, respectively; however, the maximum compressive stress of cannulated screws in the fracture site below the femoral neck were 12.4 MPa, 12.3 MPa, 10.9 MPa, and 9.4 MPa, respectively. It demonstrated that with the increase of the shortening, the maximum stress of the cannulated screws gradually increased, and there was an obvious stress concentration at the fracture site on the cannulated screws. The peak stress of three cannulated screws were 237.4 MPa, 237.6 MPa, 256.4 MPa, and 276.5 MPa, respectively, which meant that it might the place with high incidence of stress fatigue of the implants in clinical application (Figure 4).

7. Finite Element Simulation of Fracture Site with Different Degree of Femoral Neck Shortening

From normal femoral neck without shortening to shortening in 2.5 mm,7.5 mm, and 12.5 mm of the femoral neck, the maximum compressive stress of the medial bone of the femoral neck were 19.9 MPa, 18.8 MPa, 4.0 MPa, and 2.1 MPa, respectively, while the maximum compressive stress of the lateral bone of the femoral neck were 31.7 MPa, 32.5 MPa, 34.2 MPa, and 36.8 MPa, respectively. The maximum stress at the fracture site of femoral neck was 152.2 MPa, 159.3 MPa, 161.4 MPa, and 179.2 MPa, respectively. It demonstrated that with the increase of the shortening, the tensile stress of two screws above the femoral neck increased, while the compressive stress under the femoral neck decreased. It also demonstrated that the stress on the fracture site increased gradually (Figure 5). When the fracture was not healed, the increased stress might augment the possibility of implant sliding and breakage, especially in the osteoporotic patients, which the implant might bear the additional stress and subsequently affect the stability of the fracture site and increase the difficulty of fracture healing [16, 17].

8. Discussion

In recent years, the treatment of femoral neck fracture with cannulated screw has become a better method with satisfied clinical effect [18, 19]. However, neck shortening often occurs after internal fixation with cannulated screw, especially in the osteoporotic population [19]. Some clinical studies have shown that the osteoporotic femoral neck fracture, especially for the cases of neck shortening can significantly reduce the Harris score of hip joint. For example, Bartels et al. [20] pointed out that patients aged 55-70 years with a displaced femoral neck fracture might have lower bone density, higher comorbidity, and subsequently the worse function of the hip. Another example was that Chen et al. [21] compared DHS-BLADE and cannulated compression screws in the treatment of femoral neck fractures and found that the DHS-BLADE had advantages over cannulated compression screws for preventing femoral neck shortening, screw migration, and cut-out, which might keep the function of the hip in a high place. However, there is no strict biomechanical experiment to study the biomechanical effect of femoral neck shortening on the healing of femoral neck. We classify the different degrees of femoral neck shortening and divided it into four types by modeling in finite element method: normal group (without shortening), shortening mild group (shortening 2.5 mm), moderate group (shortening 7.5 mm), and severe group (shortening 12.5 mm). The stress of cannulated screw and fracture site were simulated by mechanical loading [22].

In this study, the maximum stress of three cannulated screws in four groups was increased with the increase of neck shortening. In addition, from the stress nephogram of the femoral neck, the stress concentration was obvious at the fracture site on the cannulated screws, which meant that it might the place with high incidence of stress fatigue of the implants in clinical application. It is normal to produce stress concentration because of the loading to the femoral neck in the condition of slow walking, which will lead to the extrusion between the cannulated screws and the femoral neck, so it is easy to produce stress concentration near the screw holes. At present, the yield strength of titanium alloy for implant material is about 817 MPa [22]; therefore, from this point of view, the internal fixation structure of three cannulated screws after neck shortening is still within the range of yield strength. However, the stress of implants in this experiment was measured under the condition of slow walking, which was different from the maximum stress produced by the actual movement after the operation of femoral neck fracture, so there was still a risk of breakage of cannulated screws in stress concentration. Some scholars have established the finite element model of the femoral neck shortening after internal fixation of the femoral neck fracture and found that the residual screw holes of the cannulated screws will reduce the quality of the bone structure [23]. Meanwhile, due to the loss of the support protection of the cannulated screws, the risk of fracture will be greatly increased after the removal of the cannulated screws [24].

The results also showed with the increase of the shortening, the tensile stress of two screws above the femoral neck increased, while the compressive stress under the femoral neck decreased. It also demonstrated that the stress on the fracture site increased gradually, which increased the possibility of internal fixation sliding, thus affecting the stability of the fracture site and increasing the difficulty of fracture healing. Therefore, from the biomechanical point of view, excessive stress on the fracture site might aggravate the shortening of the femoral neck, which is not conducive to the healing of the fracture, especially in the osteoporosis population. Furthermore, the shortening of femoral neck after cannulated screw fixation would affect the activity and function of hip joint and the Harris score of hip joint would decrease [25].

In summary, the healing of femoral neck fracture requires a stable environment constructed by compression between the fracture site [18, 26]; however, the shortening of the femoral neck caused by the compression between the fracture sites should not be ignored as we stated above. The increased shortening of the femoral neck will also lead to instability of fracture, increase the risk of implants breakage, and even cause the hip joint dysfunction [27]. It is suggested that we should pay attention to the effect of "excessive" compression which might cause the femoral neck shortening.

Data Availability

The data used to support the findings of this study are available from the corresponding author upon request.

Conflicts of Interest

The authors declare that there is no conflict of interest regarding the publication of this article.

Acknowledgments

We would like to acknowledge support from the Ningbo Natural Science Foundation (2019A610242), Ningbo Science and Technology Innovation 2025 Specific Project (2020Z087), Zhejiang Medical and Health Science and Technology Project (2018Ky156), Zhejiang Traditional Medicine and Technology Program (2020ZB225), and Key Research Foundation of Hwa Mei Hospital, University of Chinese Academy of Sciences (2019HMZDKY14).

References

[1] I. J. Oñativia, P. A. I. Slulittel, F. Diaz Dilernia et al., "Outcomes of nondisplaced intracapsular femoral neck fractures with internal screw fixation in elderly patients: a systematic review," *Hip International*, vol. 28, no. 1, pp. 18–28, 2018.

[2] H. H. Ma, T. F. A. Chou, S. W. Tsai, C. F. Chen, P. K. Wu, and W. M. Chen, "Outcomes of internal fixation versus hemiarthroplasty for elderly patients with an undisplaced femoral neck fracture: a systematic review and meta-analysis," *Journal of Orthopaedic Surgery and Research*, vol. 14, no. 1, p. 320, 2019.

[3] M. Zlowodzki, O. Brink, J. Switzer et al., "The effect of shortening and varus collapse of the femoral neck on function after fixation of intracapsular fracture of the hip: a multi-centre cohort study," *Journal of Bone and Joint Surgery British Volume (London)*, vol. 90, no. 11, pp. 1487–1494, 2008.

Hindawi
BioMed Research International
Volume 2024, Article ID 9852153, 1 page
https://doi.org/10.1155/2024/9852153

Retraction

Retracted: Analysis of Extended Resection of Limb Soft Tissue Leiomyosarcoma

BioMed Research International

Received 12 March 2024; Accepted 12 March 2024; Published 20 March 2024

This article has been retracted by Hindawi following an investigation undertaken by the publisher [1]. This investigation has uncovered evidence of one or more of the following indicators of systematic manipulation of the publication process:

(1) Discrepancies in scope

(2) Discrepancies in the description of the research reported

(3) Discrepancies between the availability of data and the research described

(4) Inappropriate citations

(5) Incoherent, meaningless and/or irrelevant content included in the article

(6) Manipulated or compromised peer review

The presence of these indicators undermines our confidence in the integrity of the article's content and we cannot, therefore, vouch for its reliability. Please note that this notice is intended solely to alert readers that the content of this article is unreliable. We have not investigated whether authors were aware of or involved in the systematic manipulation of the publication process.

Wiley and Hindawi regrets that the usual quality checks did not identify these issues before publication and have since put additional measures in place to safeguard research integrity.

We wish to credit our own Research Integrity and Research Publishing teams and anonymous and named external researchers and research integrity experts for contributing to this investigation.

The corresponding author, as the representative of all authors, has been given the opportunity to register their agreement or disagreement to this retraction. We have kept a record of any response received.

References

[1] Q. Liu, L. Tang, X. Hu et al., "Analysis of Extended Resection of Limb Soft Tissue Leiomyosarcoma," *BioMed Research International*, vol. 2021, Article ID 2106972, 4 pages, 2021.

Hindawi
BioMed Research International
Volume 2021, Article ID 2106972, 4 pages
https://doi.org/10.1155/2021/2106972

Research Article

Analysis of Extended Resection of Limb Soft Tissue Leiomyosarcoma

Qiang Liu,[1] **Lijun Tang**,[2] **Xinhua Hu**,[1] **Jianxing Ye**,[1] **Pengcheng Liang**,[1] **Adriana C. Panayi**,[3] **Shuhua Wang**,[1] **and Jingde Deng**[1]

[1]*Department of Orthopedics, Jiangxi Province Xing Guo People's Hospital, Wenming 699th Road, Xingguo, 342400 Jiangxi Province, China*
[2]*Department of Rehabilitation Medicine, Jiangxi Province Xingg Guo People's Hospital, Wenming 699th Road, Xingguo, 342400 Jiangxi Province, China*
[3]*Division of Plastic Surgery, Division of Plastic Surgery, Brigham and Women's Hospital, Harvard Medical School, Boston, Massachusetts, USA*

Correspondence should be addressed to Qiang Liu; 279141824@qq.com

Received 17 May 2021; Accepted 13 July 2021; Published 4 August 2021

Academic Editor: Yun-Feng Yang

Leiomyosarcoma is an uncommon soft tissue sarcoma that composed of malignant mesenchymal cells with distinct features of the smooth muscle lineage. Typically affects the uterus and gastrointestinal tract, it can rarely be seen in large blood vessels, lymphatic and glandular duts, the mesentery, the omentum, retroperitoneum, and limbs. Occurrence is particularly rare in the limb region. Retrospective study based on patient records and postoperative pathological histological features. Four patients with limb leiomyosarcoma that were operated between 2016 and 2020 were included, three of them arising in the subcutis of the thigh region and one in cubitus. Extend resection with satisfactory outcomes is reported. Pathological examination showed that masses were composed of a fascicular arrangement of hyperchromatic spindle-shaped cells, characterized by the proliferation of epithelioid cells with eosinophilic cytoplasm for epithelioid leiomyosarcoma. Leiomyosarcomas that arise in the soft tissue, although rare, should be differentiated from other lesions, such as neurilemoma, neurofibroma, liomyoma,lipomyoma, synoviosarcoma, rhabdomyosarcoma, malignant fibrous histiotoma, and malignant neurinoma.

1. Introduction

Leiomyosarcoma is an uncommon soft tissue sarcoma composed of malignant mesenchymal cells showing distinct features of a smooth muscle lineage. It usually affects the uterus and gastrointestinal tract but that may be also found in less common sites including large blood vessels, lymphatic and glandular duts, the mesentery, onmentum, and retroperitoneum as well as the limbs. However, the limb region is a rare location [1]. Leiomyosarcomas of the cubitus and subcutis of the thigh region are very infrequent occurrences. Preoperative diagnosis of leiomyosarcoma is challenging because of nonspecific symptoms and a rapidly enlarging mass, and therefore, it mainly depends on postoperative pathological examination. The histological grade, tumor size, and tumor depth are the three major clinical pathologic factors for the prognosis of leiomyosarcoma. Around 90% of leiomyosarcomas are reported to be moderate to high grade [2]. Herein, we report four cases of leiomyosarcoma and discuss possible differential diagnoses.

2. Materials and Methods

Four patients with limb leiomyosarcomas based on patient records and postoperative pathological histological features were included in this retrospective study between June 2016 and June 2020.There were 3 males and 1 female with an average age of 41.5 years (21–70 years). All the cases whose primary symptom was asymptomatic except slowly enlarging painless soft tissue masses. The course of the disease was 0.5 year to 2years.Three of them arising in the subcutis of the thigh region, one in cubitus. The masses range from 2

Table 1: Demographics of the patients and follow-up data.

Case	Gender (M/F)	Age (year)	Site	Course (year)	Max diameter (cm)	Therapies	Follow-up
1	M	70	Left thigh	0.5	7	Extended resection +chemotherapy	Survive with 2 years
2	M	35	Right cubitus	1	3	Extended resection	No recurrence or metastases 2 years
3	M	21	Right thigh	1.2	8	Extended resection	No recurrence or metastases 1.5 years
4	F	40	Right thigh	2	6	Extended resection	No recurrence or metastases 3 years

to 8 cm in diameter. Gross total extended resections with 3-5 cm of normal tissue around the tumor and wide negative margins by intraoperative frozen sections were given for all patients. All the patients were primary tumors. And one patient with pulmonary metastasis later was managed with chemotherapy. Follow-up times are from 12 to 36 months (Table 1). All patients provided informed consent preoperatively.

3. Result

The postoperative course was uneventful, and functional exercises were progressively started with the help of rehabilitation therapist. Three of the patients had an uncomplicated recovery and showed no evidence of recurrence or metastases. The patient with pulmonary metastasis survived with 2 years of postoperation (Table 1). Typical case is illustrated in pictures at the end of the article (Figures 1(a)–1(e).

4. Discussion

Most leiomyosarcomas (LMS) are located in the mesentery, omentum majus, and retroperitoneum, with rare reports in the somatic soft tissue. LMS account for about 10%-15% of limb sarcomas, with predilection for the lower limbs, especially the proximal limb. This may be related to the abundant vasalium in the proximal limb [3]. The incidence of deep bone invasion by LMS in the somatic soft tissue is estimated to be approximately 10%, as first described by Evans in 1965 [4]. Fortunately, there were no deep bone invasions by LMS for the four patients. LMS in the somatic soft tissue most commonly occur in middle-aged and elderly patients with no obvious sex ratio correlations.

Causal factors have been identified for the etiology. A high rate of LMS in somatic soft tissues has been reported in acquired immunodeficiency syndrome (AIDS) and after kidney or liver transplantation. Smooth muscle cells infected by Epstein-Barr virus may be associated with tumor pathogenesis [5]. Hematogenous spread is a frequent event in the LMS of soft tissue, with the lung the most common site of metastasis. Clinical presentation is asymptomatic except slowly enlarging painless soft tissue masses. Enlarged lymph nodes in advanced cancer have been reported [6]. Both reported cases suffered a rapidly progressive lesion which was asymptomatic that vary from 0.5 year to 2 years. Surgical resection is the essential treatment of patients with LMS localized in the somatic soft tissue. The standard surgical procedure involves a complete excision with 3-5 cm of the normal tissue around the tumor and wide negative margins by intraoperative frozen sections, which is the most important prognostic factor for survival, with or without adjuvant chemotherapy and radiation therapy. One patient with pulmonary metastasis preoperation was managed with chemotherapy in our research. LMS localized in the somatic soft tissue have better overall survival than those arising in the retroperitoneum [7].

Iconography examination plays an important role in diagnosing LMS of the soft tissue. MRI images show irregular masses with poor defined boundaries and no obvious capsule surrounding the lesion. Small areas of necrotic cystic degeneration can also be seen within the tumor. Most lesions show nonuniform equisignal on T1WI and patchy high signal on T2WI. Lesions show significantly inhomogeneous enhancement, with a patchy area of low signal and no obvious enhancement in the center of the lesion [8]. CT imaging helped us identify whether there was any bone destruction adjacent to the tumor.

Although imaging examination help for LMS identification in the soft tissue, definite diagnosis depends on postoperative pathological histological features. ELMS of the soft tissue composed of cells showing distinct features of the smooth muscle lineage, which have been characterized as intersecting, sharply marginated fascicles of spindle cells with abundant eosinophilic cytoplasm, and elongated and hyperchromatic nuclei [9]. Proliferation of epithelioid cells with eosinophilic cytoplasm is seen in epithelioid leiomyosarcoma [10]. Immunohistochemical staining showed that vimentin, desmin, SMA, Ki-67, and HHF-35 are positive.

LMS of the soft tissue should be differentiated from benign tumors such as neurilemomas and neurofibromas. If a benign tumor is misdiagnosed preoperatively, local recurrence can occur due to incomplete resection. This can be found to grow along the peripheral nerve and the well-defined margins of benign neurogenic tumors and moderately to significantly enhanced and capsular for the parenchyma of the LMS of the soft tissue, which may help to differentiated from benign tumors [11].

Secondly, there is need to exclude important likely differential diagnosis of LMS in the soft tissue such as synoviosarcoma, rhabdomyosarcoma, malignant fibrous histiotoma, and malignant neurinoma. Synoviosarcoma mainly occurs in young adults (20 to 40 year olds). Localization of

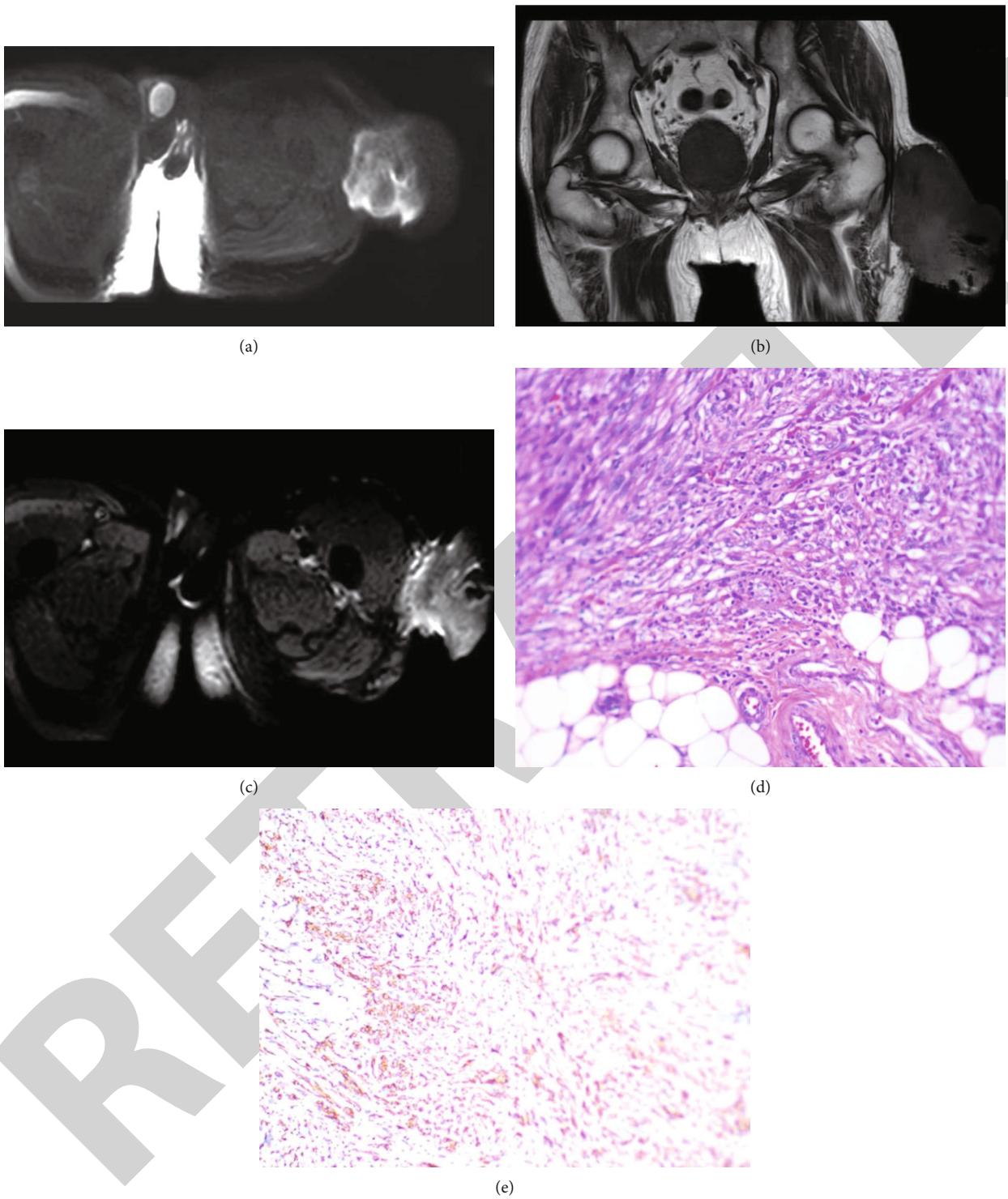

Figure 1: A 70-year-old man presented with a three-month history of a soft tissue mass in the subcutis of the left thigh. (a). Magnetic resonance imaging (MRI) revealed a fusiform mass shadow on the subcutis of the left thigh and diffusion-weighted imaging showing high signal. (b). Magnetic resonance imaging (MRI) revealed T1WI sequencing showing low signal. (c). Magnetic resonance imaging (MRI) revealed enhancement scan that showed lesion which was significantly intensify. (d). Histologic features of the lesion showed that the tumor was composed of densely arranged, abundant spindle cells with nuclei that were mild to moderately atypical, and proliferation of epithelioid cells(HE, ×200). (e). Tumor cells showing diffuse immunohistochemical positivity for SMA.

synoviosarcoma is mostly around the joints and is closely related to the joint capsule, peritendineum, and adjacent bone. The incidence of bone destruction is greater than 20%, which is higher than LMS in the soft tissue [12]. Rhabdomyosarcoma located in the muscle is another soft tissue malignant tumor that may be misdiagnosed as LMS. It is

Hindawi
BioMed Research International
Volume 2024, Article ID 9834610, 1 page
https://doi.org/10.1155/2024/9834610

Retraction

Retracted: Trophinin Is an Important Biomarker and Prognostic Factor in Osteosarcoma: Data Mining from Oncomine and the Cancer Genome Atlas Databases

BioMed Research International

Received 12 March 2024; Accepted 12 March 2024; Published 20 March 2024

This article has been retracted by Hindawi following an investigation undertaken by the publisher [1]. This investigation has uncovered evidence of one or more of the following indicators of systematic manipulation of the publication process:

(1) Discrepancies in scope

(2) Discrepancies in the description of the research reported

(3) Discrepancies between the availability of data and the research described

(4) Inappropriate citations

(5) Incoherent, meaningless and/or irrelevant content included in the article

(6) Manipulated or compromised peer review

The presence of these indicators undermines our confidence in the integrity of the article's content and we cannot, therefore, vouch for its reliability. Please note that this notice is intended solely to alert readers that the content of this article is unreliable. We have not investigated whether authors were aware of or involved in the systematic manipulation of the publication process.

Wiley and Hindawi regrets that the usual quality checks did not identify these issues before publication and have since put additional measures in place to safeguard research integrity.

We wish to credit our own Research Integrity and Research Publishing teams and anonymous and named external researchers and research integrity experts for contributing to this investigation.

The corresponding author, as the representative of all authors, has been given the opportunity to register their agreement or disagreement to this retraction. We have kept a record of any response received.

References

[1] P. Cai, Y. Lu, Z. Yin, X. Wang, X. Zhou, and Z. Li, "Trophinin Is an Important Biomarker and Prognostic Factor in Osteosarcoma: Data Mining from Oncomine and the Cancer Genome Atlas Databases," *BioMed Research International*, vol. 2021, Article ID 6885897, 9 pages, 2021.

Hindawi
BioMed Research International
Volume 2021, Article ID 6885897, 9 pages
https://doi.org/10.1155/2021/6885897

Research Article

Trophinin Is an Important Biomarker and Prognostic Factor in Osteosarcoma: Data Mining from Oncomine and the Cancer Genome Atlas Databases

Pan Cai,[1] Yan Lu,[2] Zhifeng Yin,[3] Xiuhui Wang,[1] Xiaoxiao Zhou,[1] and Zhuokai Li[1]

[1]*Department of Orthopedics, Zhoupu Hospital, Affiliated to Shanghai University of Medicine & Health Sciences, Shanghai 201318, China*
[2]*Department of Laboratory Medicine, Zhoupu Hospital, Affiliated to Shanghai University of Medicine & Health Sciences, Shanghai 201318, China*
[3]*Department of Orthopedics, Shanghai Zhongye Hospital, 200941 Shanghai, China*

Correspondence should be addressed to Zhuokai Li; zhuokaibone@163.com

Received 9 April 2021; Revised 5 May 2021; Accepted 8 June 2021; Published 7 July 2021

Academic Editor: Yun-Feng Yang

Osteosarcoma (OS) is a type of bone malignancy with a high rate of treatment failure. To date, few evident biomarkers for the prognostic significance of OS have been established. Oncomine was used to integrate RNA and DNA-seq data from the Gene Expression Omnibus (GEO), The Cancer Genome Atlas (TCGA), and the published literature. The correlation of the gene Trophinin (TRO) and different types of cancers was generated using the Cancer Cell Line Encyclopedia (CCLE) online tool. Prognostic values of featured Melanoma Antigen Gene (MAGE) members were further assessed by establishing the overall survival using the Kaplan-Meier plotter. Moreover, the online tool, Database for Annotation, Visualization and Integrated Discovery version (DAVID), was used to understand the biological meaning list of the genes. MAGEB10, MAGED2, TRO, MAGEH1, MAGEB18, MAGEB6, MAGEB4, MAGEB1, MAGED4B, MAGED1, MAGEB2, and MAGEB3 were significantly overexpressed in sarcoma. TRO was further demonstrated to be distinctively upregulated in osteosarcoma cell lines and associated with shorter overall survival. TRO may play an important role in the development of OS and may be a promising potential biomarker and prognostic factor.

1. Introduction

Osteosarcoma (OS) is the most common bone malignancy in young people, with over 50% of cases occurring in the first two decades of life [1]. Tremendous progress has been achieved in the past few decades in the field of OS therapy development including advances in surgical and diagnostic strategies and the use of combined chemotherapy [2]. Despite this progress, curative treatment of OS remains challenging with subsequent poor prognosis and shortened life expectancy [3]. Early diagnosis and treatment of OS, particularly with nonmetastatic OS, is crucial for improving the prognosis of OS patients [4]. Unfortunately, few distinctive diagnostic and prognostic biomarkers have been identified. A better understanding of the molecular and cellular biology and an identification of effective biomarkers involved in tumor initiation and progression are crucial for optimizing diagnosis and treatment of OS.

The TRO gene encodes for Trophinin, a member of the Melanoma Antigen Gene (MAGE) family, mediate the initial attachment of the blastocyst to the uterine epithelial cells during embryo implantation through a cell adhesion molecule complex in combination with bystin and tastin [5]. Furthermore, a prior study indicated that TRO is overexpressed in many trophoblastic cancers, which is of great importance for the progression of trophinin-expressing cancers [6]. TRO may therefore have a critical role in the development of different cancers, with a possible role in OS initiation and prognosis remaining elusive.

Rank	*P* value	Fold change	Gene	Reporter	Gene
1555	0.002	1.10	MAGEB10	23-027743364	MAGEB10
1625	0.002	1.13	MAGED2	23-054855032	MAGED2
1626	0.002	1.13	TRO	23-054969281	TRO
1760	0.002	1.14	MAGEH1	23-055495993	MAGEH1
1777	0.002	1.09	MAGEB18	23-026067578	MAGEB18
1778	0.002	1.09	MAGEB6	23-026122080	MAGEB6
1846	0.002	1.11	MAGEB4	23-030171159	MAGEB4
1847	0.002	1.11	MAGEB1	23-030175922	MAGEB1
1957	0.003	1.11	MAGED4B	23-051948381	MAGED4B
1973	0.003	1.11	MAGED1	23-051612542	MAGED1
2628	0.014	1.09	MAGEB2	23-030145860	MAGEB2
2629	0.014	1.09	MAGEB3	23-030162000	MAGEB3
4948	0.089	1.05	MAGEL2	15-021441028	MAGEL2
4949	0.089	1.05	NDN	15-021482594	NDN
8158	0.340	1.01	NDNL2	15-027348479	NDNL2
10795	0.625	−1.01	MAGEF1	03-185911689	MAGEF1
13322	0.852	−1.08	MAGEE2	23-074920671	MAGEE2
13324	0.852	−1.08	MAGEE1	23-075566334	MAGEE1
13617	0.868	−1.05	MAGEA1	23-152137012	MAGEA1
15031	0.943	−1.05	MAGEA6	23-151619685	MAGEA6

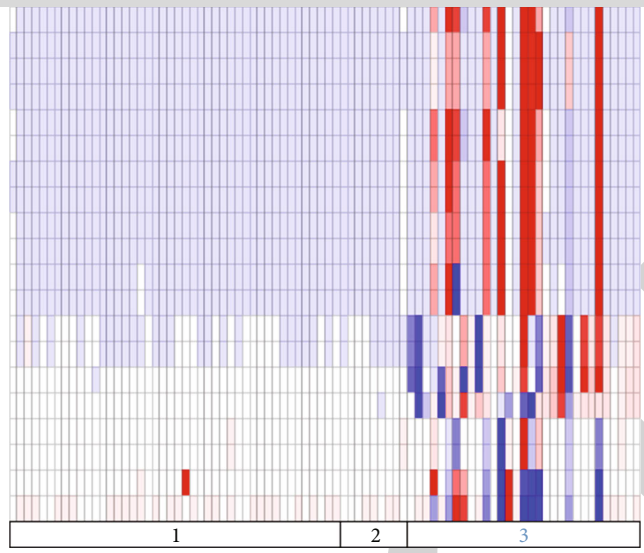

Figure 1

Median rank	*P* value	Gene
829.0	2.48*E*-4	TRO
1747.0	0.012	MAGED4B
1770.5	0.010	MAGED2
1973.0	0.003	MAGED1
3030.5	0.092	MAGEB10
3793.0	0.090	MAGEA5
4514.0	0.057	MAGEF1
4743.0	0.010	MAGEA3
4811.0	0.193	MAGEA12
4856.0	0.127	MAGEA9
4953.0	0.081	MAGEA6
5460.0	0.179	MAGEB18
5546.5	0.228	MAGEB4
5966.0	0.308	MAGEB2
5989.0	0.332	MAGEC1
6076.5	0.392	MAGEH1
6258.0	0.177	MAGEB1
6359.0	0.378	MAGEA1
6565.0	0.065	MAGEB6
6663.0	0.455	MAGEL2

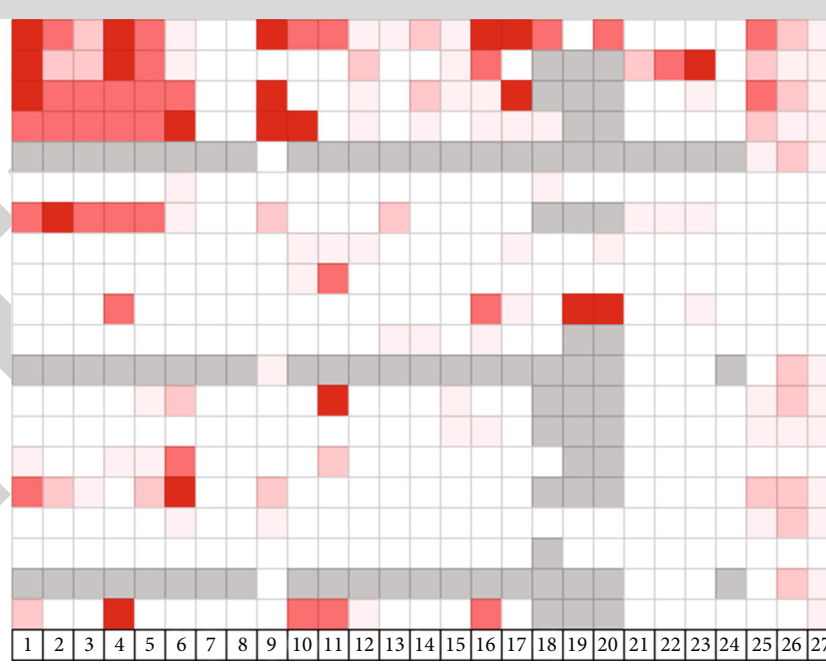

Figure 2

In the present research, we first investigated the diagnostic role and prognostic value of TRO in OS. Additionally, the underlying biological mechanism of TRO in OS was explored.

2. Materials and Methods

2.1. Oncomine Analysis. The Oncomine (https://www.oncomine.org) database integrates RNA and DNA-seq data from GEO, TCGA, and published literature. We can use Oncomine for differentially expressed gene analysis, clinical correlation analysis, and multigene coexpression analysis. The expression information of the MAGE family in sarcoma and coexpressed genes of the MAGE family were retrieved from Oncomine with the default setting of fold change > 2 and *P* value < 0.01.

2.2. CCLE Analysis. The CCLE database (https://portals.broadinstitute.org/ccle/home) is an online encyclopedia of a compilation of gene expression, chromosomal copy number, and massively parallel sequencing data from 1457 human cancer cell lines and 136,488 unique data sets, to

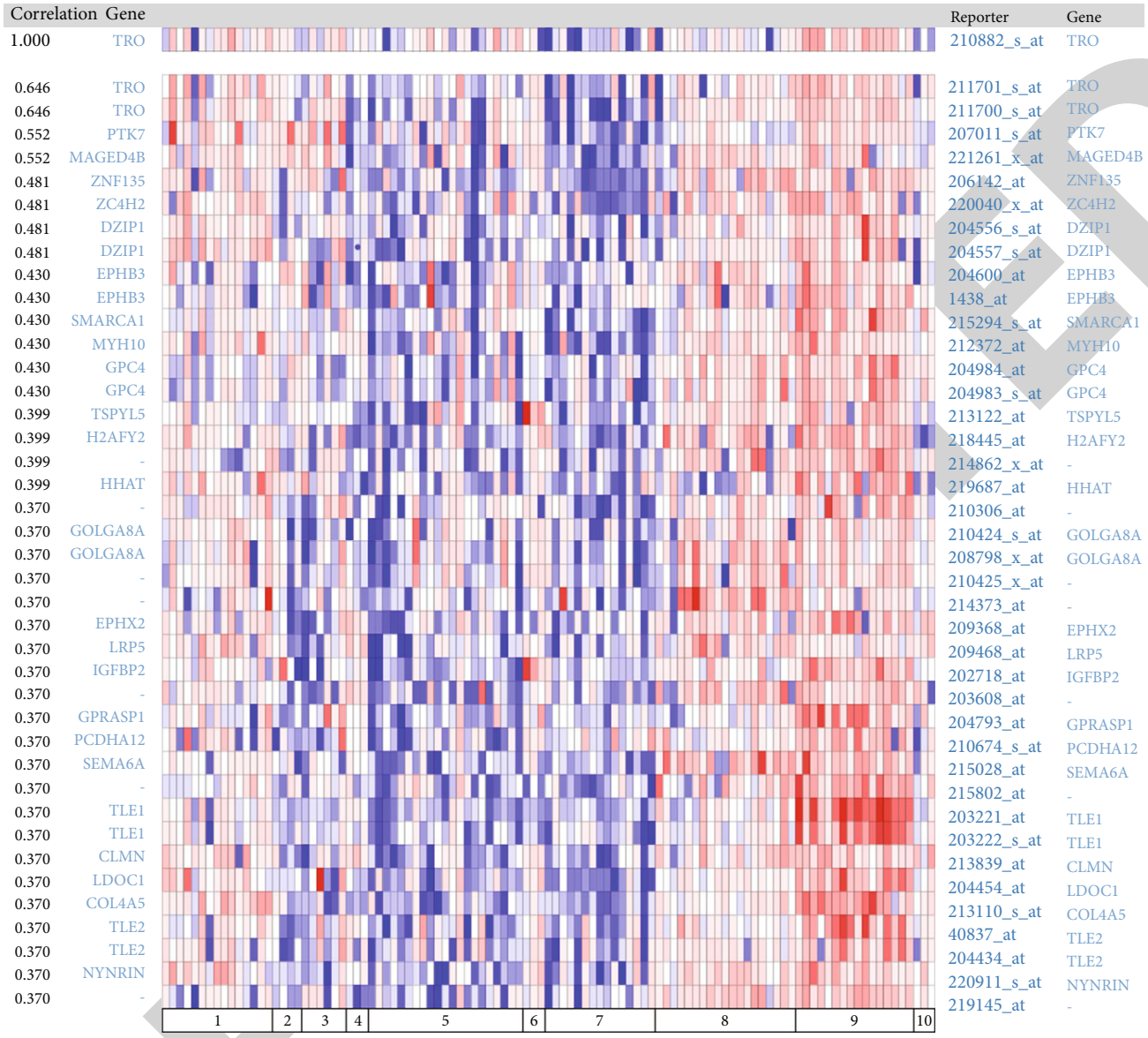

Figure 3

facilitate the identification of genetic, lineage, and predictors of drug sensitivity. The correlation of gene TRO and different types of cancers was generated using the CCLE online tool.

2.3. The Kaplan-Meier Plotter Survival Analysis. The MAGE members that were shown to be specifically highly expressed in sarcoma samples and their coexpressed genes were further assessed by displaying the overall survival using the Kaplan-Meier plotter (http://kmplot.com/analysis/). The Kaplan-Meier plotter is an online tool applied to assess the effect of 54,675 genes on survival using 13,316 cancer samples in 21 cancer types. Sources for the databases include GEO, EGA, and TCGA. The primary purpose of the tool is a meta-analysis-based discovery and validation of survival biomarkers. $P < 0.01$ was considered to indicate a statistically significant result.

2.4. Gene Ontology (GO) and Kyoto Encyclopedia of Genes and Genomes (KEGG) Pathway Enrichment Analysis. The online tool Database for Annotation, Visualization and Integrated Discovery version (DAVID) Bioinformatics Resources 6.8 was used to understand the biological meaning of the list of genes. GO enrichment and KEGG pathway analyses were performed with DAVID. The GO and KEGG pathway analysis result was visualized by the ggPlot2 R package. The relationship between GO terms was calculated in Cytoscape 3.7.2, using the plug-in software ClueGO.

3. Results and Discussion

3.1. Oncomine Analysis. Oncomine analysis revealed that for MAGE family, MAGEB10, MAGED2, TRO, MAGEH1, MAGEB18, MAGEB6, MAGEB4, MAGEB1, MAGED4B, MAGED1, MAGEB2, and MAGEB3 were significantly

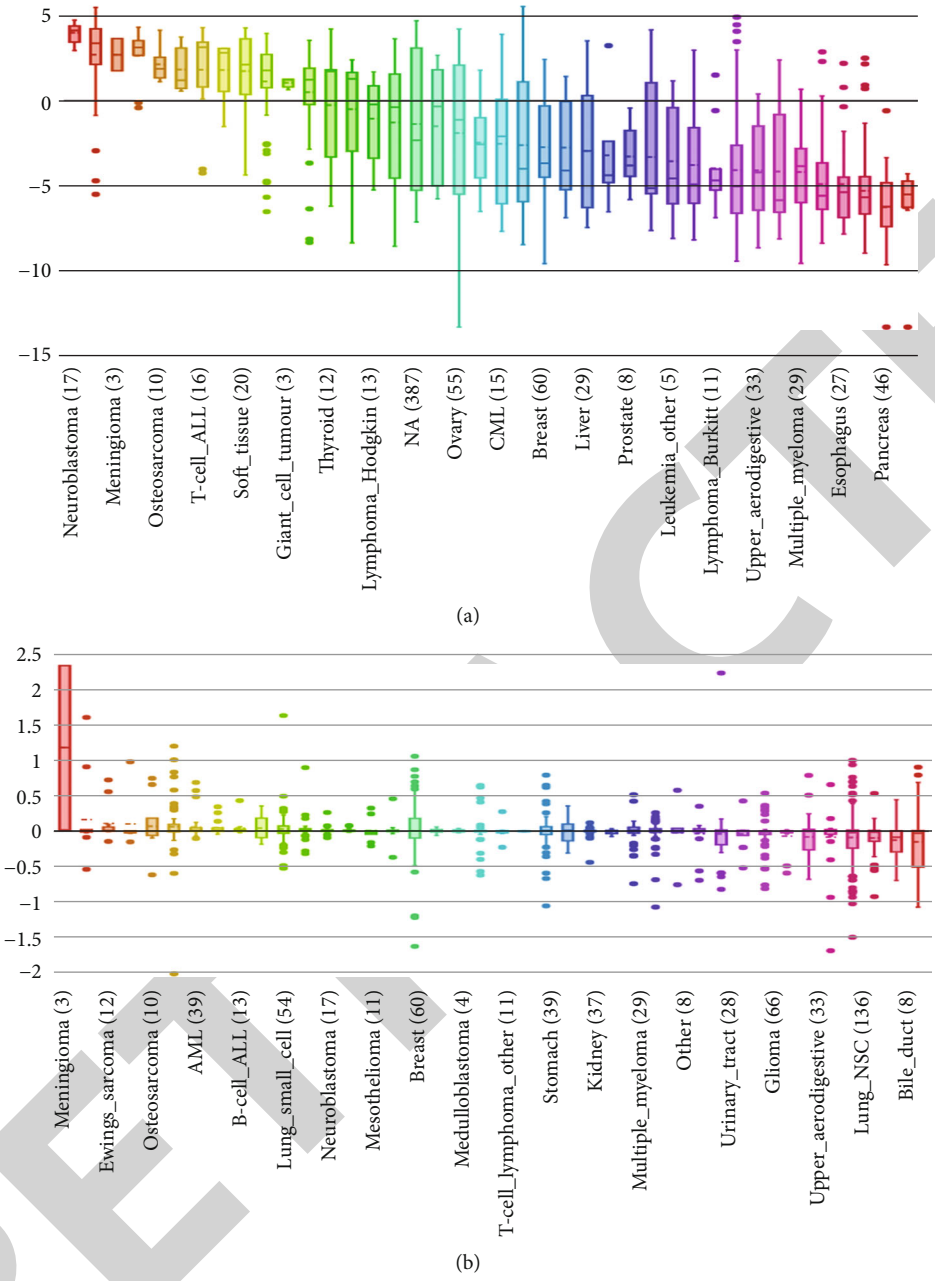

Figure 4: Continued.

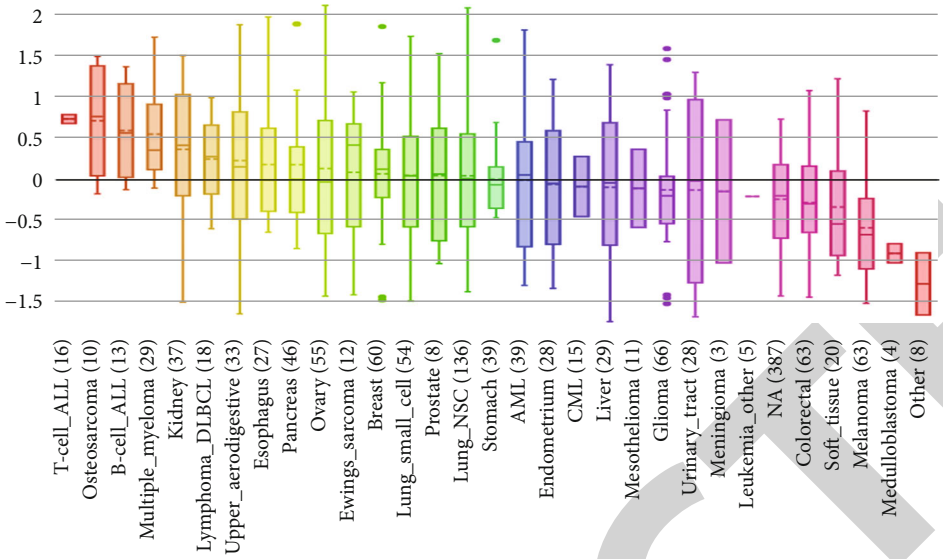

(c)

Figure 4

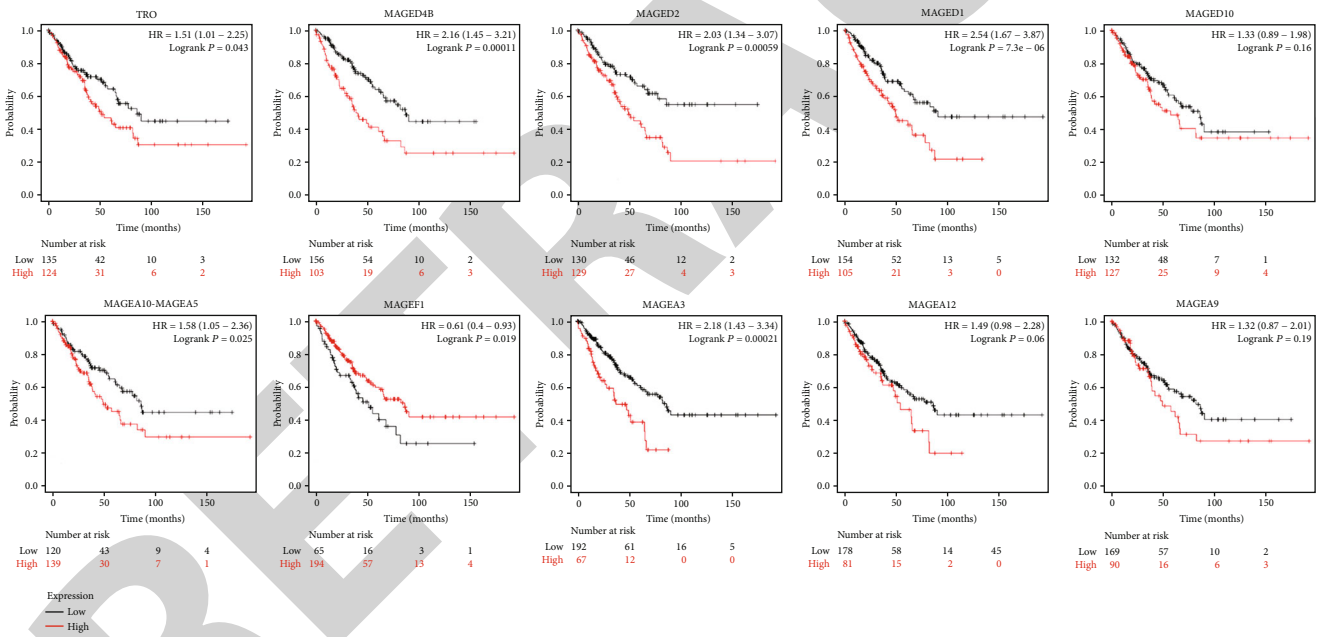

Figure 5

overexpressed in sarcoma, based on the TCGA database (Figure 1). The meta-analysis combined 27 studies ranking the MAGE family genes expressed in sarcoma by P value and median. TRO was the top gene which was significantly upregulated in sarcoma (Figure 2). The coexpressed genes of TRO were identified using the coexpression online tool in Oncomine. The top ten genes were PTK7, ZNF135, ZC4H2, DZIP1, EPHB3, SMARCA1, MYH10, GPC, TSPYL5, and H2AFY2 (Figure 3).

3.2. CCLE Analysis. CCLE analysis agreed with the Oncomine results demonstrating that TRO was distinctively upregulated in the osteosarcoma cell lines (Figure 4(a)). In addition, the DNA copy number was relatively high in osteosarcoma (Figure 4(b)). Moreover, the Achilles shRNA knockdown results showed osteosarcoma was ranked second when ordered by dependency probability with TRO (Figure 4(c)).

3.3. The Kaplan-Meier Plotter Survival Analysis. For the top 10 MAGE family genes of TRO, MAGED4B, MAGED2, MAGED1, MAGEA5, MAGEF1, and MAGEA3 were associated with shorter overall survival ($P < 0.05$) (Figure 5). For the top 10 coexpressed genes of TRO, PTK7, ZNF135, DZIP1, EPHB3, SMARCA1, GPC4, and TSPYL5 were associated with shorter overall survival ($P < 0.05$) (Figure 6).

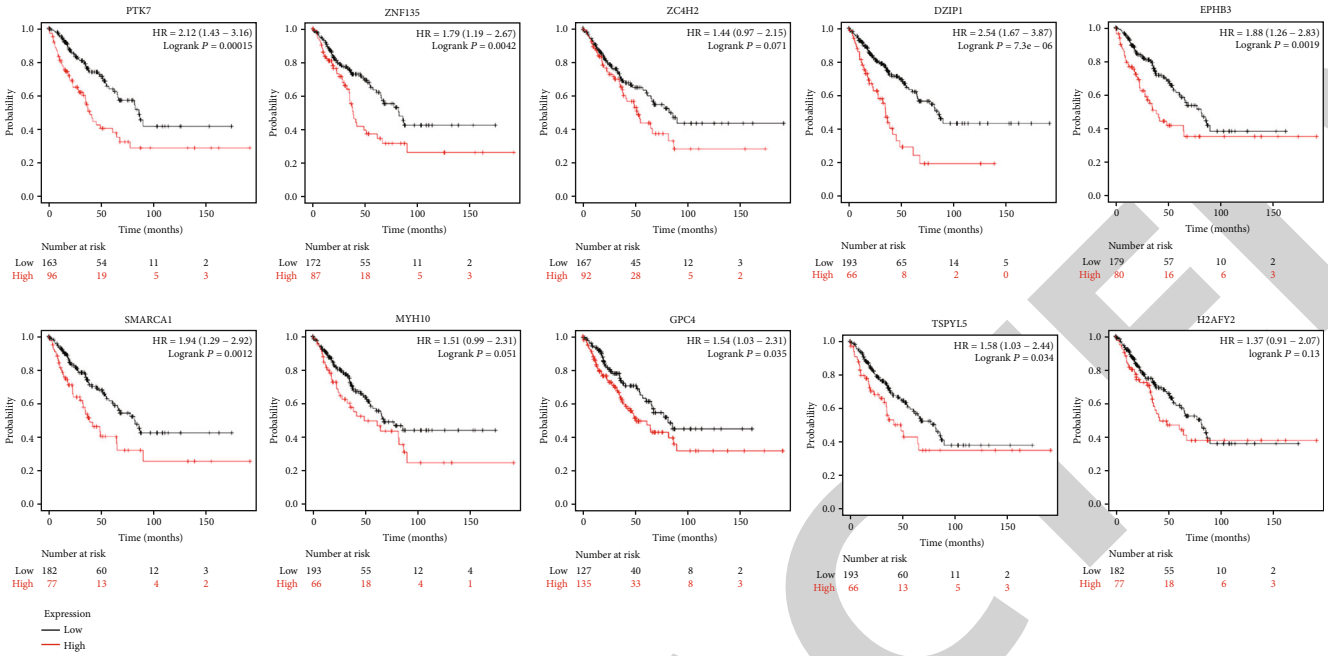

Figure 6

3.4. Gene Ontology (GO) and Kyoto Encyclopedia of Genes and Genomes (KEGG) Pathway Enrichment Analysis. The MAGE family and coexpressed genes were significantly enriched in the biological progress of nervous system development, cochlea morphogenesis, and positive regulation of mesenchymal cell proliferation; in cellular components of coreceptor activity involved in the Wnt signaling pathway, protein binding, and transmembrane-ephrin receptor activity; in molecular functions of integral component of plasma membrane, synapse, and intrinsic component of plasma membrane; in KEGG pathways of Wnt signaling pathway, axon guidance pathways, and signaling pathways regulating pluripotency of stem cells (Figure 7 and Table 1).

4. Discussion

OS is the most common type of bone malignancy with a high incidence in teenagers [7]. Early diagnosis and effective treatment of OS could remarkably decrease the high OS-related mortality [8, 9]. However, current therapies for advanced OS remain poor due to the lack of specific molecular targets. In this study, we first aimed to investigate the diagnostic role and prognostic value of TRO in OS.

TRO is a member of MAGE family members of which have previously been reported as effective targets for cancer immunotherapy [10]. TRO is a type of adhesion molecule with specific expression on human trophoblast cells [11]. Trophoblastic cancer patients with high expression of this molecule often have poor prognosis [12]. Among those with positive expression of TRO, HMGB1/RAGE are often coexpressed, suggesting that TRO can promote tumor invasion through an HMGB1/RAGE signaling pathway [13]. Similarly, high levels of TRO were found to be related with poor prognosis in liver and gallbladder cancer [14, 15]. It has also been demonstrated that TRO enhanced invasion and promoted colorectal cancer through a mechanism involving HMGB1/RAGE [11]. However, the function of TRO in the prognosis and progression of OS had not yet been fully elucidated.

This study first investigated the function and clinical significance of TRO in OS patients via the clinical data of OS patients and public expression profiles. The results indicated that the members of the MAGE family, including MAGEB10, MAGED2, TRO, MAGEH1, MAGEB18, MAGEB6, MAGEB4, MAGEB1, MAGED4B, MAGED1, MAGEB2, and MAGEB3, were significantly overexpressed in sarcoma tissues. And TRO was further demonstrated to be distinctively upregulated in OS cell lines and associated with shorter overall survival. Moreover, it was indicated from the statistical analysis that there was an evident correlation between TRO expression levels and a relatively poor prognosis. It was verified by further univariate and multivariate analyses that TRO could be used as a potential prognostic biomarker for OS patients.

To the best of our knowledge, the regulation of the expression of TRO in OS patients has not yet been explored. A limited number of studies have reported that overexpression of other MAGE family numbers, such as melanoma antigen family A (MAGEA), and preferentially expressed antigen in melanoma (PRAME) are related to OS progression [16]. However, the specific mechanism of MAGE family contribution to the occurrence, development, and prognosis of OS is still unknown. The present study suggested that TRO can act as a promising biomarker for OS diagnosis and prognosis. Nevertheless, the current study presented results derived solely from bioinformatics analyses, and further experimental evidence is required to validate these findings.

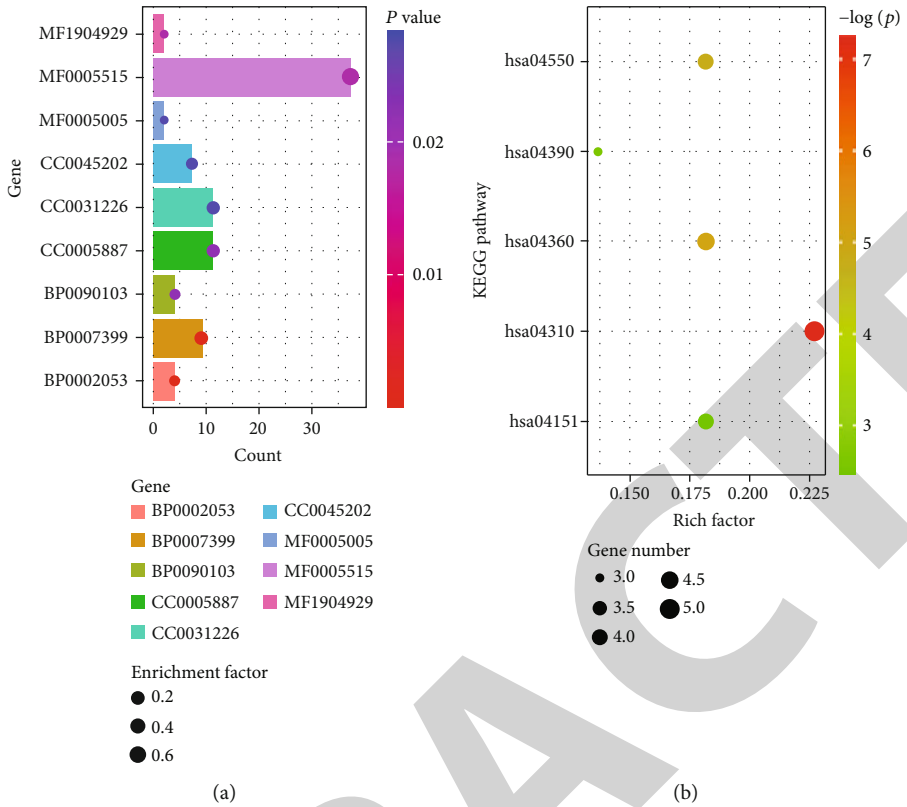

(a) (b)

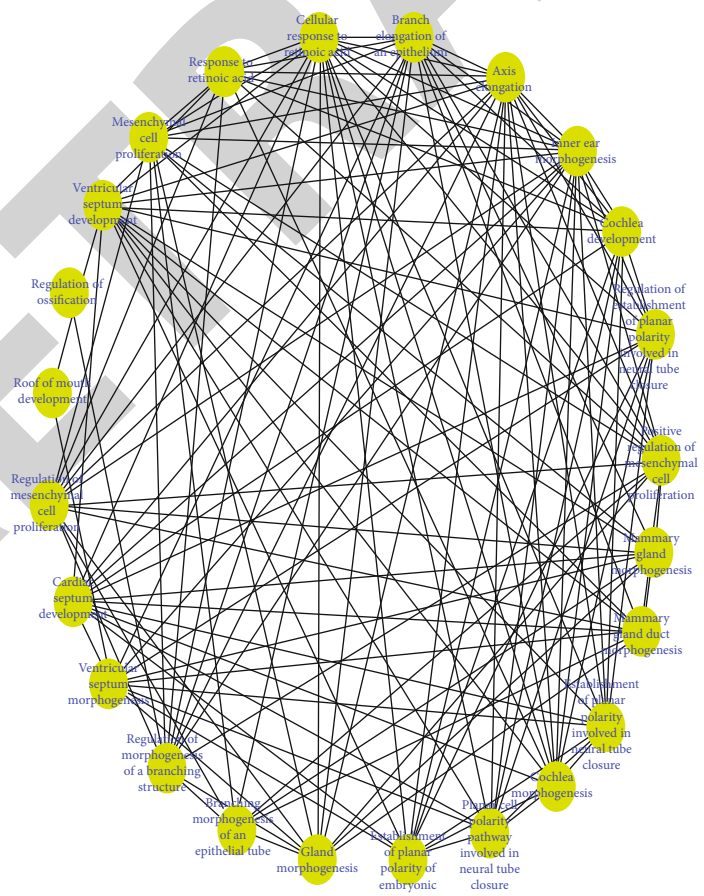

(c)

Figure 7

Table 1: Functional and KEGG pathway enrichment analysis of MAGE family and co-expressed genes. Top 3 terms were selected according to P-value.

(a) Biological processes

Term	Name	Count	P-value	Genes
GO:0007399	Nervous system development	9	2.22E-6	SEMA6A, EFNB3, DPYSL4, MDK, ZC4H2, PCDHB3, APBA2, PAFAH1B3, GPM6B
GO:0090103	Cochlea morphogenesis	4	3.90E-5	FZD2, PTK7, WNT5A, SOX9
GO:0002053	Positive regulation of mesenchymal cell proliferation	4	6.53E-5	WNT5A, LRP5, SOX9, FGFR2

(b) Molecular functions

Term	Name	Count	P-value	Genes
GO:1904929	Coreceptor activity involved in Wnt signaling pathway	2	1.83E-2	PTK7, GPC4
GO:0005515	Protein binding	36	1.85E-2	ISYNA1, MAGED1, ZC4H2, MAGEF1, LRP5, EFNA4, MAGEA9, TRO, CCND2, DPYSL4, SOX9, GPRASP1, MYH10, MAGEA3, TLE2, SEMA6A, FZD2, TLE1, CADM1, IGFBP2, WNT5A, LDOC1, SMARCA1, TBX3, PTK7, ADGRL1, ZNF415, MAGED2, BCOR, DZIP1, APBA2, ZNF334, PAFAH1B3, FGFR2, TSPYL5, ITM2C
GO:0005005	Transmembrane-ephrin receptor activity	2	2.74E-2	EFNB3, EFNA4

(c) Cellular components

Term	Name	Count	P-value	Genes
GO:0005887	Integral component of plasma membrane	11	2.19E-2	TRO, SEMA6A, EFNB3, CADM1, TUSC3, PTK7, PCDHB3, GPC4, EFNA4, FGFR2, EPHB3
GO:0045202	Synapse	7	2.53E-2	CADM1, ZC4H2, COL4A5, ADGRL1, APBA2, MYH10, FGFR2
GO:0031226	Intrinsic component of plasma membrane	11	2.82E-2	TRO, SEMA6A, EFNB3, CADM1, TUSC3, PTK7, PCDHB3, GPC4, EFNA4, FGFR2, EPHB3

(d) KEGG pathways

Term	Name	Count	P-value	Genes
hsa04310	Wnt signaling pathway	4	7.12E-4	FZD2, CCND2, WNT5A, LRP5, GPC4
hsa04360	Axon guidance	4	6.41E-3	SEMA6A, EFNB3, EFNA4, EPHB3
hsa04550	Signaling pathways regulating pluripotency of stem cells	4	8.39E-3	FZD2, WNT5A, FGFR2, TBX3

5. Conclusions

Overall, as TRO is overexpressed in human OS tissues, a poor prognosis can be predicted by a high level of TRO. Therefore, our findings highlight that TRO may be an important biomarker for the prognosis and progression of OS.

Data Availability

The data used to support the findings of this study are available from the corresponding author upon request.

Conflicts of Interest

The authors declare that there is no conflict of interest regarding the publication of this paper.

Authors' Contributions

Pan Cai and Yan Lu contributed equally to this work.

Acknowledgments

This study was supported by the Construction of Key Medical Specialties in Shanghai (ZK2019-B05), the Shanghai

Hindawi
BioMed Research International
Volume 2024, Article ID 9826076, 1 page
https://doi.org/10.1155/2024/9826076

Retraction

Retracted: Nomogram for Predicting Deep Venous Thrombosis in Lower Extremity Fractures

BioMed Research International

Received 12 March 2024; Accepted 12 March 2024; Published 20 March 2024

This article has been retracted by Hindawi following an investigation undertaken by the publisher [1]. This investigation has uncovered evidence of one or more of the following indicators of systematic manipulation of the publication process:

(1) Discrepancies in scope

(2) Discrepancies in the description of the research reported

(3) Discrepancies between the availability of data and the research described

(4) Inappropriate citations

(5) Incoherent, meaningless and/or irrelevant content included in the article

(6) Manipulated or compromised peer review

The presence of these indicators undermines our confidence in the integrity of the article's content and we cannot, therefore, vouch for its reliability. Please note that this notice is intended solely to alert readers that the content of this article is unreliable. We have not investigated whether authors were aware of or involved in the systematic manipulation of the publication process.

Wiley and Hindawi regrets that the usual quality checks did not identify these issues before publication and have since put additional measures in place to safeguard research integrity.

We wish to credit our own Research Integrity and Research Publishing teams and anonymous and named external researchers and research integrity experts for contributing to this investigation.

The corresponding author, as the representative of all authors, has been given the opportunity to register their agreement or disagreement to this retraction. We have kept a record of any response received.

References

[1] Z. Lin, B. Mi, X. Liu et al., "Nomogram for Predicting Deep Venous Thrombosis in Lower Extremity Fractures," *BioMed Research International*, vol. 2021, Article ID 9930524, 8 pages, 2021.

Hindawi
BioMed Research International
Volume 2021, Article ID 9930524, 8 pages
https://doi.org/10.1155/2021/9930524

Research Article

Nomogram for Predicting Deep Venous Thrombosis in Lower Extremity Fractures

Ze Lin,[1] **Bobin Mi**,[1] **Xuehan Liu**,[2] **Adriana C. Panayi**,[3] **Yuan Xiong**,[1] **Hang Xue**,[1] **Wu Zhou**,[1] **Faqi Cao**,[1] **Jing Liu**,[1] **Liangcong Hu**,[1] **Yiqiang Hu**,[1] **Lang Chen**,[1] **Chenchen Yan**,[1] **Xudong Xie**,[1] **Junfei Guo**,[4,5] **Zhiyong Hou**,[4,5] **Yun Sun**,[1] **Yingze Zhang**,[4,5] **Yu Hu**,[6] **and Guohui Liu**[1]

[1]*Department of Orthopaedics, Union Hospital, Tongji Medical College, Huazhong University of Science and Technology, Jiefang Road. 1277#, Wuhan, 430022 Hubei, China*
[2]*Tongji Medical College, Huazhong University of Science and Technology, Wuhan 430022, China*
[3]*The Division of Plastic Surgery, Brigham and Women's Hospital, Harvard Medical School, Boston, MA, USA*
[4]*Department of Orthopaedic Surgery, The Third Hospital of Hebei Medical University, No. 139 Ziqiang Road, Shijiazhuang, 050051 Hebei, China*
[5]*Key Laboratory of Biomechanics of Hebei Province, Shijiazhuang, 050051 Hebei, China*
[6]*Institute of Hematology, Union Hospital, Tongji Medical College, Huazhong University of Science and Technology, Wuhan, 430022 Hubei, China*

Correspondence should be addressed to Yun Sun; 627224540@qq.com, Yingze Zhang; dryzzhang@126.com, Yu Hu; dr_huyu@126.com, and Guohui Liu; liuguohui@hust.edu.cn

Received 23 March 2021; Accepted 29 May 2021; Published 23 June 2021

Academic Editor: Andrea Scribante

Deep venous thrombosis (DVT) is a common complication in patients with lower extremity fractures, causing delays in recovery short-term and possible impacts on quality of life long-term. Early prediction and prevention of thrombosis can effectively reduce patient pain while improving outcomes. Although research on the risk factors for thrombosis is prevalent, there is a stark lack of clinical predictive models for DVT occurrence specifically in patients with lower limb fractures. In this study, we aim to propose a new thrombus prediction model for lower extremity fracture patients. Data from 3300 patients with lower limb fractures were collected from Wuhan Union Hospital and Hebei Third Hospital, China. Patients who met our inclusion criteria were divided into a thrombosis and a nonthrombosis group. A multivariate logistic regression analysis was carried out to identify predictors with obvious effects, and the corresponding formulas were used to establish the model. Model performance was evaluated using a discrimination and correction curve. 2662 patients were included in the regression analysis, with 1666 in the thrombosis group and 996 in the nonthrombosis group. Predictive factors included age, Body Mass Index (BMI), fracture-fixation types, energy of impact at the time of injury, blood transfusion during hospitalization, and use of anticoagulant drugs. The discriminative ability of the model was verified using the C-statistic (0.676). For the convenience of clinical use, a score table and nomogram were compiled. Data from two centers were used to establish a novel thrombus prediction model specific for patients with lower limb fractures, with verified predictive ability.

1. Introduction

Lower limb fractures account for approximately one-third of fracture patients [1–3], with a higher incidence in the elderly population. Consequently, given the aging population, lower limb fractures are on the rise. Among hospitalized patients, trauma patients have the highest risk of developing deep venous thrombosis (DVT), with the risk reported to be 13-fold higher than nontrauma patients [4, 5].

Further, lower limb fractures are a well-known risk factor for DVT occurrence [6]. DVT is in turn the third leading cause of cardiovascular death worldwide [7, 8] and also a major complication limiting recovery in patients with lower limb fractures [6, 9].

Thrombosis in patients with fractures is primarily formed in the deep veins of the lower extremities, which may result in swelling and pain in the patient's lower extremities. When the thrombus dislodges, it may cause life-threatening complications such as pulmonary embolism [7, 10–12]. A large number of studies have investigated the diagnosis and treatment of DVT. Specific advances include the combination of ultrasound, D-dimer, and clinical evaluation for thrombosis diagnosis [13, 14]; the use of small RNA molecules as new diagnostic markers [15, 16],; and the combination therapy and standard treatment with anticoagulation and antithrombotic drugs [7, 9]. In comparison to the large strides that have been made in the treatment of thrombosis, efforts to increase early prediction and prevention of DVT—which are arguably more effective and more efficient—have been minimal. Therefore, early prediction of thrombosis has become a major focus of current research.

An increasing number of studies have strove to identify the factors associated with DVT occurrence during hospitalization of patients with lower limb fractures [8, 17–19]. Such studies have offered a better understanding of the factors associated with increased DVT risk. However, whether to take the prevention of DVT is usually based on a physician's experience and on patient symptoms. Although practical, this approach may delay the prevention and treatment of DVT. Identification of patients who are at the highest risk of DVT may enable the provision of timely and effective therapies, thereby avoiding DVT occurrence.

Although there are several prediction models for venous thrombosis, like Caprini Risk Assessment Model, these are not specific to lower extremity fractures and, hence, have several limitations if used in that context. First, some tools already used in clinic fail to include factors that may affect thrombosis which are specific to fracture patients, including energy of impact and surgical method. This highlights the need for a more targeted prediction model. Second, some studies focus on the effect of a single risk factor for thrombosis in fracture patients [20, 21]. However, the occurrence of thrombosis is a relatively complicated, multifactorial process [6]. Therefore, the ability of single factor prediction is limited. Furthermore, some studies that do include multiple influencing factors fail to establish a clear clinical predictive model or a scoring table that can be applied by physicians in a healthcare setting [22–24]. In order to be able to translate such research results to patient care, a prediction model must be established. The primary aim of this study is to develop a model for predicting the risk of DVT following a lower limb fracture and, ultimately, offers a straight-to-clinic/hospital nomogram that can change current practice.

2. Materials and Methods

2.1. Study Population. This retrospective cohort study consisted of two groups (thrombosis group and nonthrombosis group) of patients with lower limb fractures who underwent surgery at Wuhan Union Hospital and Hebei Third Hospital, China. Patients with hip, femur, or tibial fibula fractures were included in the study. At the same time, patients who had experienced a DVT prior to the fracture were excluded from the study. The time frame for the collection of medical records was from January 2016 to January 2019. The information collected consisted of 18 risk factors linked to DVT occurrence in the lower extremities, such as sex, age, site of fracture, history of cardiovascular disease, and BMI. The current study was approved by the Ethics Committee of Union Hospital, Tongji Medical College, Huazhong University of Science and Technology.

2.2. Clinical Outcomes and Definitions. The defined outcome was the occurrence of lower extremity DVT. Venous ultrasound is the gold standard for establishing whether DVT has formed in the lower extremities [25, 26]. When the patient's lower extremity venous ultrasound results show that venous thrombosis has formed, the patient was included in the thrombosis group. All lower extremity venous ultrasound findings included in this study were recorded in the patient's medical history data during hospitalization. In patients with femur or tibia/fibula fractures, the venous ultrasound was performed on the noninjured lower extremity. In patients with hip fractures, the test was performed on both lower limbs, and the result of the side with the more severe thrombosis was recorded. Patients who did not undergo a lower limb venous ultrasound examination during hospitalization were excluded from the analysis.

2.3. Selection of Predictors. Firstly, we selected the factors that significantly affect the formation of thrombus as potential predictors. A list of potential predictors was compiled from a search of the relevant literature as well as through clinical judgment. These variables were sex, age, BMI, fracture site, energy of the traumatic impact, open wound, traumatic brain injury, cardiovascular history, history of type II diabetes, smoking history, triglyceride (TG), high-density lipoprotein (HDL), low-density lipoprotein (LDL), D-dimer, prothrombin time (PT), activated partial thromboplastin time (APTT), thrombin time (TT), fibrinogen (FIB), duration of surgery, fracture fixation types, blood transfusion during hospitalization (red blood cells), and anticoagulation drugs (low-molecular-weight heparin sodium; Table 1). The fracture sites were divided into hip, femur, and tibia/fibula. Traumatic brain injury was determined through head imaging. Fracture fixation types included internal fixation, external fixation, and others.

2.4. Missing Data. In this retrospective study, 19.33% ($n = 638$) of patients had missing medical history information or test results due to the long review period. Participants with missing ultrasound results were also excluded. In the case of participants with missing basic information, a multiple filler method was used to supplement the data.

2.5. Model Building. Data analysis of the individual variables was performed using χ^2 or CMH-χ^2, Fisher exact probability

Table 1: Patients characteristics and univariate associations for thrombosis-related risk factors.

Risk factor	Thrombosis group ($n = 1666$)	Nonthrombosis group ($n = 996$)	p value
Sex [n (%)]			0.0018[#]
Male	870 (52.22%)	458 (45.98%)	
Female	796 (47.78%)	538 (54.02%)	
Age [median (IQR)]	73 (25.5)	64 (34)	<0.0001[@]
BMI [median (IQR)]	23.46 (4.72)	23.88 (4.89)	0.0023[@]
Fracture site [n (%)]			0.001[#]
Tibia/fibula	299 (17.95%)	88 (8.84%)	
Femur	1199 (71.97%)	835 (83.84%)	
Hip	168 (10.08%)	73 (7.33%)	
Energy [n (%)]			0.1085[#]
Low	1209 (72.57%)	751 (75.40%)	
High	457 (27.43%)	245 (24.60%)	
Open wound [n (%)]			0.0014[#]
No	1481 (88.90%)	923 (92.67%)	
Yes	185 (11.10%)	73 (7.33%)	
Traumatic brain injury [n (%)]			0.1611[#]
No	1553 (93.22%)	942 (94.58%)	
Yes	113 (6.78%)	54 (5.42%)	
Cardiovascular history [n (%)]			<0.0001[#]
No	1102 (66.15%)	579 (58.13%)	
Yes	564 (33.85%)	417 (41.87%)	
History of type II diabetes [n (%)]			0.0151[#]
No	1447 (86.85%)	831 (83.43%)	
Yes	219 (13.15%)	165 (16.57%)	
Smoking history [n (%)]			0.5171[#]
No	1482 (88.96%)	894 (89.76%)	
Yes	184 (11.04%)	102 (10.24%)	
Blood lipid [median (IQR)]			
TG	1.04 (0.72)	1.04 (0.67)	0.3573[@]
HDL	1.17 (0.5)	1.20 (0.44)	0.0971[@]
LDL	2.24 (0.95)	2.27 (0.92)	0.1570[@]
D-dimer [median (IQR)]	2.2 (3.82)	1.99 (3.14)	0.1570[@]
Clotting function [median (IQR)]			
TT	15.3 (2.8)	15.1 (2.4)	0.0209[@]
PT	12.4 (2.00)	12.1 (1.7)	<0.0001[@]
APTT	29.4 (6.3)	30.8 (7.9)	<0.0001[@]
FIB	3.6 (1.6)	3.6 (1.3)	0.4257[@]
Duration of surgery [median (IQR)]	2.0 (1.3)	2.0 (1.2)	0.3389[@]
Fracture fixation type [n (%)]			<0.0001[#]
Internal fixation	1266 (75.99%)	882 (88.55%)	
External fixation	117 (7.02%)	22 (2.21%)	
Other types	283 (16.99%)	92 (9.24%)	

Table 1: Continued.

Risk factor	Thrombosis group ($n = 1666$)	Nonthrombosis group ($n = 996$)	p value
Blood transfusion during hospitalization [n (%)]			<.0001[#]
No	879 (52.76%)	348 (34.94%)	
Yes	787 (47.24%)	648 (65.06%)	
Anticoagulation drugs [n (%)]			<0.0001[*]
No	312 (18.73%)	42 (4.22%)	
Yes	1354 (81.27%)	954 (95.78%)	

[#]Comparison among groups using χ^2 or CMH-χ^2; [*]Comparison among groups using Fisher's exact probability test; [@]Comparison among groups using the Wilcoxon rank-sum test; IQR: interquartile range.

Table 2: Multivariate logistic regression analysis.

Risk factor	Coef (β)	Wald-χ^2	p value	OR	95% CI for OR
Intercept	-5.0642	-11.37	<.0001	—	—
Age	0.0192	7.16	<.0001	1.02	1.01-1.02
BMI	0.0484	4.05	<.0001	1.05	1.03-1.07
Energy	0.4054	3.51	0.0004	1.45	1.16-1.88
Fracture fixation type					
External fixation	Ref				
Other types	0.3807	1.38	0.1677	1.46	0.85-2.51
Internal fixation	0.9015	3.63	0.0003	2.46	1.51-4.01
Blood transfusion during hospitalization	0.3868	4.26	<.0001	1.47	1.23-1.76
Anticoagulation drugs	1.1537	6.49	<.0001	3.17	2.24-4.49

test, and Wilcoxon rank-sum test for between-group comparison to identify variables significantly associated with DVT. Risk factors with significant univariate associations ($p < 0.05$) were incorporated into the multivariate model. The regression coefficients β, OR, and 95% CI for each risk factor were estimated by constructing a multivariate logistic regression model that incorporated the risk factors primarily considered in the regression model. Nomogram coefficients for each variable were calculated based on coefficients from logistic regression and data according to the formula: $\text{Nomogram}i = (\max(Wi) - \min(Wi)) * \beta i$. In this formula, max (W) and min (W) represent the maximum and minimum values of each variable. Subsequently, we selected age as the scoring scale, with a total score of 100. After clarifying the score corresponding to age, we calculated the score corresponding to each variable according to the coefficient: $\text{Point}i = 100 * (\text{Nomogram}i/\text{Nomogramage})/(\max(Wi) - \min(Wi))$. In the model testing process, internal validation of the models was conducted using the bootstrap method with 1000 replicates. And we used the c-statistic to measure the discrimination of our model. This study was performed according to the Transparent Reporting of a multivariable prediction model for Individual Prognosis or Diagnosis (TRIPOD) statement.

2.6. Sample Size. In this retrospective study, we collected 3300 medical records from two centers. 638 records were not eligible for use in the model building process due to missing data or examination results. The remaining 2662 were included in the clinical prediction model building. According to established criteria for constructing clinical prediction models, this amount of data is adequate for model construction [27].

2.7. General Statistical Methods. Model building and nomogram plotting were performed using the rms package in R (version 3.6.1; Windows; R Core Team [28]) through RStudio (version 1.2.5001; R Studio Team [29]).

3. Results

3.1. Sample Characteristics and Outcomes. Patient characteristics are summarized in Table 1. We collected the medical records of thrombotic patients ($n = 1666$) and nonthrombotic patients ($n = 996$). 2034 patients were diagnosed with femur fractures and 387 patients were diagnosed with tibia/fibula fractures. In the thrombosis group, 870 (52.22%) of the patients were male, the median age was 73 years old, the majority (66.15%) of patients had a history of cardiovascular disease, 1447 (86.85%) patients did not have a history of type II diabetes, and nearly half (47.24%) of the patients had a blood transfusion during their hospitalization. In the nonthrombosis group, median BMI was 23.88, 73 (7.33%) patients had an open wound, most (94.58%) patients did not have a traumatic brain injury, and only a few (4.22%) patients were not treated with anticoagulation drugs. There was no significant difference between the groups in terms of traumatic brain injury occurrence, smoking history, blood lipid levels,

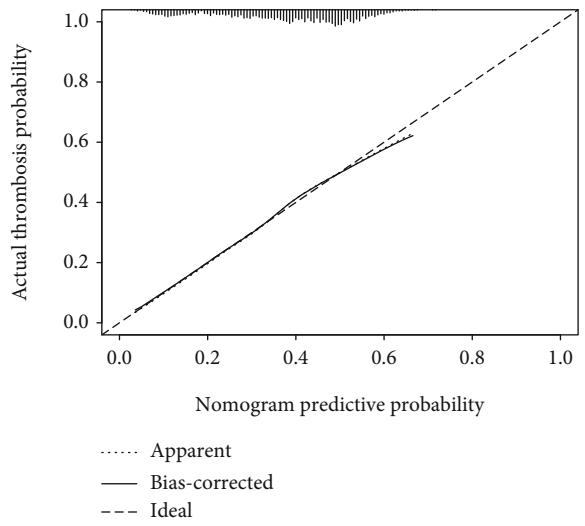

Figure 1: Calibration curve of the clinical prediction model. On the calibration curve, x-axis is the nomogram predicted probability of thrombosis for low limb fracture patients, and y-axis is the actual probability of thrombosis for these patients.

TT, FIB, and duration of surgery. Comparisons between the groups for each variable are also shown in Table 1.

3.2. Model Development. Multivariate logistic regression analysis was performed on identified potential predictors of thrombosis ($p < 0.05$). After completion of the regression analysis, variables lacking statistical significance were eliminated. Regression coefficients for each predictor in the final prediction model are recorded in Table 2. The predictors included in this thrombosis prediction model were age, BMI, energy of impact, fracture fixation type, blood transfusion during hospitalization, and use of anticoagulation drugs. The c-statistic of this thrombus-related clinical prediction model is 0.676, highlighting the model's good discriminatory ability. During the internal validation of the model, a correction curve was drawn using R (Figure 1). The curve shows that the prediction model has a good fit to the real scenario.

3.3. Computing the Risk Estimate and Nomogram Presentation. After completing the multivariate logistic regression analysis, we calculated the nomogram coefficient of age as per the formula defined in the methods ($\text{Nomogram}_{\text{Age}} = 1.728$). As we intended to use age as the scoring scale (with a total score of 100), we used 10 years as a baseline reference (i.e., $\text{Point}_{\text{age=10}} = 0$) with the total score increasing by 1 for each additional year of age. After completing the score-assignment for age, we used the other formula defined in the methods to assign values to each of the other variables (Table 3).

The risk probability corresponding to each score was calculated using the formula: $p = [1 + \exp(lp)]^{-1}$. In this formula, the linear predictor (lp) was obtained by multiplying the value of each variable with its associated regression coefficient and summing all the values ($lp = -\sum_{i=0}^{p} \beta_i X_i$). The results are shown as a nomogram (Figure 2).

Table 3: Risk score chart for thrombosis in patients with lower extremity fractures.

Risk factor		Coef	Nomogram	Point
		0.0192	1.728	
Age	10			0
	20			10
	30			20
	40			30
	50			40
	60			50
	70			60
	80			70
	90			80
	100			90
	110			100
		0.0484	2.45	
BMI	10			0
	12			5
	14			10
	16			15
	18			20
	20			25
	22			29
	24			34
	26			39
	28			44
	30			49
	32			54
	34			59
	36			64
	38			69
	40			74
Fracture fixation type	External fixation	Ref	Ref	0
	Other types	0.3808	0.3808	20
	Internal fixation	0.9015	0.9015	52
Energy	Low	Ref	Ref	0
	High	0.4054	0.4054	23
Blood transfusion	No	Ref	Ref	0
	Yes	0.3868	0.3868	22
Anticoagulation drugs	Yes	Ref	Ref	0
	No	1.1537	1.1537	58

4. Discussion

Venous thrombosis of the lower extremity is a well-known complication following lower limb fracture. Extensive

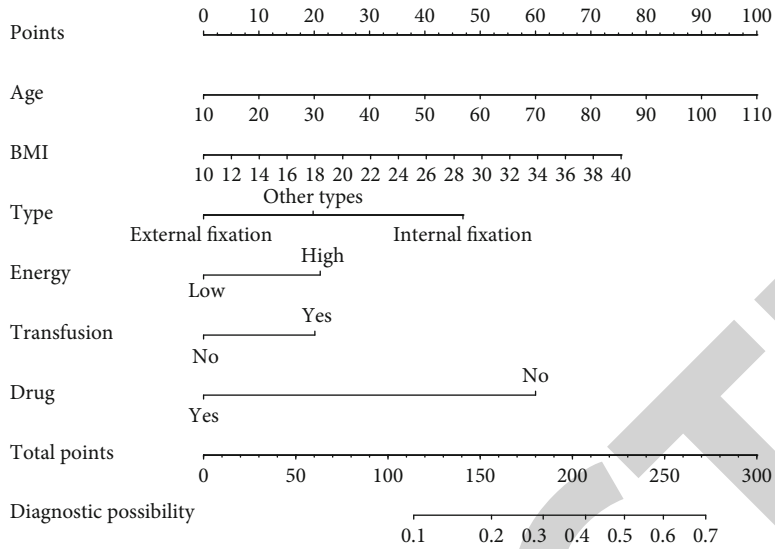

Figure 2: Nomogram for the computation of percentage risk of lower extremity fracture-related thrombosis.

research has been dedicated to the prevention and treatment of thrombosis, but early prediction of thrombosis is now appearing as an important research direction. In this paper, we analyzed clinical data of patients with lower extremity fractures from two centers from the past three years to develop a clinical prediction model for establishing the risk of DVT in such patients. The predictors used in this model are common and easily identified in clinical practice. Our final model showed strong predictive capability during the validation process (c – statistic = 0.676). This model will be effective in a clinical setting in the prediction of thrombosis in patients with lower extremity fractures. It is worth noting that the medical records of the thrombosis group and the nonthrombosis group are collected separately to compare the impact of each risk factor on thrombosis, so the number of medical records does not represent the incidence of thrombosis.

Numerous studies have been published on the prediction or screening of thrombosis in patients with lower extremity fractures or orthopedic surgery of the lower extremity. Some studies have evaluated the effect of a single factor on thrombosis. Monreal et al. collected the test results of 1033 patients undergoing large joint replacement surgery both at the time of discharge and during follow-up [20]. Using these clinical data, they assessed the efficacy of a combined strategy, that is, physical examination and compression ultrasound, to detect DVT prior to discharge. They found that a diagnostic testing for DVT before discharge has the capacity to identify 44% of patients who will experience symptoms after discharge. Madhav et al. conducted a retrospective analysis of 169 patients who were treated with open reduction and internal fixation for hip fractures and found that BMI is a significant predictive indicator of postoperative complications following an acetabular fracture [21]. Although the authors analyzed the impact of multiple factors on thrombosis, no clear scoring table or model was established. Rogers et al. conducted a cross-case study of 16,781 participants and found that factors predisposing to thrombosis included the following: infection, erythropoietin and blood transfusion, surgery, fracture, immobilization, and chemotherapy [22]. Park et al. performed a retrospective analysis of 901 lower limb fracture cases and identified several risk factors for increased DVT, including increased age, cardiovascular disease, and chronic lung disease [23]. Consequently, the predictive ability of some of the factors that we have identified as predictors has been verified in previous studies, verifying the validity of our results.

Overall, using a large multicenter sample, we analyzed multiple possible risk factors that have evident influence and have developed an easy-to-use model, which would be convenient for a clinical setting. Notably, in contrast with the Caprini score, our model includes energy at the time of impact and the type of surgical fixation of the fracture site, making our tool more specific for trauma patients with lower limb fractures. In addition, the risk factors included in the final model are well-defined and easy to be collected. Finally, calculating the final results through a score table or nomogram increases the practicality and accuracy of our model.

The limitations of this study should be acknowledged. First, as this is a retrospective study, issues with the patients' examination and treatment plans became apparent when collecting medical records. For example, in older records, doctors would only perform ultrasound test on patients with high thrombosis risk. Therefore, some patients without thrombosis or some patients with asymptomatic thrombosis did not undergo ultrasound testing during hospitalization. Since the thrombosis of these patients cannot be confirmed, such patients had to be excluded from the analysis. This reason may help explain why factors that are well-known predictors of thrombosis, such as D-dimer, were not included in our final model [8]. Therefore, this model may be more likely to be applied to a population at high risk of thrombosis, with a narrower scope than originally planned. Ideally, in future studies, we would seek to refine this model, by verifying the model in a clinical setting, as well as prospectively, comprehensively documenting case data and analyzing the

correlation between factors which were not included in the model and DVT. Second, in this study, anticoagulation therapy for all patients was low-molecular-weight heparin sodium. However, anticoagulation drugs that are known to be effective and are clinically used include low-molecular-weight heparin, vitamin K antagonists, direct thrombin inhibitors, and direct FXa inhibitors [7, 9, 30]. Hence, in future studies, cases using different anticoagulation drugs should be included in the analysis for comparison. Moreover, although the risk factors included in the final model are simple and easy to complete, the addition of some inspection indicators and test results will improve the predictive ability of the model. For example, studies have shown that microRNA-495 and Stat3 proteins in the circulating blood can be used as biomarkers for the prognosis and prediction of lower extremity DVT [15]. Finally, our model was built using data from Wuhan, Hubei, and Shijiazhuang, Hebei, China, where all of the patients are Asian. Verification of our model in the white and black population is necessary.

5. Conclusion

Our study is the first, to the best of our knowledge, to provide a prediction model that can be used to guide decisions regarding primary prevention of venous thrombosis in patients with lower extremity fractures. During validation, the model showed good predictive ability. Our proposed score calculation method corresponding to the chart is designed to be convenient for clinical use. Overall, this model offers promising potential as a tool for the prevention and treatment of thrombosis in patients with lower limb fractures.

Data Availability

If the original data is reasonably required, the permission to obtain can be applied to Professor Guohui Liu.

Conflicts of Interest

The authors declare that there is no conflict of interest regarding the publication of this paper.

Authors' Contributions

Z. Lin, B. Mi, and X. Liu contributed equally to this work.

Acknowledgments

This study was supported by the Wuhan Science and Technology Bureau (Grant No. 2017060201010192) and the Health Commission of Hubei Province (Grant No. WJ2019Z009).

References

[1] J. A. Kaye, "Epidemiology of lower limb fractures in general practice in the United Kingdom," *Injury Prevention.*, vol. 10, no. 6, pp. 368–374, 2004.

[2] C. M. Court-Brown and B. Caesar, "Epidemiology of adult fractures: a review," *Injury*, vol. 37, no. 8, pp. 691–697, 2006.

[3] M. S. H. Beerekamp, R. J. O. de Muinck Keizer, N. W. L. Schep, D. T. Ubbink, M. J. M. Panneman, and J. C. Goslings, "Epidemiology of extremity fractures in the Netherlands," *Injury*, vol. 48, no. 7, pp. 1355–1362, 2017.

[4] F. B. Rogers, M. D. Cipolle, G. Velmahos, G. Rozycki, and F. A. Luchette, "Practice management guidelines for the prevention of venous thromboembolism in trauma patients: the EAST practice management guidelines work group," *The Journal of Trauma*, vol. 53, no. 1, pp. 142–164, 2002.

[5] M. H. Meissner, W. L. Chandler, and J. S. Elliott, "Venous thromboembolism in trauma: a local manifestation of systemic hypercoagulability?," *The Journal of Trauma*, vol. 54, no. 2, pp. 224–231, 2003.

[6] J. A. Heit, F. A. Spencer, and R. H. White, "The epidemiology of venous thromboembolism," *Journal of Thrombosis and Thrombolysis.*, vol. 41, no. 1, pp. 3–14, 2016.

[7] N. Mackman, "Triggers, targets and treatments for thrombosis," *Nature*, vol. 451, no. 7181, pp. 914–918, 2008.

[8] M. Di Nisio, N. van Es, and H. R. Büller, "Deep vein thrombosis and pulmonary embolism," *The Lancet.*, vol. 388, no. 10063, pp. 3060–3073, 2016.

[9] Y. Falck-Ytter, C. W. Francis, N. A. Johanson et al., "Prevention of VTE in orthopedic surgery patients," *Chest*, vol. 141, no. 2, pp. e278S–e325S, 2012.

[10] C. Tovey and S. Wyatt, "Diagnosis, investigation, and management of deep vein thrombosis," *BMJ (Clinical research ed).*, vol. 326, no. 7400, pp. 1180–1184, 2003.

[11] N. Rosencher, C. Vielpeau, J. Emmerich, F. Fagnani, and C. M. Samama, "Venous thromboembolism and mortality after hip fracture surgery: the ESCORTE study," *Journal of Thrombosis and Haemostasis*, vol. 3, no. 9, pp. 2006–2014, 2005.

[12] A. S. Wolberg, F. R. Rosendaal, J. I. Weitz et al., "Venous thrombosis," *Nature Reviews Disease Primers*, vol. 1, no. 1, 2015.

[13] T. L. Fancher, R. H. White, and R. L. Kravitz, "Combined use of rapid D-dimer testing and estimation of clinical probability in the diagnosis of deep vein thrombosis: systematic review," *Bmj*, vol. 329, no. 7470, p. 821, 2004.

[14] L. A. Linkins and L. S. Takach, "Review of D-dimer testing: good, bad, and ugly," *International Journal of Laboratory Hematology*, vol. 39, pp. 98–103, 2017.

[15] N. X. Li, J. W. Sun, and L. M. Yu, "Evaluation of the circulating MicroRNA-495 and Stat3 as prognostic and predictive biomarkers for lower extremity deep venous thrombosis," *Journal of Cellular Biochemistry*, vol. 119, no. 7, pp. 5262–5273, 2018.

[16] R. Jafarzadeh-Esfehani, S. M. Parizadeh, A. S. Aghabozorgi et al., "Circulating and tissue microRNAs as a potential diagnostic biomarker in patients with thrombotic events," *Journal of Cellular Physiology*, vol. 235, no. 10, pp. 6393–6403, 2020.

[17] F. Xing, L. Li, Y. Long, and Z. Xiang, "Admission prevalence of deep vein thrombosis in elderly Chinese patients with hip fracture and a new predictor based on risk factors for thrombosis screening," *BMC Musculoskeletal Disorders*, vol. 19, no. 1, 2018.

[18] F. A. Anderson, "Risk factors for venous thromboembolism," *Circulation*, vol. 107, no. 90231, pp. 9I-–916, 2003.

[19] M. M. Knudson, D. G. Ikossi, L. Khaw, D. Morabito, and L. S. Speetzen, "Thromboembolism after trauma," *Annals of Surgery.*, vol. 240, no. 3, pp. 490–498, 2004.

[20] M. Monreal, L. Peidro, C. Resines et al., "Limited diagnostic workup for deep vein thrombosis after major joint surgery," *Thrombosis and haemostasis.*, vol. 99, no. 6, pp. 1112–1115, 2008.

Hindawi
BioMed Research International
Volume 2024, Article ID 9782859, 1 page
https://doi.org/10.1155/2024/9782859

Retraction

Retracted: Increased EHHADH Expression Predicting Poor Survival of Osteosarcoma by Integrating Weighted Gene Coexpression Network Analysis and Experimental Validation

BioMed Research International

Received 12 March 2024; Accepted 12 March 2024; Published 20 March 2024

This article has been retracted by Hindawi following an investigation undertaken by the publisher [1]. This investigation has uncovered evidence of one or more of the following indicators of systematic manipulation of the publication process:

(1) Discrepancies in scope

(2) Discrepancies in the description of the research reported

(3) Discrepancies between the availability of data and the research described

(4) Inappropriate citations

(5) Incoherent, meaningless and/or irrelevant content included in the article

(6) Manipulated or compromised peer review

The presence of these indicators undermines our confidence in the integrity of the article's content and we cannot, therefore, vouch for its reliability. Please note that this notice is intended solely to alert readers that the content of this article is unreliable. We have not investigated whether authors were aware of or involved in the systematic manipulation of the publication process.

Wiley and Hindawi regrets that the usual quality checks did not identify these issues before publication and have since put additional measures in place to safeguard research integrity.

We wish to credit our own Research Integrity and Research Publishing teams and anonymous and named external researchers and research integrity experts for contributing to this investigation.

The corresponding author, as the representative of all authors, has been given the opportunity to register their agreement or disagreement to this retraction. We have kept a record of any response received.

References

[1] J. Cui, G. Yi, J. Li, Y. Li, and D. Qian, "Increased EHHADH Expression Predicting Poor Survival of Osteosarcoma by Integrating Weighted Gene Coexpression Network Analysis and Experimental Validation," *BioMed Research International*, vol. 2021, Article ID 9917060, 13 pages, 2021.

Hindawi
BioMed Research International
Volume 2021, Article ID 9917060, 13 pages
https://doi.org/10.1155/2021/9917060

Research Article

Increased EHHADH Expression Predicting Poor Survival of Osteosarcoma by Integrating Weighted Gene Coexpression Network Analysis and Experimental Validation

Juncheng Cui,[1] Guoliang Yi,[1] Jinxin Li,[1] Yangtao Li,[1] and Dongyang Qian [2]

[1]*Department of Orthopedic Surgery, The First Affiliated Hospital of University of South China, 69 Chuanshan Road, Hengyang, Hunan 421001, China*
[2]*Department of Orthopaedics, The First Affiliated Hospital, Guangzhou Medical University/Guangdong key Laboratory of Orthopaedic Technology and Implant Materials, Guangzhou 510120, China*

Correspondence should be addressed to Dongyang Qian; 2011681099@gzhmu.edu.cn

Received 26 March 2021; Revised 13 April 2021; Accepted 17 April 2021; Published 4 May 2021

Academic Editor: Yun-Feng Yang

Enoyl-CoA hydratase and 3-hydroxyacyl CoA dehydrogenase (EHHADH), a member of the 3-hydroxyacyl-CoA dehydrogenase family, were previously demonstrated to be involved in the tumorigenesis of various cancer types. This study is aimed at determining of the diagnostic and prognostic value of EHHADH in osteosarcoma (OS). The overexpression of EHHADH was found both in OS and also other sarcoma types, and according to the retrospective cohort study, the EHHADH level was related to the overall survival and disease-free survival of the OS patients. Furthermore, knockdown of EHHADH under the influence of EHHADH small interfering RNA significantly suppressed the proliferation ability of the tumor cells. Moreover, EHHADH overexpressed was found in human OS tissues. In summary, the progression of OS could be enhanced by EHHADH, which may be a potential diagnostic and prognostic biomarker for OS patients.

1. Introduction

Osteosarcoma (OS) is one of the commonly occurring malignant tumors in bone tissues [1]. OS is derived from the mesenchymal cell line, and the frequent growth of the tumor is associated with the development of tumor osteoid (either direct or indirect manner) and bone tissue through the cartilage stage [2]. OS can typically be characterized by the high proliferation of the tumor cells, rapid metastasis, and high mortality rate [3]. However, medical failure of OS is the main issue which in turn results in the poor curative effect for OS [4]. Despite the huge development of therapeutic strategies, only lesser advancement in the treatment of OS patients has been obtained [5]. Currently, there are very few feasible biomarkers present that are involved in the determination of tumor burden and assess the therapeutic response for OS [6]. Hence, the discovery of efficient biomarkers for early diagnosis and prognostic evaluation of OS is greatly required. Therefore, the survival of the patients can be improved because of the development of early therapy for OS.

Enoyl-CoA hydratase and 3-hydroxyacyl CoA dehydrogenase (EHHADH), a member of the 3- hydroxyacyl-CoA dehydrogenase family, previously been reported to be involved in tumorigenesis of various types of cancer [7, 8]. Various studies have reported that several tumor-related diseases are enriched with EHHADH, which is of great importance for the progression of cancers [9, 10]. Thus, it is reasonably assumed that EHHADH is involved in the development of tumor-related diseases. However, only a few reports are suggesting the diagnostic role of EHHADH in the development of OS.

Therefore, this study initially pursued the investigation of the prognostic value of EHHADH in OS. The overexpression of EHHADH was observed in both OS and other sarcoma types. According to the retrospective cohort study, the EHHADH level was related to the disease-free survival and

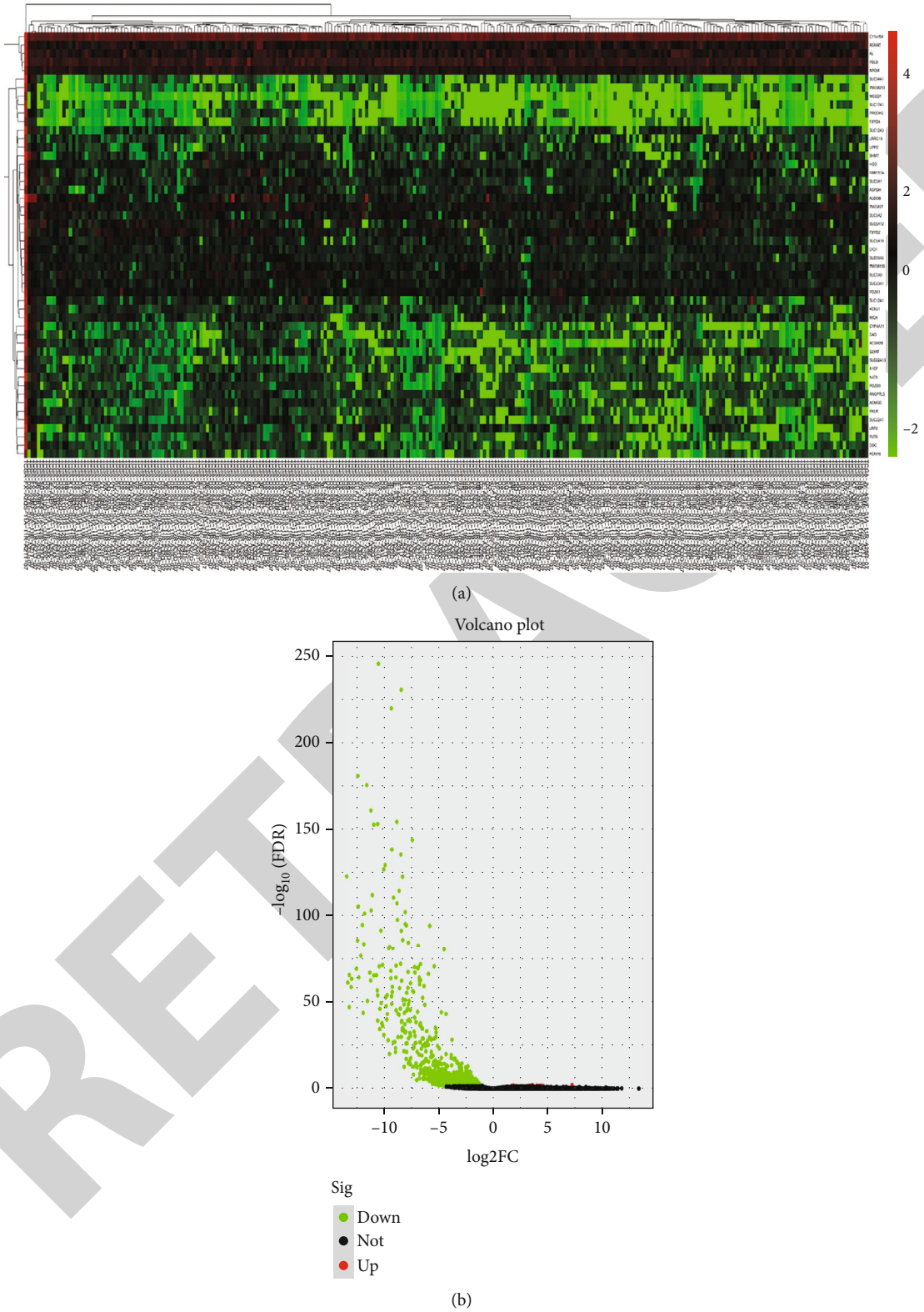

Figure 1: Identification of differentially expressed genes in sarcoma base on the TCGA database. (a) The heat map of mRNA expression information of 263 sarcoma patients and 2 normal people. (b) The volcano result of included datasets.

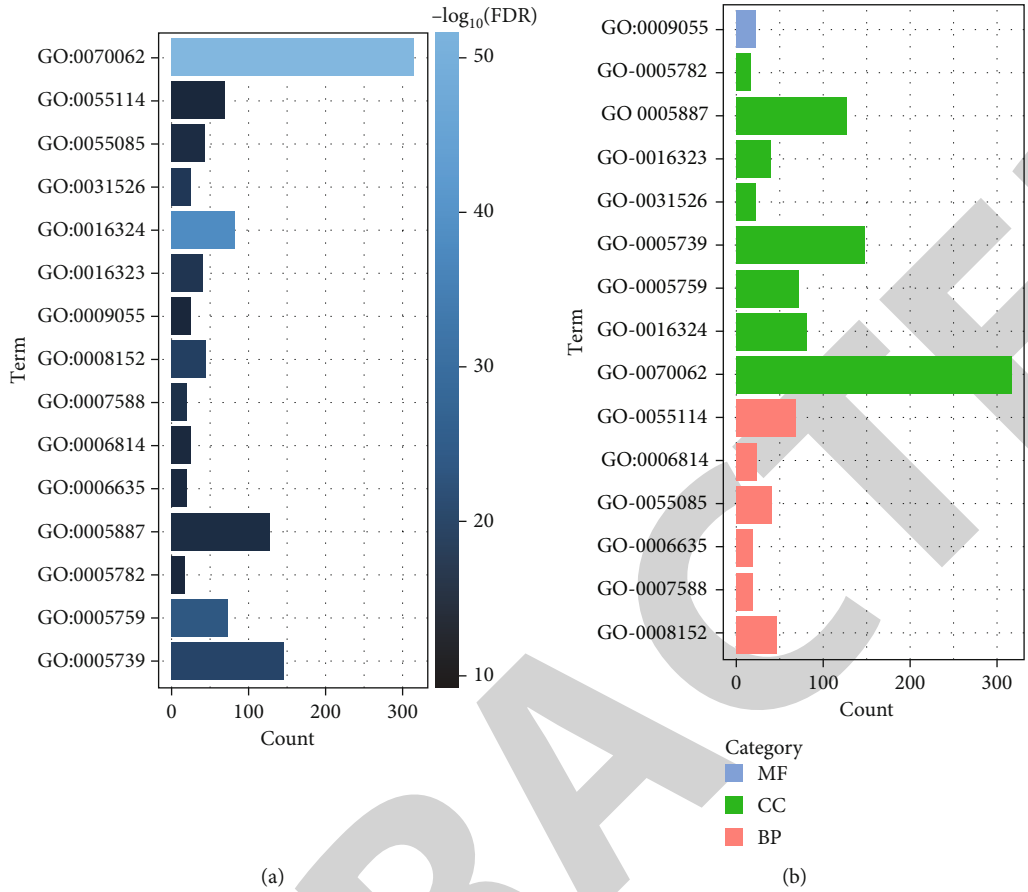

Figure 2: Continued.

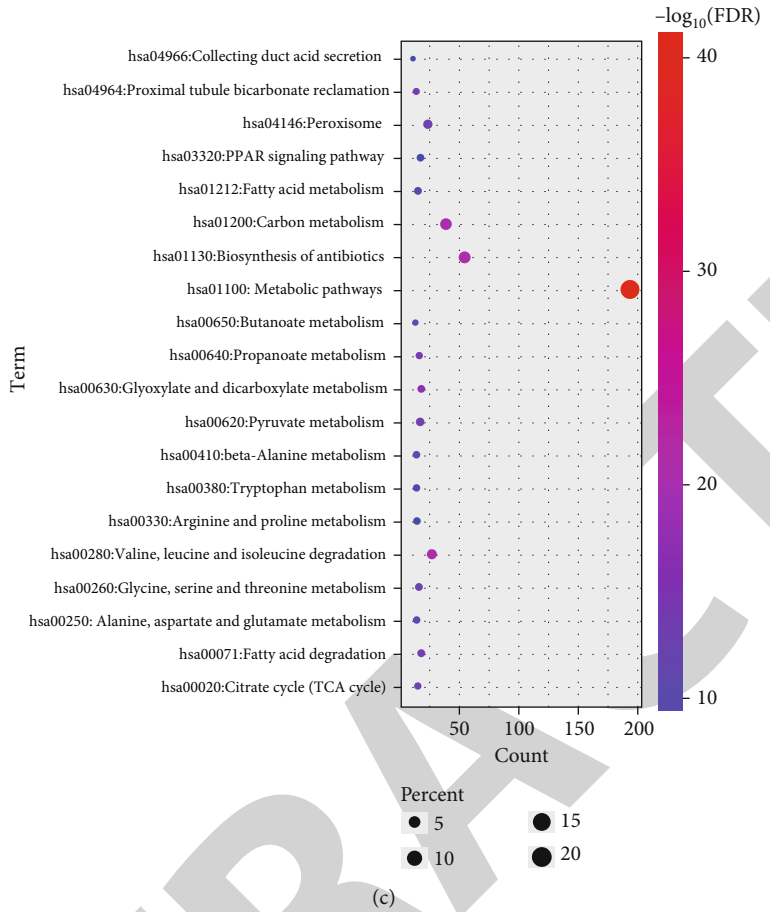

Figure 2: GO and KEGG enrichment analysis results of differentially expressed genes. (a) The information of FDR and count of significantly enriched GO terms. (b) The information of category and count of significantly enriched GO terms. (c) The information of enrich factor, FDR, and count of enriched KEGG pathways.

Table 1: GO function enrichment analysis of DEGs. Top 15 GO terms were selected.

Term	Name	Count	FDR
A, biological processes			
GO: 0008152	Metabolic process	46	1.50*E*-18
GO: 0007588	Excretion	20	5.97*E*-13
GO: 0006635	Fatty acid beta-oxidation	20	2.42*E*-11
GO: 0055085	Transmembrane transport	44	5.10*E*-11
GO: 0006814	Sodium ion transport	24	1.02*E*-09
GO: 0055114	Oxidation-reduction process	70	2.06*E*-09
B, molecular functions			
GO: 0009055	Electron carrier activity	25	5.06*E*-09
C, cellular components			
GO: 0070062	Extracellular exosome	317	1.51*E*-52
GO: 0016324	Apical plasma membrane	84	1.18*E*-39
GO: 0005759	Mitochondrial matrix	73	1.61*E*-26
GO: 0005739	Mitochondrion	147	1.97*E*-20
GO: 0031526	Brush border membrane	24	1.13*E*-15
GO: 0016323	Basolateral plasma membrane	41	8.68*E*-15
GO: 0005887	Integral component of plasma membrane	129	3.56*E*-11
GO: 0005782	Peroxisomal matrix	18	6.33*E*-10

Table 2: KEGG pathway enrichment analysis of DEGs. Top 20 KEGG pathways were selected.

KEGG pathways Term	Name	Count	FDR
hsa01100	Metabolic pathways	194	2.12*E*-41
hsa01130	Biosynthesis of antibiotics	53	5.46*E*-17
hsa00280	Valine, leucine, and isoleucine degradation	26	6.03*E*-17
hsa01200	Carbon metabolism	38	1.39*E*-16
hsa00630	Glyoxylate and dicarboxylate metabolism	17	7.89*E*-12
hsa00640	Propanoate metabolism	15	4.88*E*-09
hsa00071	Fatty acid degradation	17	3.06*E*-08
hsa04964	Proximal tubule bicarbonate reclamation	13	4.15*E*-08
hsa04146	Peroxisome	23	5.39*E*-08
hsa00620	Pyruvate metabolism	16	9.28*E*-08
hsa00020	Citrate cycle (TCA cycle)	14	1.13*E*-07
hsa00260	Glycine, serine, and threonine metabolism	15	4.71*E*-07
hsa00410	Beta-alanine metabolism	13	1.70*E*-06
hsa00650	Butanoate metabolism	12	2.90*E*-06
hsa00250	Alanine, aspartate, and glutamate metabolism	13	6.95*E*-06
hsa00380	Tryptophan metabolism	13	3.29*E*-05
hsa01212	Fatty acid metabolism	14	4.26*E*-05
hsa03320	PPAR signaling pathway	16	9.57*E*-05
hsa04966	Collecting duct acid secretion	10	1.95*E*-04
hsa00330	Arginine and proline metabolism	13	3.27*E*-04

overall survival of the OS patients. Furthermore, the clinical importance of EHHADH level in human OS and the regulatory effect of EHHADH on OS cell proliferation were explored.

2. Materials and Methods

2.1. TCGA Analysis. We obtained the data sets of sarcoma patients from TCGA Data Portal (https://tcga-data.nci.nih.gov/tcga/). The DEGs analysis was performed with the edge*R* package and visualized using the pheatmap *R* package. The volcano result was visualized with the ggplot2 *R* package. Results were reported as the average expression value of repeated genes. A two-tailed test was carried out between the two groups. $p < 0.05$ and $|\log FC| > 1$ were considered as differentially expressed genes.

2.2. Enrichment Analysis for Gene Ontology (GO) and Kyoto Encyclopedia of Genes and Genomes (KEGG) Pathway. The online tool Database for Annotation, Visualization, and Integrated Discovery version (DAVID) Bioinformatics Resources 6.8 was used to recognize the biological meaning of the listed genes. Analyses for the enrichment of the KEGG pathway and GO were performed with DAVID. We selected the GO and KEGG terms with FDR < 0.05.

2.3. Construction of the Protein-Protein Interaction (PPI) Network and Identification of Hub Genes. With the help of the PPI network, further information was obtained regarding the functional interactions between the DEGs. DEGs were imported into Search Tool for the Retrieval of Interacting Genes (STRING, http://www.string-db.org), and interactions with a combined score of >0.9 were identified. After that, with the help of the Cytoscape software (version 3.7.2), a PPI network was built. With the plugin software cytoHubba, hub genes were identified by degree analysis. The interaction between GO terms was visualized with clueGO, a plugin software of Cytoscape.

2.4. Oncomine Analysis. Oncomine (http://www.oncomine.org) integrates RNA and DNA-seq data from GEO, TCGA, and published literature. We can use Oncomine for the analysis of the differentially expressed genes, clinical correlation, and multigene coexpression. The coexpressed genes of EHHADH in sarcoma were retrieved from Oncomine with the default setting of fold change > 2 and p value < 0.01.

2.5. The Analysis of Kaplan-Meier Plotter Survival. DEG prognostic values and coexpressed genes of EHHADH in sarcoma were further assessed by the examination of overall survival using the Kaplan-Meier plotter (http://kmplot.com/analysis/). It is an online tool that is used to assess the role of 54,675 genes on the survival of 13,316 cancer samples in 21 cancer types. The database sources include the EGA, GEO, and TCGA. The main purpose of the tool is the discovery and validation of meta-analysis-based biomarkers. Statistically significant results were showed $p < 0.01$.

2.6. Cell Culture and Transfection. OS cell line MG63 was obtained from the Shanghai Cell Bank (Shanghai, China), and DMEM and 10% fetal bovine serum (Thermo Fisher Scientific, Waltham, MA, USA) were applied to the cell culture

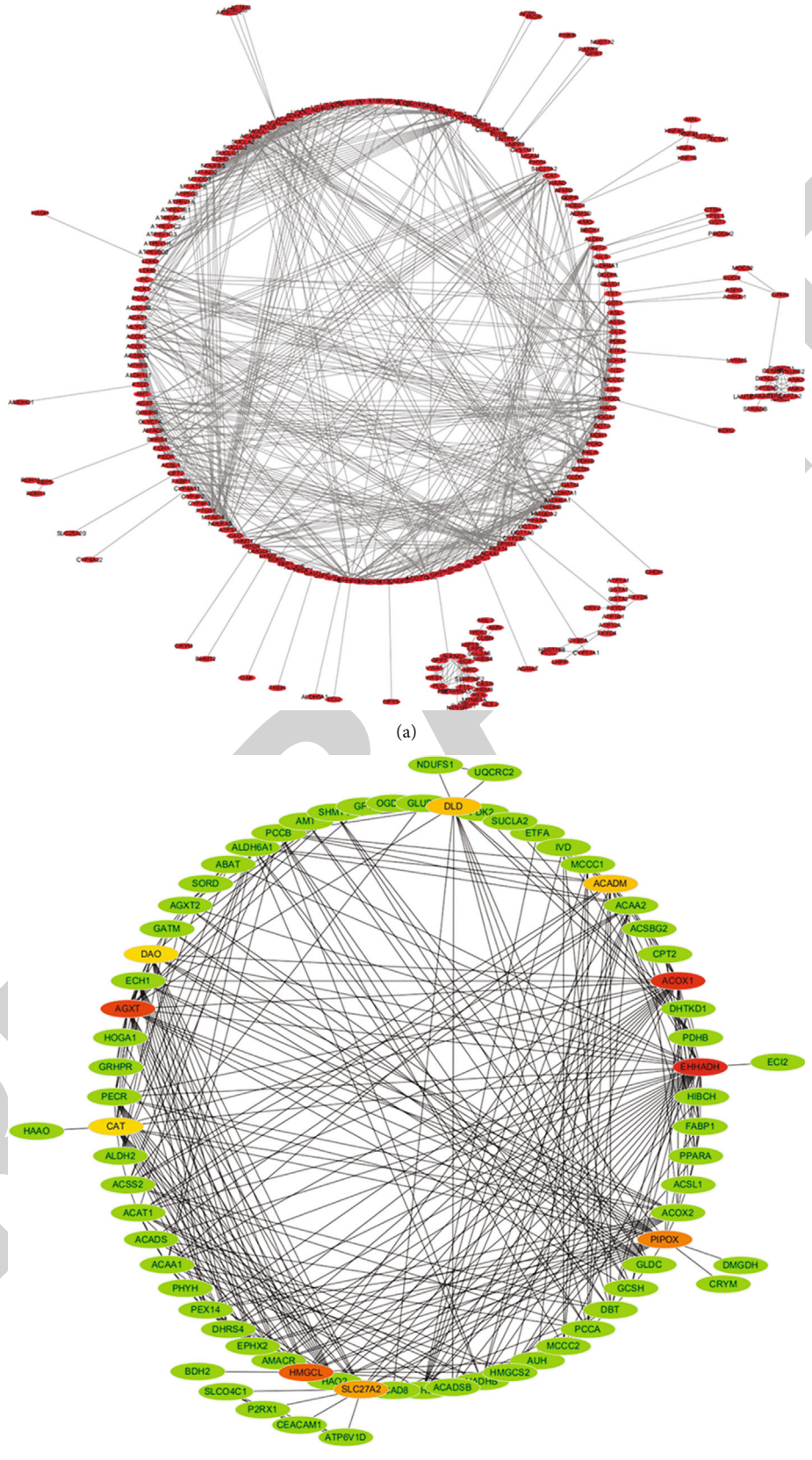

(a)

(b)

Figure 3: PPI network construction and hub genes identification of DEGs. (a) PPI network of DEGs constructed with Cytoscape. (b) DEGs in the network were ranked by degree. The top ten genes were EHHADH, ACOX1, AGXT, HMGCL, PIPOX, SLC27A2, DLD, ACADM, CAT, and DAO.

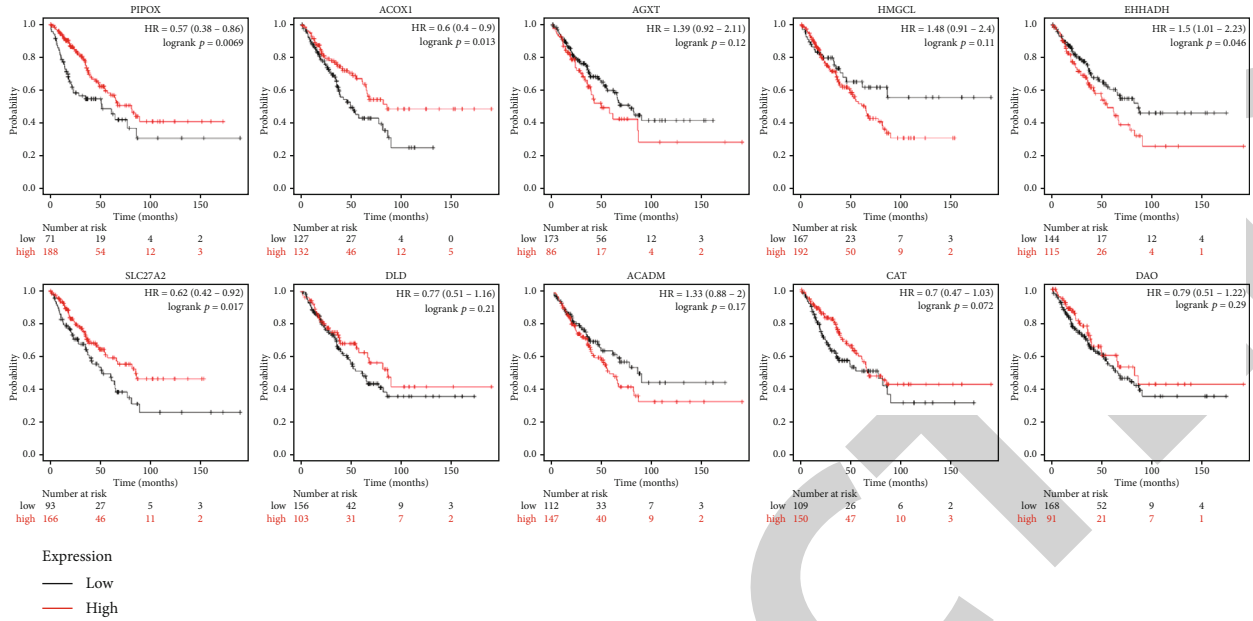

Figure 4: The prognostic values of hub genes in sarcoma. It is depicted that EHHADH was associated with shorter overall survival, and PIPOX, ACOX1, and SLC27A2 were associated with longer overall survival ($p < 0.05$).

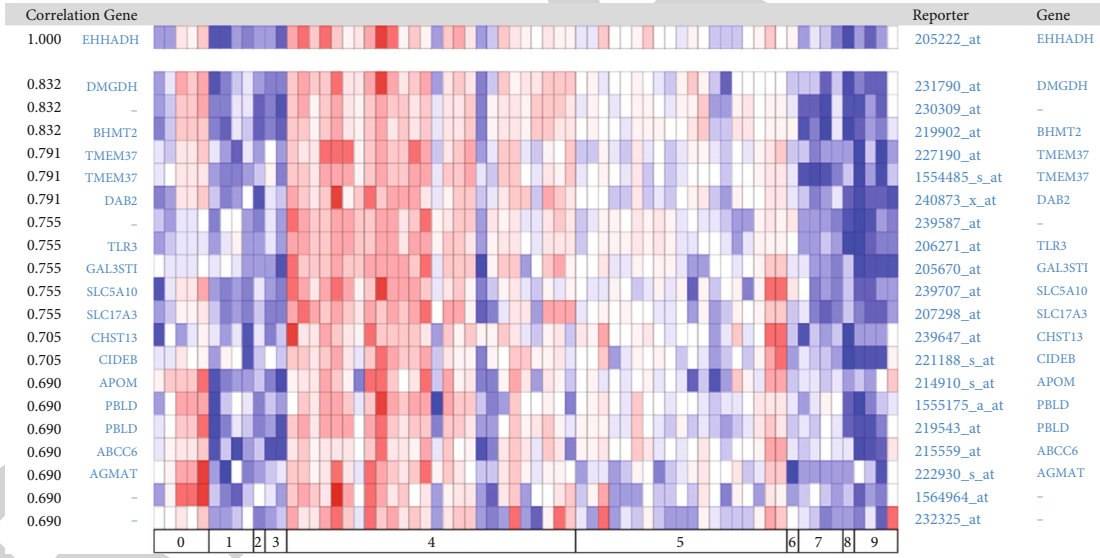

Figure 5: The coexpressed genes of EHHADH in sarcoma ranked by correlation factor. The top ten genes were DMGDH, BHMT2, TMEM37, DAB2, TLR3, GAL3ST1, SLC5A10, SLC17A3, CHST13, and CID3B.

at 37°C in 5% CO_2. For transfection, the negative control small interfering RNA (siRNA) and EHHADH siRNA were designed by Suzhou GenePharma Biotechnology Co., Ltd. (Suzhou, China). Transfection of MG63 cells was performed with 50 nM NC siRNA or EHHADH siRNA and Lipofectamine 3000 (Thermo Fisher Scientific, Waltham, MA, USA).

2.7. Quantitative Reverse Transcription Polymerase Chain Reaction (qRT-qPCR). Invitrogen TRIzol (ThermoFisher, Waltham, MA, USA) was used for the extraction of the total RNA from the OS cells and tissues according to the instructions of the manufacturer. To assess the EHHADH mRNA level, the qRT-PCR analysis was applied using a One-Step RT-PCR kit (Beijing Suolaibao Bio, Inc., Beijing, China) according to the instruction provided by the manufacture. The CBX3 primers were designed by Suzhou GenePharma Co., Ltd. (Suzhou, China) and are as follows: EHHADH forward, 5′-ATGGCTGAGTATCTGAGGCTG-3′ and reverse, 5′-ACCGTATGGTCCAAACTAGCTT-3′; and GAPDH forward, 5′-ACTGCGAATGGCTCATTAAATCA-3′ and reverse, 5′-AGCTCTAGAATTACCACAGTTATCCA AGT-3′. Cyclin D1 forward, 5′-TTGCCCTCTGTGCCAC AGAT-3′ and reverse, 5′-TCAGGTTCAGGCCTTGCACT-

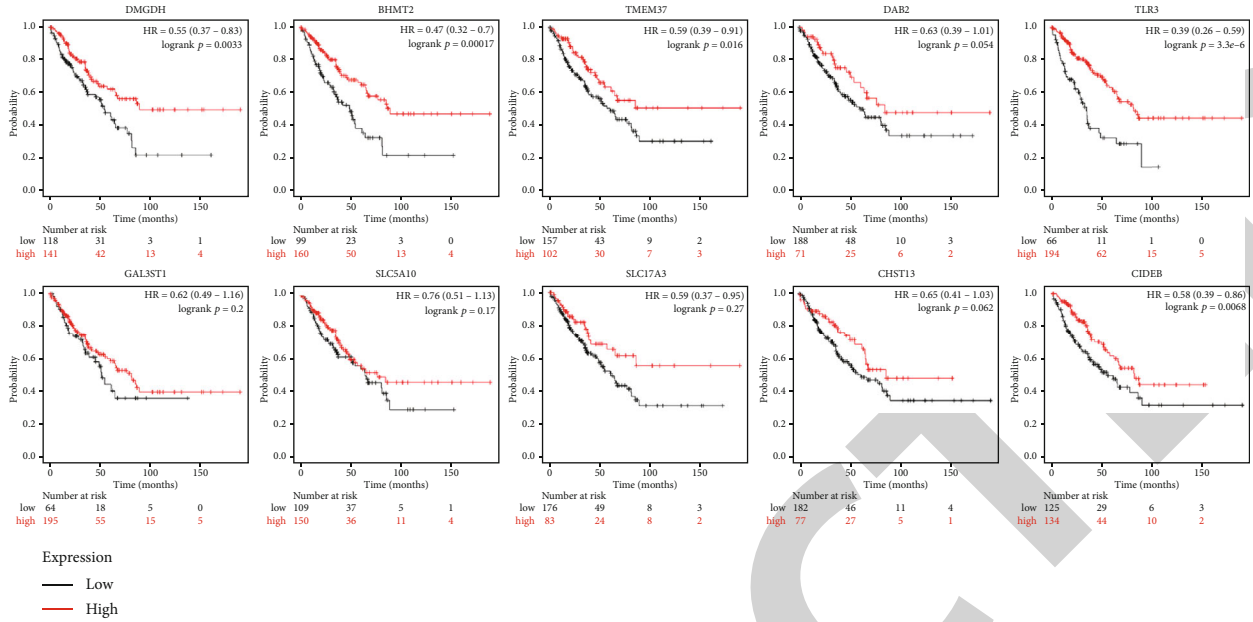

Figure 6: The prognostic values of coexpressed genes of EHHADH in sarcoma. DMGDH, BHMT2, TMEM37, TLR3, SLC17A3, and CID3B were associated with longer overall survival ($p < 0.05$).

3′. Cyclin D3 forward, 5′-CTGGCCATGAACTACCTGGA-3′ and reverse, 5′-CCAGCAAATCATGTGCAATC-3′.The $2^{-\Delta\Delta Cq}$ approach was used to quantify the EHHADH mRNA level.

2.8. Western Blot (WB) Analysis. The BCA method (ThermoFisher, Waltham, MA, USA) was applied to assess the concentration of proteins. Subsequently, the separation of equal amounts of the total protein was performed by using 12.5% SDS-PAGE, and then we transferred the separated proteins onto polyvinylidene difluoride membranes. To block the membrane, 5% skim milk was used at room temperature for 2 hours and was subjected to incubation with anti-EHHADH (1 : 800 dilution) (cat. no. Ab136059, Abcam) antibody or anti-GAPDH (1: 2,500 dilution) (cat. no. ab9485, Abcam). GAPDH was used as the internal reference to normalize the expression EHHADH.

2.9. Statistical Analysis. Data are depicted as means ± SD, and all the statistical analyses were conducted by using GraphPad Prism 8.0 (GraphPad Software, CA, USA). Data comparison was based on Student's *t*-tests and one-way ANOVAs with Tukey's posthoc test as appropriate. The significant threshold was mentioned as $p < 0.05$.

3. Results and Discussion

3.1. TCGA Analysis. Through the TCGA database, we obtained the mRNA expression and clinical information of 265 cases (263 sarcoma patients and 2 normal people). After normalization of the data and comprehensive analysis, 912 downregulated and 21 upregulated DEGs were identified (Figure 1).

3.2. GO and KEGG Pathway Enrichment Analysis of DEGs. The DEGs were significantly involved in the biological progress of the metabolic process, excretion, fatty acid beta-oxidation, transmembrane transport, sodium ion transport, and oxidation-reduction process; in cellular components of the extracellular exosome, apical plasma membrane, mitochondrial matrix, mitochondrion, brush border membrane, an integral component of the plasma membrane, basolateral plasma membrane, and peroxisomal matrix; in molecular functions of electron carrier activity (Figures 2(a) and 2(b), Table 1); and in KEGG pathways of metabolic pathways, biosynthesis of antibiotics pathway, degradation pathway of leucine valine, and isoleucine, metabolism pathways of carbon, glyoxylate and dicarboxylate, propanoate, and fatty acid degradation pathway, proximal tubule bicarbonate reclamation pathway, peroxisome pathway, pyruvate metabolism pathway, etc. (Figure 2(c), Table 2).

3.3. Construction of the PPI Network and Identification of Hub Genes. The construction of an interaction network of DEGs was accomplished in Cytoscape (Figure 3(a)). DEGs were ranked by degree value in Cytoscape (Figure 3(b)). The top ten genes were EHHADH, ACOX1, AGXT, HMGCL, PIPOX, SLC27A2, DLD, ACADM, CAT, and DAO. They are considered hub genes. EHHADH was ranked No. 1 with a lesser *p* value.

3.4. The Kaplan-Meier Plotter Survival Analysis of Hub Genes. EHHADH was found to be linked with a shorter overall survival rate among ten hub genes while longer overall survival was associated with PIPOX, ACOX1, and SLC27A2 ($p < 0.05$) (Figure 4).

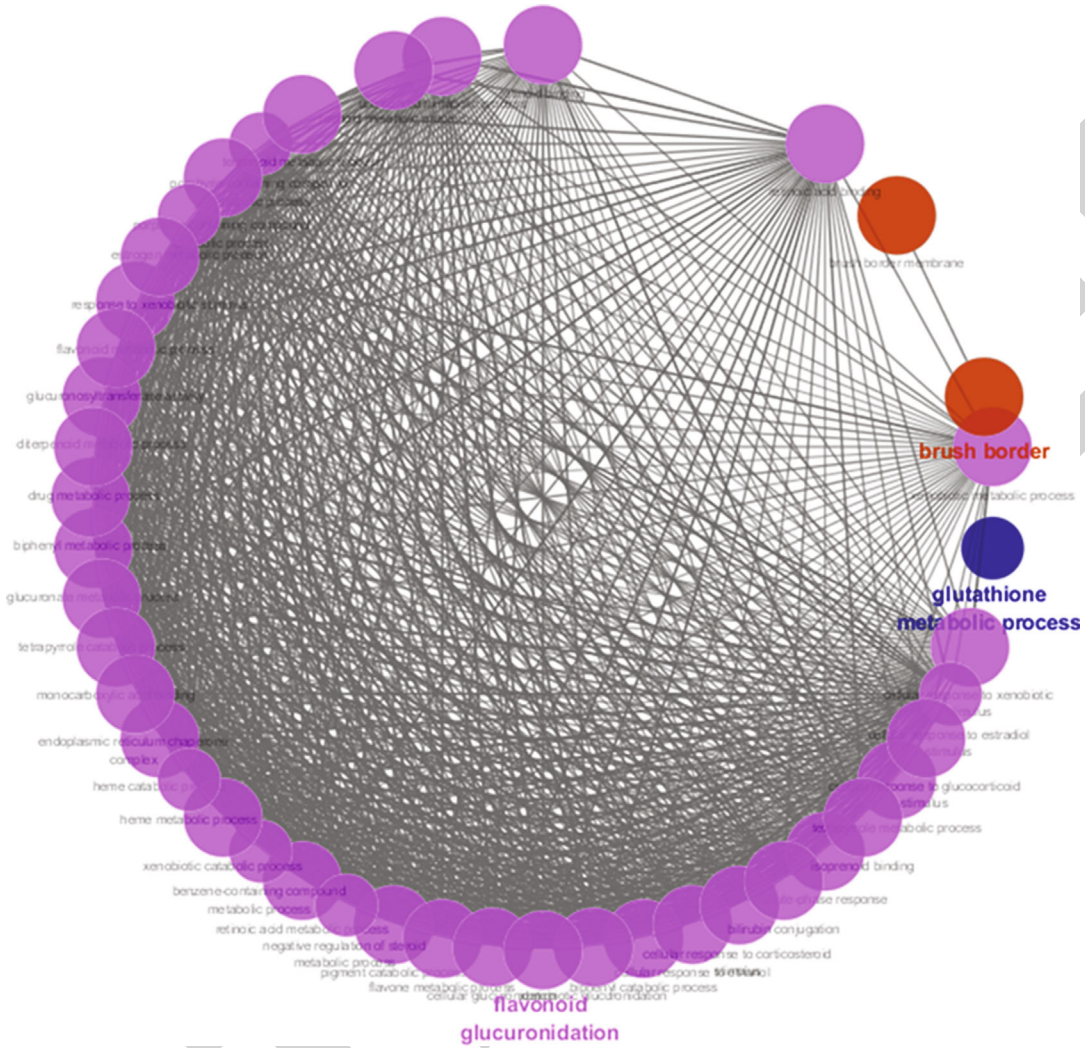

(a)

Figure 7: Continued.

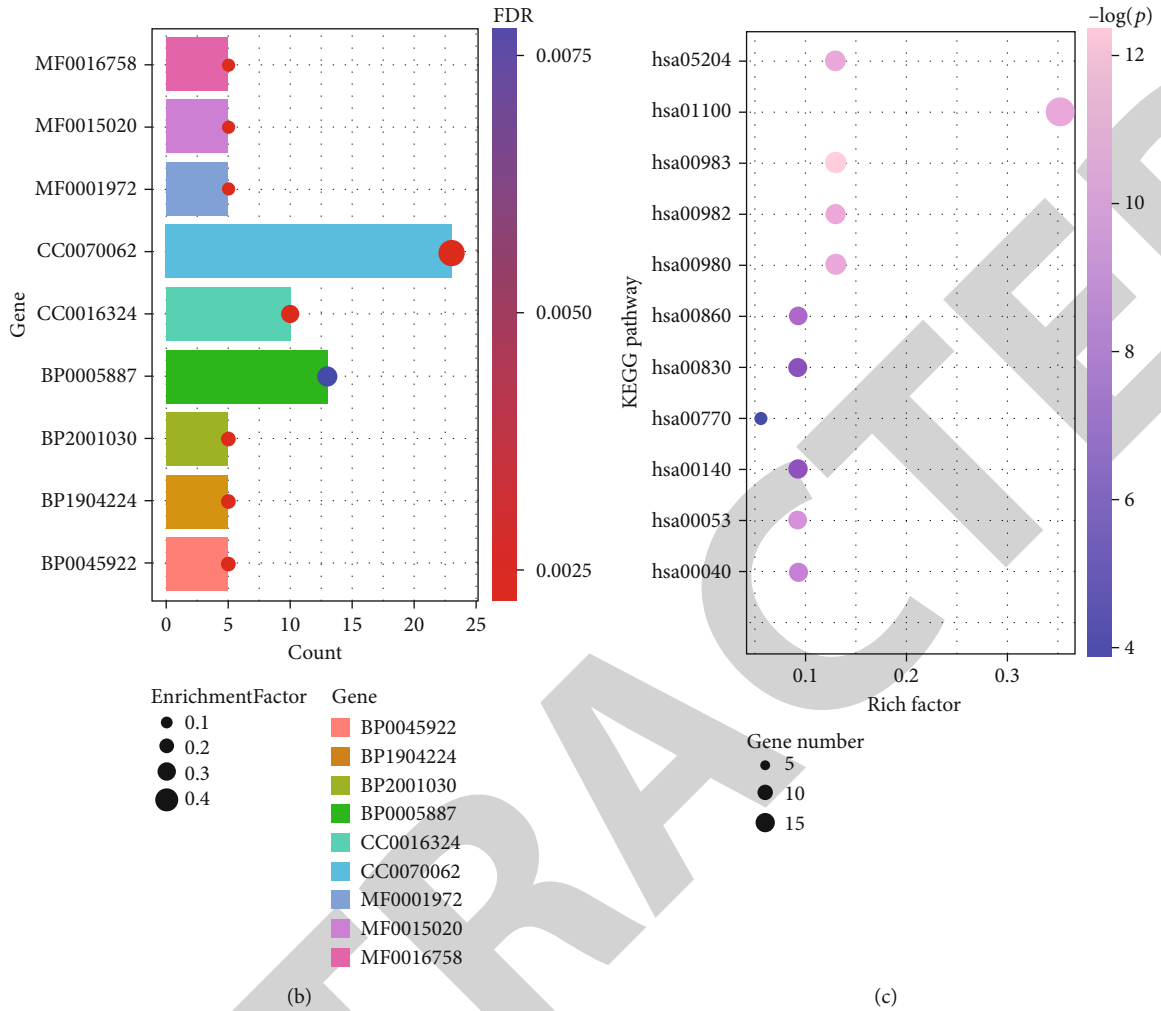

Figure 7: GO and KEGG enrichment analysis results of EHHADH and its coexpressed genes. (a) Relationship and interactions between enriched GO terms. (b) Enriched KEGG pathways. hsa00983: drug metabolism-other enzymes, hsa00982: drug metabolism-cytochrome P450, hsa00980: metabolism of xenobiotics by cytochrome P450, hsa05204: chemical carcinogenesis, hsa01100: metabolic pathways, hsa00053: ascorbate and aldarate metabolism, hsa00040: pentose and glucuronate interconversions, hsa00860: porphyrin and chlorophyll metabolism, hsa00140: steroid hormone biosynthesis, hsa00830: retinol metabolism, and hsa00770: pantothenate and CoA biosynthesis. (c) Enriched GO terms. MF0001972: retinoic acid binding, MF0015020: glucuronosyltransferase activity, MF0016758: transferase activity, transferring hexosyl groups, CC0016324: apical plasma membrane, CC0070062: extracellular exosome, CC0005887: integral component of plasma membrane, BP1904224: negative regulation of glucuronosyltransferase activity, BP2001030: negative regulation of cellular glucuronidation, and BP0045922: negative regulation of fatty acid metabolic process.

3.5. Oncomine Analysis. The coexpressed genes of EHHADH were identified using a coexpression online tool in Oncomine. Results of the analysis revealed that the top ten coexpressed genes with the smallest correlation factor include DMGDH, BHMT2, TMEM37, DAB2, TLR3, GAL3ST1, SLC5A10, SLC17A3, CHST13, and CID3B (Figure 5).

3.6. The Kaplan-Meier Plotter Survival Analysis of EHHADH-Coexpressed Genes. For the ten coexpressed genes of EHHADH in sarcoma, DMGDH, BHMT2, TMEM37, TLR3, SLC17A3, and CID3B were associated with longer overall survival ($p < 0.05$) (Figure 6).

3.7. GO and KEGG Pathway Enrichment Analysis of EHHADH-Coexpressed Genes. EHHADH-coexpressed genes were significantly involved in the biological progress of negative regulation of the following: glucuronosyltransferase activity, cellular glucuronidation, and fatty acid metabolic process; in cellular components of the extracellular exosome, apical plasma membrane, and integral plasma membrane components; in molecular functions of retinoic acid binding, glucuronosyltransferase activity, transferring hexosyl groups, and transferase activity (Figures 7(a) and 7(b)); and in KEGG pathways of drug metabolism—other enzyme pathway, drug metabolism—cytochrome P450 pathway, metabolism of xenobiotics by cytochrome P450 pathway, etc. (Figure 7(c), Table 3).

3.8. Inhibition of EHHADH Suppresses MG63 Cell Proliferation. To detect the EHHADH expression in the OS

Table 3: Functional and KEGG pathway enrichment analysis of EHHADH and its coexpressed genes. Top 3 GO terms and KEGG terms with $p < 0.05$ were selected.

Term	Name	Count	FDR
A, biological processes			
GO: 1904224	Negative regulation of glucuronosyltransferase activity	5	5.78*E*-07
GO: 2001030	Negative regulation of cellular glucuronidation	5	5.78*E*-07
GO: 0045922	Negative regulation of fatty acid metabolic process	5	5.78*E*-07
B, molecular functions			
GO: 0001972	Retinoic acid binding	5	8.33*E*-05
GO: 0015020	Glucuronosyltransferase activity	5	8.46*E*-05
GO: 0016758	Transferase activity, transferring hexosyl groups	5	8.46*E*-05
C, cellular components			
GO: 0016324	Apical plasma membrane	10	6.69*E*-06
GO: 0070062	Extracellular exosome	23	7.17*E*-05
GO: 0005887	Integral component of plasma membrane	13	9.71*E*-03
D, KEGG pathways			
hsa00983	Drug metabolism—other enzymes	7	4.20*E*-06
hsa00982	Drug metabolism—cytochrome P450	7	2.28*E*-05
hsa00980	Metabolism of xenobiotics by cytochrome P450	7	2.51*E*-05
hsa05204	Chemical carcinogenesis	7	2.51*E*-05
hsa01100	Metabolic pathways	19	2.51*E*-05
hsa00053	Ascorbate and aldarate metabolism	5	8.08*E*-05
hsa00040	Pentose and glucuronate interconversions	5	1.58*E*-04
hsa00860	Porphyrin and chlorophyll metabolism	5	3.67*E*-04
hsa00140	Steroid hormone biosynthesis	5	1.17*E*-03
hsa00830	Retinol metabolism	5	1.55*E*-03
hsa00770	Pantothenate and CoA biosynthesis	3	2.01*E*-02

tissue, qRT-PCR analysis was used to compare the EHHADH level between OS tissue and the adjunct bone tissue, and as shown in Figure 8(a), significantly increased level of EHHADH mRNA was found in the OS tissues compared with adjacent bone tissues. Next, to explore the function of EHHADH in OS, EHHADH siRNA was used to knock down the EHHADH expression in MG63 cells. The western blotting and qRT-PCR analysis indicated the knockdown efficiency (Figures 8(b) and 8(c)). Besides, to assess the role of EHHADH on the growth of the MG63 cells, a qRT-PCR assay was accomplished to detect the proliferation-related gene expression in the different treated groups. According to Figure 8(d), knockdown of the EHHADH expression markedly inhibit the proliferation rate of the MG63 cells than that of the NC siRNA group.

EHHADH, an L-bifunctional enzyme, is a part of the classical peroxisomal fatty acid β-oxidation pathway. A powerful way to trigger this pathway is the activation of the peroxisome proliferator-activated receptor α (PPARα) [11]. The abnormal EHHADH expression can lead to several human diseases, such as Fanconi's syndrome and burn sepsis [12–14]. Previously, a high level of EHHADH has been found in various cancers, which can be correlated with cancer development, and therefore considered as a potential therapeutic target for cancers [15–18]. For instance, it was reported that EHHADH was a significant biomarker in renal cell carcinoma with a significant prognostic value [19–21]. Similarly, a recent study indicated that EHHADH was found to be correlated with the elucidation of the pathogenesis of hepatocellular carcinoma, and it was assumed that the EHHADH expression is an indicator of poor prognosis of hepatocellular carcinoma patients. However, the diagnostic and prognostic role of EHHADH in OS has not yet been fully understood.

In the present research, we first sought to discover the clinical importance and prognostic value of EHHADH in OS patients with the help of clinical and the public database. Our results indicated that the EHHADH expression was upregulated in sarcoma tissues as compared to the normal tissues. Furthermore, compared with the adjacent bone tissues, human OS tissues showed the overexpression of EHHADH. Moreover, the statistical results revealed a clear relationship between the EHHADH expression and the survival of OS patients, which was further supported by multivariate and univariate analyses, indicating that EHHADH could be designed as a possible prognostic index to monitor the progress of OS.

Furthermore, to examine the influence of the expression of the EHHADH on the OS cell proliferation, the siRNA of EHHADH was developed and used to transfect the human MG63 cells. The qRT-PCR analysis was performed to measure the proliferation-related genes *Cyclin D1* and *Cyclin D3*, and the results indicated that the proliferation of OS cells

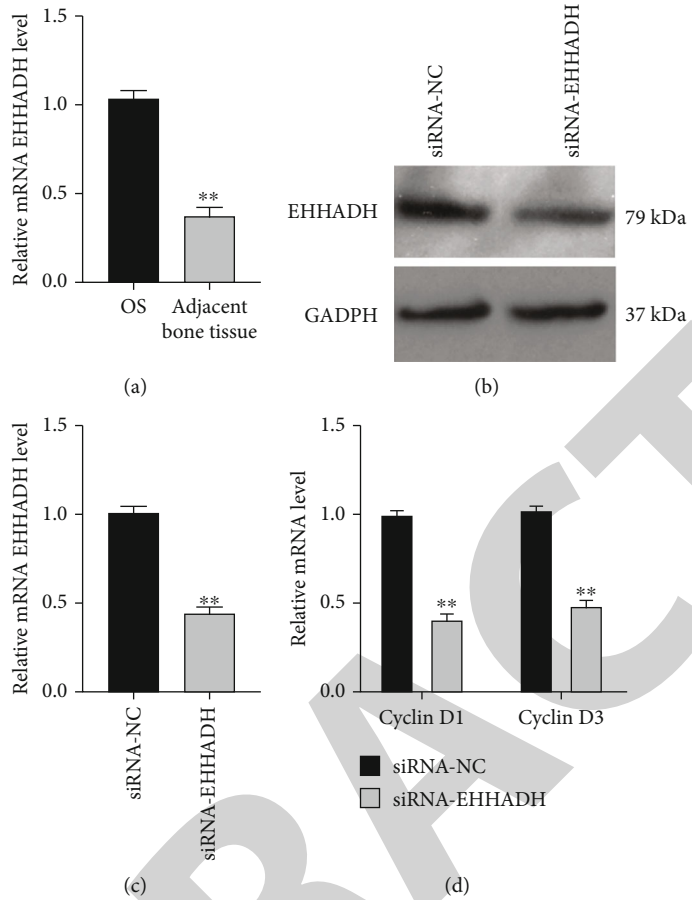

Figure 8: Inhibition of EHHADH suppresses MG63 cell proliferation. (a) qRT-PCR results of the EHHADH expression in OS tissue and the bone tissue. (b) The level of EHHADH following the siRNA EHHADH treatment in MG63 cells. (c) qRT-PCR results of the EHHADH expression in MG63 cells receiving different treatments. (d) The expression of proliferation-related genes cyclin D1 and cyclin D3 in the different groups was assessed by qRT-PCR analysis. $^{*}p < 0.05$, $^{**}p < 0.01$, $^{**}p < 0.01$. Data are the means ± SDs of three independent experiments.

can be repressed by knockout EHHADH in vitro. However, much more evaluation and validation should be performed to study the role of EHHADH in OS cells and investigate the underlying molecular mechanism of this correlation.

4. Conclusions

The research indicated that EHHADH possesses significant importance in the diagnosis and prognosis of OS, while the dismal prognosis of OS patients can be predicted by the expression level of EHHADH. Additionally, the inhibited proliferation of MG63 cells under the influence of the reduction of EHHADH also supported the conclusion that EHHADH may perform a function of a valuable prognostic biomarker for OS patients.

Data Availability

The data used to support the findings of this study are available from the corresponding author upon request.

Conflicts of Interest

The authors declare that there is no conflict of interest regarding the publication of this paper.

Authors' Contributions

Juncheng Cui and Guoliang Yi contributed equally to this work.

Acknowledgments

This work was supported by grants from the Health Commission of Hunan Province (20201907) and Natural Science Foundation of Hunan (2018JJ3468).

References

[1] R. Chen, G. Wang, Y. Zheng, Y. Hua, and Z. Cai, "Drug resistance-related microRNAs in osteosarcoma: translating basic evidence into therapeutic strategies," *Journal of Cellular and Molecular Medicine*, vol. 23, no. 4, pp. 2280–2292, 2019.